Une stratégie d'identification multi-échelles générale pour la caractérisation du comportement des matériaux hétérogènes.

Lorenzo Cappelli

HESAM UNIVERSITÉ

Arts et Métiers Sciences et Technologies

ÉCOLE DOCTORALE SCIENCES DES MÉTIERS DE L'INGÉNIEUR
I2M - Institut de mécanique et d'ingénierie (CNRS UMR 5295) –
Campus de Bordeaux

THÈSE

présentée par : **Lorenzo CAPPELLI**

soutenue le : **06 Mai 2020**

pour obtenir le grade de : **Docteur d'HESAM Université**

préparée à : **École Nationale Supérieure d'Arts et Métiers**

Spécialité : **Mécanique**

A general multi-scale identification strategy for the characterisation of the material behaviour of heterogeneous media

THÈSE dirigée par :
M. GUILLAUMAT Laurent

et co-encadrée par :
M. MONTEMURRO Marco et M. DAU Frédéric

Jury

M. El-Mostafa DAYA, PU, LEM3, Université de Lorraine	Président
M. Djimédo KONDO PU, Institut d'Alembert, Sorbonne Université	Rapporteur
M. Patrick ROZYCKI, MCF HDR, GEM, Ecole Centrale de Nantes	Rapporteur
M. Yves CHEMISKY, PU, I2M, Université de Bordeaux	Examinateur
Mme. Alina KRASNOBRIZHA, MCF, LEME, Université Paris Nanterre	Examinatrice
M. Laurent GUILLAUMAT, PU, LAMPA, Ecole Nationale Supérieure d'Arts et Métiers	Examinateur
M. Frédéric DAU, MCF, I2M, Ecole Nationale Supérieure d'Arts et Métiers	Examinateur
M. Marco MONTEMURRO, MCF HDR, I2M, Ecole Nationale Supérieure d'Arts et Métiers	Examinateur

T H È S E

Alla mia Famiglia,
Lorenzo.

Contents

List of Figures

Acknowledgements

I wish to express my sincerest gratitude to my supervisors Marco Montemurro, Frédéric Dau and Laurent Guillaumat, who have directly contributed to the realisation of this work, making it possible. In particular, I would like to thank Marco for all the scientific knowledge that he transmitted to me and for the patience he had in following my work constantly during these years, showing a great passion for Science and Engineering. Thanks to Frédéric and to Laurent for continually supervising my work, giving valuable technical advices, the result of a long experience in the engineering field.

I thank all the members of the FULLCOMP project, in particular Erasmo Carrera and Marco Petrolo, without whom this project would never existed. During this experience I met *eleven* special people: Guohong Li, Alberto García de Miguel, Ibrahim Kaleel, Margarita Akterskaia, Sander van den Broek, Yanchuan Hui, Gabriele De Pietro, Sergio Minera, Mayank Patni, Pietro del Sorbo and Georgios Balokas, with which I gave rise to a unique international friendship, through the sharing of every moment of this experience, travelling around the Europe.

A special thanks to three guys: Michele Iacopo Izzi, Pietro del Sorbo and Giulio Costa, who daily supported and advised me both scientifically and personally, showing people full of passion and dedication to their work, as well as being honest and with a unique kindness. A special mention for Ilan Raphael, who, with his constant smile, has always tried to make me feel welcomed in his native country, showing an infinite humanity.

I would like to thank Martina, because your affection allowed me to go on, able to overcome an unbridgeable distance: without you, this would not have been possible.

Finally, I thank my Parents Paolo and Sandra and my Brother Francesco for having supported me at all times, despite their distance, helping me to overcome any harshness.

Ringraziamenti

Vorrei esprimere la mia più sincera gratitudine ai miei inquadranti Marco Montemurro, Frédéric Dau e Laurent Guillaumat, i quali hanno contribuito direttamente alla realizzazione di questo lavoro, redendolo possibile. In particolare, vorrei ringraziare Marco per tutte le conoscenze scientifiche che mi ha trasmesso e per la grande pazienza che ha avuto nel seguire il mio operato pedissequamente in questi anni, mostrando una grande passione per la Scienza e l'Ingegneria. Un grazie a Frédéric ed a Laurent per aver supervisionato continuamente il mio lavoro, dando preziosi consigli tecnici, frutto di una lunga esperienza in campo ingegneristico.

Ringrazio tutti i membri del progetto FULLCOMP, in particolare Erasmo Carrera e Marco Petrolo, senza i quali tale progetto non sarebbe mai esistito. Durante questa esperienza ho conosciuto 11 persone speciali: Guohong Li, Alberto García de Miguel, Ibrahim Kaleel, Margarita Akterskaia, Sander van den Broek, Yanchuan Hui, Gabriele De Pietro, Sergio Minera, Mayank Patni, Pietro del Sorbo e Georgios Balokas, con i quali è nata un'amicizia internazionale unica, attraverso la condivisione di ogni istante di questa esperienza, viaggiando per l'Europa.

Un grazie speciale a tre ragazzi: Michele Iacopo Izzi, Pietro del Sorbo e Giulio Costa, i quali mi hanno sostenuto e consigliato quotidianamente sia dal punto di vista scientifico che personale, mostrandosi persone piene di passione e dedizione per il proprio lavoro, oltre che oneste e di una gentilezza unica. Una menzione speciale per Ilan Raphael, il quale, con un sorriso costante, ha sempre cercato di farmi sentire accolto nel suo paese natio, mostrando un'umanità infinita.

Vorrei ringraziare Martina, perché il tuo affetto mi ha permesso di andare avanti, capace di superare una distanza incolmabile: senza di te, tutto ciò non sarebbe stato possibile.

Infine, ringrazio i miei Genitori Paolo e Sandra e mio Fratello Francesco per avermi supportato in ogni momento, nonostante la lontananza, aiutandomi a superare ogni asperità.

Introduction

The thesis context and the FULLCOMP project

The word *composite* in the engineering context means that two, or more, different materials are combined together with the purpose of manufacturing a third material characterised by a set of material properties responding to a specific need. By conducting a macroscopic examination, the constitutive elements can be identified by the naked eye (e.g. multilayer composites) or can show a macroscopic homogeneous appearance (e.g. short fibre composites). These features highlight the huge variety of structural configurations and properties that can be obtained/designed through composite materials [2].

Composites can be conceived in different format and topologies. Usually they are designed in order to highlight the best qualities of the constitutive components and, often, to show properties that neither of their constituents possesses. Composite materials are massively employed due to their outstanding strength-to-weight and stiffness-to-weight ratii, fatigue life, thermal conductivity, acoustical insulation, etc. Accordingly, it is possible to understand why, nowadays, the use of composite materials in the engineering field grows continuously. Composites involve a multibillion market in which automotive, aerospace and wind energy sectors are the main players. The success of composites stems from their superior specific properties and the possibility of creating fit-for-purpose materials and structures. However, the lack of knowledge still undermines the cost-effectiveness of composites and overweight characterising some solutions (especially in the aerospace field). [3].

The development of the scientific knowledge on this topic requires synergistic approaches in which, the multi-scale and the multi-physics modelling, characterisation, design/optimisation and validation phases must be considered. These aspects should be taken into account at all stages of the composite specimen life: from the preliminary design to the manufacturing process, from the numerical modelling to the experimental validation. Only in this way, it is possible to take advantage from the peculiar features of composite materials.

To facilitate the transition between design, modelling, manufacturing and experimentation, a paradigm shift in the field of composite materials, under a multidisciplinary point of view, is required. This paradigm change constitutes the main topic of the FULLCOMP (FULLy integrated analysis, design, manufacturing and health-monitoring of COMPosite structures) project. In particular, the FULLCOMP project deals with the advances in predictive models and techniques for numerical analyses of the composite materials.

FULLCOMP is an H2020 Marie Sklodowska-Curie project which is dedicated to the training of *twelve* Ph.D. students in the field of advanced models for composite materials and structures. The most relevant common thread of the contributions is the increment of the numerical efficiency, in terms of simulation, with an increment of accuracy for a given computational costs, when compared to the existing methodologies. The FULLCOMP

project started in 2015 as an European Training Network (ETN). The consortium is composed by *seven* Universities (Politecnico di Torino, University of Bristol, Leibniz Universität Hannover, École Nationale Supérieure d'Arts et Métiers of Bordeaux, Universidade do Porto, University of Washington and RMIT), *one* research institute (Luxembourg Institute of Science and Technology) and *one* company (ELAN-AUSYGmbH).

The training of the Ph.D. students followed *five* main work packages, i.e. analysis and computational methods, design and optimisation, damage and failure analysis, multi-scale methods, and experimental approaches. Other forms of training included three courses on entrepreneurship and project management, *four* workshops on composite materials and structures, *one* spring school, and *ten* seminars or courses. Also, each student spent *two* secondment periods of several weeks in academic and non-academic institutions to increase the multidisciplinary aspects, facilitate cross-fertilisation and the transfer of knowledge toward industry.

The research activities , constituting the kernel of the FULLCOMP project, can be summarised in three main research axes.

- *Advanced finite element models.*
  Numerical techniques focusing on enhanced one-dimensional (1D) and two-dimensional (2D) models, commonly referred to as beams and shells, are developed. The implementation of such theories/models allows to predict accurately 3D displacements and stress fields, without requiring a strong computational effort with respect to classical 3D finite element (FE) models. The proposed models are based on the Carrera Unified Formulation (CUF) [4, 5] and employed for multi-field and multi-scale analyses.

- *Damage and failure models.*
  New models for damage prediction and failure analysis of composite materials, together with studies on the structural health monitoring (SHM) are also carried out. Concerning the modelling strategies, they are developed at the level of the structural theory (e.g. by implementing the CUF), in order to obtain accurate 3D stress fields and reducing, at the same time, the computational effort. By coupling special modelling strategies (such as global-local methods) it is possible to limit the detailes (and expensive) FE analyses to local zones and to extend the predictive tools to complex structures. In particular, the material non-linearities are included into 1D structural models to deal with damage mechanisms and failure.

  For example one of the main applications, presented in the FULLCOMP project, focuses on dry fabrics and their ballistic application. The modelling approach deals with hyperelastic constitutive laws for the yarn structure and full characterisation via experimental/numerical approaches. Various numerical models exist for dry fabric layers in literature [6]: among them, the so-called mesoscopic models are the most efficient in terms of accuracy and computational costs. In particular, the Gasser's mesoscopic model [7] for dry fabrics is universally adopted. However, the characterisation of the yarn transverse behaviour remains unsolved: unfortunately this last aspect assumes a fundamental role in determining the ballistic performances and, for this reason, these aspects are investigated.

  Finally, suitable SHM tools, ensuring structural integrity during service and reducing substantially the operating costs are developed. In this context, the guided ultrasonic waves (GUW) are a suitable candidate to detect, localize and characterise

the defects [8]. However, in laminated structures the phenomena is highly complex: the anisotropy of the material causes distorted wave-fronts and the heterogeneity of the material might result in mode couplings. Numerical models are necessary and, to this purpose, high-order theories based on the CUF [5] are used to simulate wave propagation analysis in composite laminates.

- *Virtual characterisation and manufacturing.*
  Real structures are imperfect, despite advances in the manufacturing processes and quality controls. A real composite structure is characterised by a number of differences in terms of geometry and material properties with respect to its numerical model, due to the variability in the manufacturing process throughout the production line [9, 10]. The main contribution of the FULLCOMP project on this topic focuses on the development of suitable models able to properly integrate the uncertainty (at each pertinent scale) in the analysis of composite materials and structures. A particular attention is put on the correlation between mechanical response and the spatial variation of material properties which allows identifying the areas in which variability of material properties has a relevant effect. This aspect is of paramount importance in order to define the product inspection zones and to improve the performances of a structure.

  Concerning the issues related to the uncertainty, the composite materials heterogeneous nature is the main cause of the variability of the mechanical response (e.g. stiffness, strength, etc.) at the macroscopic scale. Classical examples are the aleatory uncertainty related to the fibre and matrix properties, together with their geometrical features. Many efforts are devoted to simulate the random fibre distributions [11] and uncertainty propagation through the scales.

  Finally, the multi-scale nature of composite materials makes mandatory, analysis and design purposes, the characterisation of the full set of material properties, at each pertinent scale, i.e. the mesoscopic scale of the elementary lamina and the microscopic scale of the constituent phases. Moreover, from the industrial point of view, the cost reduction of the experimental characterisation tests is of outstanding importance: usually, destructive tests are conducted and a significant number of samples is needed to get reliable results [12]. However, as far as the characterisation of the composite behaviour at the mesoscopic scales, common standard ASTM tests are not able to provide the full set of 3D properties of the composite. Moreover, in the case of laminates, the elastic behaviour of the lamina is, generally, anisotropic due to the mechanical behaviour of the constituent phases at the microscopic scale. Concerning the identification of elastic properties at the microscopic scale, only few standard tests are available in the literature and usually non-standard tests are used [13–15], yet they show major shortcomings (complex experimental set-up, significant dispersion of results, etc.).

  In this context, the need of a general multi-scale identification strategy, able to smartly combine the information resulting from both suitable numerical model and cheap non-destructive tests, is of paramount importance. The identification procedure should be as general as possible in order to include the uncertainty related to both the material and the manufacturing process. This is precisely the goal of this third research axis.

This Ph.D. thesis belongs to the third researc axis of the FULLCOMP project.

Identification of composite material properties: issues and challenges

When dealing with the characterisation of the composite material behaviour, one of the main issues is related to the difficulty of characterising the material properties of the constitutive phases (microscopic scale).

Experimental destructive tests are commonly used to carry out the characterisation procedure, though they lead to an expensive experimental campaigns. As outlined in [12] they can be divided into mesoscopic and microscopic identification tests. The most relevant tests at the mesoscopic/macroscopic scale can be summarised as follows: the tension test for flat specimens (ASTM D3039 [16]), three/four points bending test (ASTM D790 [17]), compression tests (shear loading methods ASTM D3410 [18], end loading methods ASTM D695 [19], combined loading methods ASTM D6641 [20]) and shear tests (in-plane shear tests ASTM D5379 [21]-D7078 [22]-D3518 [23], out-of-plane - interlaminar shear tests ASTM D2344 [24]-D5379). These tests are often used to determine the elastic constants of the constitutive lamina. However, they do not allow identifying the full set of 3D elastic properties required to uniquely describe the lamina stiffness tensor. For example, an unidirectional fibre-reinforced pre-preg lamina has an orthotropic behaviour. The ASTM standard tests conducted at the lamina-level are able to provide only the in-plane elastic properties, together with an approximation of the out-of-plane shear moduli.

Concerning the identification of the material properties of the constituent phases, i.e. fibres and matrix, only few standard tests can be performed at the microscopic scale: single fibre test to obtain the Young's modulus along the fibre axis (ASTM D3379 [25]) and the matrix tensile test (ASTM D638 [26]). Conversely, to characterise the rest of the elastic properties, only non-standard tests are available in the literature: the pull-out test [13], the micro-indentation test [14], the fragmentation test [15], etc. However, non-standard microscopic tests present some major shortcomings: the experimental set-up is usually difficult to be realised and the results often show significant dispersions, as outlined in [27].

In this context, the main challenge is to identify the composite behaviour, at each pertinent scale, avoiding destructive tests. To overcome these limitations, a dedicated multi-scale identification strategy (MSIS) should be developed.
Firstly, the MSIS should be as general as possible in order to allow for characterising both linear and non-linear behaviour of the composite at each scale.

For example, under dynamic loads, the characterisation of the composite damping capability is of outstanding importance [28]. The macroscopic dynamic response of the composite is strongly affected by the viscoelastic behaviour of the fibre and the matrix. However, the characterisation of the viscoelastic behaviour of the constitutive phases is anything but trivial.

From the experimental point of view, two methods are commonly used in the literature: the direct technique and the indirect one. On the one hand, the direct techniques are mainly based on the measurement of the dissipated energy per load cycle, through the evaluation of the area hysteresis loop [29]. On the other hand, the indirect methods allow evaluating the dissipated energy through the specimen spectrum response. Typical indirect techniques for damping characterisation are: the free vibration-decay, the resonant-dwell, the bandwidth and the impedance methods [30]. However, all the aforementioned methods are able to provide information only at the mesoscopic scale: the

viscoelastic behaviour of the microscopic constituents cannot be characterised through these techniques.

Secondly, the MSIS should take into account for the variability of the composite material at each scale. This aspect is very important, especially in large-scale production, where a large amount of variability arises from unavoidable manufacturing imperfections both for geometrical and material properties, affecting, hence, the macroscopic response of the composite. As outlined in [31], the uncertainty can be classified as follows: aleatory (variability of material parameters), epistemic (lack of adequate information about the system) and prejudicial (absence of stochastic characterisation of the structural system). Composite structures are affected by these forms of uncertainty and the characterisation of the parameters tuning the model describing the uncertainty becomes of prime importance. However, experimental methods that are commonly used to characterise the uncertainty require a huge number of standard ASTM tests [32]. Moreover, these tests are only suited to evaluate mesoscopic uncertainty, in terms of material and geometrical properties at the mesoscopic scale, without providing useful information about the variability characterising the properties of the constitutive phases at the microscopic scale.

In order to get statistical representative results, the aforementioned tests must be performed a huge number of times. Of course, this implies significant costs (and time) and the variability results (i.e. mean and standard deviation of material properties) are strongly affected by the errors introduced to carry out the experimental campaign, especially for those tests conducted at the microscopic scale. To this purpose, Sepahvand *et al.* developed the inverse stochastic method based on the general polynomial chaos (gPC) to identify uncertain lamina elastic parameters from experimental modal data. Further examples of probabilistic methods are the parametric probabilistic approach [33] and the Bayesian inference techniques wherein all information are included into a prior distribution model [34–37]. However, in the case of composite structures, the uncertainty affecting the ply elastic behaviour is strictly related to the variability of the elastic properties of the constitutive phases. Up to now, the aforementioned probabilistic techniques have never been extended to the identification of the variability parameters characterising the elastic properties of the microscopic constituents of the composite. This aspect represents the main challenge concerning the uncertainty identification of composite structures, together with the need to use macroscopic non-destructive techniques.

The thesis objectives

In the light of the issues and challenges listed beforehand, this Ph.D. thesis aims to develop a general MSIS exploiting the information restrained in non-destructive tests and making use of pertinent FE models at each scale of the composite. In particular, the research activity carried out in this thesis focuses on four main goals.

1. A general, multi-purpose MSIS should be developed in the framework of *inverse problems*.

2. The MSIS should allow characterising both the linear and the non-linear behaviour of the composite at each scale.

3. The MSIS should be able to integrate the material properties variability, at each scale. Moreover, it should take into account the uncertainty propagation among scales.

4. The MSIS should efficiently exploit the information hidden into macroscopic non-destructive tests.

Of course, point (1) requires the formulation of an opportune constrained non-linear programming problem (CNLPP). The idea is to propose a CNLPP formulation free from simplifying hypotheses (or at least reducing the number of such hypotheses) which allows characterising, in a reliable way, the behaviour of the composite (linear and non-linear) at each scale. // The proposed formulation should also reduce/avoid the user's intervention, i.e. the MSIS should be, ideally, problem-independent. Morevoer, the CNLPP formulation should integrate all the variables involved into the definition of the composite behaviour at each scale. Obviously, the price to pay is an increased problem complexity in terms of both lack of uniqueness of the solution and sophistication of models and tools to perform the solution search for the CNLPP.// As far as the numerical tool used to perform the solution search for the (multi-scale) inverse problem, formulated as a CNLPP, a particular care should be put in choosing an adequate optimisation algorithm. Due to the increased problem complexity, the best choice is the use of a hybrid global/local optimisation tool composed by the union of a meta-heuristic algorithm (to perform the global exploration) and of a deterministic algorithm (to refine the local search).

Finally, points (2)-(4) require the development of pertinent numerical models. These models should be, on the one hand, as accurate as possible to properly describe the behaviour of the composite at each scale. On the other hand, they should be computationally efficient in order to be integrated in an optimisation loop and to provide a solution in a reasonable time.

The thesis outline

The manuscript is articulated in six chapters.

Chapter 1 presents a literature survey on inverse problems and their application to the characterisation of composite material properties.

Inasmuch as the work carried out in this thesis makes use of optimisation methods, a brief overview on deterministic and on meta-heuristic algorithms is provided in Chapter 2.

Chapters 3, 4 and 5 constitute the core of this thesis: the effectiveness of the MSIS is tested on some meaningful real-world engineering problems. Each one of these chapters directly reports the related paper, published in an international journal.

In particular, Chapter 3 deals with the problem of the multi-scale characterisation of the elastic properties of composites. In this work the identification process is conducted at both the lamina-level and at the microconstituents-level. The MSIS makes use of the information provided by a linear harmonic analysis.

In Chapter 4 the MSIS is generalised to the identification of the viscoelastic behaviour of the composite at both the mesoscopic and microscopic scales. In this case, the MSIS uses the information restrained in non-linear modal and harmonic analyses.

Chapter 5 further extend the MSIS by integrating the characterisation of the parameters tuning the variability of elastic properties of the composite material at each pertinent scale. In this case, the multi-scale identification makes use of the information restrained in buckling tests.

Finally, Conclusions and Perspectives of this Ph.D. work are presented in Chapter 5.2.

Chapter 1

Literature survey

1.1 Inverse problems: generalities and application to composite materials

1.1.1 General comments

Given a physical system, the *forward* or *direct* problem consists in using a physical theory to predict the outcome of possible experiments [38]. In classical physics this problem has a unique solution. For instance, for a given mathematical model describing the behaviour of a system (e.g. an aircraft uniquely defined by a set of material and geometrical parameters) and for a given model of the external inputs (e.g. applied loads, environmental conditions, etc.), it is possible to predict the static and dynamic responses of the system.

The *inverse* problem arises when a good model of the considered system or a good model of the inputs are not available, but only a set of experimental data is available. These information can be used to infer the main features characterising the system behaviour, or a model of the external inputs. Generally speaking, inverse problems have not a unique solution. Two classical examples can be found in the field of heterogeneous, anisotropic materials. The first one concerns laminates: different stacking sequences can correspond to the same macroscopic behaviour in terms of membrane, bending and membrane-bending coupling stiffness tensors. The second one is about cellular structures: different microscopic representative volume elements (RVEs), e.g. cubic, octahedron, gyroid topologies, can show the same macroscopic stiffness.

1.1.2 Historical review

The use of optimisation techniques to solve inverse problems has a long history. Laplace explicitly stated the least absolute values criterion. This formulation together with the least-squares criterion were later popularised by Gauss [39]. While Laplace and Gauss were mainly interested in *overdetermined* problems, Hadamard [40] introduced the notion of an *ill-posed* problem, that can be viewed in many cases as an *underdetermined* problem. The period from late sixties to early seventies was a *golden age* for the theory of inverse problems. In this period the first attempts of using the Monte Carlo theory to obtain Earth models were made by Keilis-Borok and Yanovskaya [41] and by Press [42]. At about the same time, Backus and Gilbert [43–48] made original contributions to the theory of inverse problems, focusing on the problem of obtaining an unknown function from discrete data. Although the resulting mathematical theory is elegant: its initial

predominance over the Monte Carlo theory was only possibly due to the quite limited capacities of the computers at that time. An investigation of the connection between analogue models, discrete models and Monte Carlo models can be found in a paper by Kennett and Nolet [49]. Important developments of inverse theory were also made by Wiggins [50] with the method of suppressing the *small eigenvalues* and by Franklin [51], by introducing the right mathematical setting for the Gaussian functional, i.e. infinite dimensional inverse problem. A reference on the probabilistic approach of Akaike can be found in Parzen *et al.* [52].

1.1.3 Probabilistic formulation of inverse problems

As stated above, an inverse problem must be formulated when a set of measured data are available and information on unknown parameters of the physical system are sought. For standard inverse problems all the variables can be separated in two groups, the *directly observable parameters* and the *model parameters*. In particular, for a given physical system, it is possible to describe its behaviour by assigning values to a given set of parameters $\mathbf{m} = \{m_1, m_2, ..., m_{NM}\}$, defined as the model parameters, that may not be directly observable. Indirect measurements are then performed and the set of (directly) observable parameters $\mathbf{d} = \{d_1, d_2, ..., d_{ND}\}$ can be defined.

The second ingredient is the mathematical model describing a given physical theory that can be used to solve the forward problem, i.e. given a mathematical model uniquely defined by the set $\mathbf{m}$, it can be used to predict the theoretical data $\mathbf{d}$ that an ideal measurement should produce. The generally non-linear function that can be associated to this model can be represented as

$$\mathbf{d} = \mathbf{f}(\mathbf{m}). \tag{1.1}$$

Usually, mathematical models are characterised also by *a priori* information, i.e. the information that do not depend upon of the measurements. These information show a generally complex probability distribution over the model space and, for this reason, one can introduce the probability density function $\rho_m(\mathbf{m})$, as outlined in [53].

Similarly, the observation of the considered physical phenomena is represented by the set $\mathbf{d}$: as in any measurement, the data are determined with an associated uncertainty, which can be described by a probability density function over the data parameter space, denoted as $\rho_d(\mathbf{d})$.

Assuming that the probability density in the model space does not depend upon the measurements, it is possible to define a joint probability density $\rho(\mathbf{x})$ in the space $X = (M, D)$, defined as

$$\rho(\mathbf{x}) = \rho(\mathbf{m}, \mathbf{d}) = \rho_m(\mathbf{m})\,\rho_d(\mathbf{d}). \tag{1.2}$$

In the $(M, D) = M \times D$ space, the natural and common way to compose the probability density $\rho(\mathbf{m}, \mathbf{d})$ and the hypersurface $\mathbf{d} = \mathbf{f}(\mathbf{m})$ is to define the conditional probability density $\sigma_m(\mathbf{m})$ [38]:

$$\sigma_m(\mathbf{m}) = \rho_{m|d(m)}(\mathbf{m} \mid \mathbf{d} = \mathbf{f}(\mathbf{m})) = k\rho(\mathbf{m}, \mathbf{d}) \left.\frac{\sqrt{det(\mathbf{g}_m + \mathbf{F}^T\mathbf{g}_d\mathbf{F})}}{\sqrt{det(\mathbf{g}_m)}\sqrt{det(\mathbf{g}_d)}}\right|_{\mathbf{d}=\mathbf{f}(\mathbf{m})}, \tag{1.3}$$

where $\mathbf{F} = \mathbf{F}(\mathbf{m})$ is the matrix of partial derivatives, with components $F_{i\alpha} = \frac{\partial f_i}{\partial m_\alpha}$; where $\mathbf{g}_m$ and $\mathbf{g}_d$ are the metric in the model parameter space M and in the data space D, respectively.

Once the conditional probability density $\sigma_m(\mathbf{m})$ is defined, there are different ways of using it. If the model space M is characterised by a small number of dimensions the values of $\sigma_m(\mathbf{m})$ can be computed at every point of a grid and a graphical representation of $\sigma_m(\mathbf{m})$ can be obtained. Conversely, if the model space M has a large number of dimensions (e.g. grather than five), then an exhaustive exploration of the space is not possible and the Monte Carlo sampling method can be implemented to extract information from $\sigma_m(\mathbf{m})$, as outlined in [54].

1.1.4 Solution techniques for inverse problems

The solution techniques for inverse problems are substantially three: the examination of the combined probability density, the Monte Carlo and the optimisation methods. The examination of the probability density consists of directly plotting $\sigma_m(\mathbf{m})$, when few parameters are investigated (i.e. from one to five). However, when the number of parameters increases, the Monte Carlo algorithm or the optimisation methods are mandatory to solve the inverse problem.

On the one hand, an extensive systematic exploration of the model space is needed and, concerning the meta-heuristic algorithms, different sampling methods are available in the literature: the inversion method, the rejection method, the sequential realisation, the Gibbs sampler, the Metropolis algorithm and the genetic algorithms [55] (GAs). Nowadays, the most well-established techniques are the Metropolis algorithm [56–58] and the GAs: the basic idea is to perform a random exploration of the model space and the main differences are that the Metropolis algorithm is based on a sort of Brownian motion, while the GA is a biological metaphor exploiting the mechanisms at the basis of genetics and of the Natural selection.

On the other hand, deterministic methods can also be used. Roughly speaking, the solution of an inverse problem essentially consists of a probability distribution over the space of all possible models of the physical system under study. In general, if the model dimension is high (i.e. greater than five) the only way to explore it is by means of the Monte Carlo method. However, if the probability distributions are *bell-shaped* (i.e. a generalised Gaussian shape), it is possible to simplify the problem by calculating the point around which the probability is maximum. Common deterministic methods based on the gradient of the function are: maximum likelihood point, misfit, steepest descent algorithm and quasi-Newton methods (for more general methods, the reader is addressed to [54, 59–62] and to Chapter 2).

When the non-linearity is weak, inverse problems can be solved with the *least-absolute-values* and the *min-max* criteria (l_1-norm criteria) introduced by Laplace [63], or the *least-squares* criterion (l_2-norm criterion) introduced by Legendre and Gauss [39]. Least-squares are popular for solving inverse problems because they lead to the easiest computations. The only drawback is their lack of robustness, i.e. their strong sensitivity to a small number of large errors in the data set.

1.1.5 Material properties characterisation as an inverse problem

This Ph.D. thesis deals with the characterisation of the behaviour of composite materials at each pertinent scale, ideally by using non-destructive tests. Unfortunately, the set of material properties provided by manufactures is often not sufficient to describe completely the behaviour of the composite for all its potential applications [64]. For example, the technical sheet for standard fibre-reinforced pre-pregs [65–67] includes only basic information, like fibre volume fraction, in-plane Young's moduli (tension and flexural), density, etc. However, very often the out-of-plane elastic constants are not provided, thus experimental tests reveal necessary to fully characterise the 3D elastic response of the pre-preg. Furthermore, as far as the non-linear behaviour is concerned, no information are available.

Different techniques are commonly applied to deal with material properties characterisation. The experimental tests are of two types: destructive and non-destructive tests. Usually, when the characterisation of the material properties of a composite is formulated as an inverse problem the data provided by non-destructive tests are employed. In particular, the identification of the material behaviour by means of inverse methods has recently seen a significant growth, mainly because of the availability of efficient and modern technologies such as automated testing, full-field measurement techniques [68], and inexpensive computing resources [69]. Two exhaustive surveys on this topic are available in [70, 71]. These works highlight that the vibration-based techniques (based on the evaluation of natural frequencies and the related modal shapes) are the most popular non-destructive tests associated to inverse problems for material properties identification. The researchers dealing with this topic make use of deterministic algorithms to carry out the solution search of the inverse problem [72, 73]. When possible the sensitivity analysis (i.e. the evaluation of the gradient of either objective function or constraint functions) is performed analytically or by means of surrogate models like artificial neural networks (ANNs) [74]. When the inverse problem is strongly non-convex meta-heuristic algorithms, like GAs, are adopted [75]. Often the inverse problem is solved for single-layer [72–74] or multilayer composite plates [75].

As stated above, the identification of the material properties of composites can be formulated as an inverse problem, as widely discussed in [76]. Although often the aim is to find static material data, eigenfrequencies and/or modal shapes are measured for a given specimen. In a pilot project by Markworth and Petersen [76] this technique was found very promising (some of the results can be found in Pedersen and Frederiksen [77]). The same conclusions were reported in the Ph.D. thesis by Sol [78]. The research groups in Brussels and in Eindhoven have continuously refined the method and obtained impressive results. The proceedings from an Euromech colloquium, edited by Sol and Oomens [79], give a picture of the state of the art. A doctoral thesis by Kuttenkeuler [80] shows the importance of these techniques for composite materials characterisation and design. Combination with the FE method and thick plate kinematics formulation are investigated and the relative issues and challenges are discussed in the work by Mota Soares *et al.* [81].

1.2 Multi-scale characterisation of composite material properties

Due to their nature, composite materials show a behaviour significantly different from that of conventional materials, such as metals. For metals, the hypothesis of homogeneous isotropic behaviour is consistent in most cases. In addition, in the framework of linear

elasticity the stiffness tensor of metals depends only upon the Young's modulus and the Poisson's ratio [82]. In the case of composite materials, the assumption of homogeneous-isotropic behavior is not possible, and more complex models have to be used depending on the problem at hand [83]. The complex behaviour of composites is actually due to two intrinsic properties of these materials, i.e. the heterogeneity and the anisotropy. The heterogeneity is involved mainly at the micro-scale (i.e. the scale of constitutive "phases"). Conversely, the anisotropy intervenes at both mesoscale (that of the constitutive lamina) and macro-scale (that of the laminate). As a consequence of the anisotropy, the mechanical response of the material depends upon a considerable number of parameters, i.e. 21 for a general triclinic material, 13 for the monoclinic case, nine for the orthotropic one, five for the transverse isotropic case and two for an isotropic material. Accordingly, composite materials need the development of suitable multi-scale models and theories. To this purpose, they are conveniently studied from two points of view: the micro-mechanics and the macro-mechanics.

In this work, the characterisation of the behaviour of the composite material is performed at each characteristic scale. In particular, the main goal is the identification of the behaviour of the microscopic constituents starting from the evaluation of a macroscopic mechanical response, as the dynamic response or the first buckling load. More precisely, this thesis focuses on the multi-scale characterisation of the elastic and viscoelastic properties of composite materials, eventually in presence of uncertainty. Therefore, a state-of-the-art concerning the application of characterisation techniques and inverse problems to the above topics is presented in the following sections.

1.2.1 Identification of the elastic properties

The heterogeneity and anisotropy typical of composite materials require more sophisticated experimental procedures for characterising their behaviour. The standards normally used for homogeneous isotropic materials are inadequate for the complete identification of the composite response [82]. In fact, even under the hypothesis of linear elastic behaviour, the anisotropy requires that the material response must be measured along several directions. The microconstituents, in turn, implies a local variation of the mechanical properties, which requires the averaging of deformations over areas sufficiently larger than the heterogeneity characteristic sizes.

For these reasons, multiple standard destructive tests have been developed. The most important tests aiming at characterising the composite behaviour at the mesoscopic scale (i.e. lamina-level) are the tension test for flat specimens (ASTM D3039 [16]), three/four points bending test (ASTM D790 [17]), compression tests (shear loading methods ASTM D3410 [18], end loading methods ASTM D695 [19], combined loading methods ASTM D6641 [20]) and shear tests (in-plane shear tests ASTM D5379 [21]-D7078 [22]-D3518 [23], out-of-plane - interlaminar shear tests ASTM D2344 [24]-D5379). Nevertheless, ASTM standard tests conducted at the lamina level are not able to provide the full set of 3D elastic properties: only the in-plane material properties together with an approximated value of the out-of-plane shear moduli can be retrieved through these tests.

Conversely, only few standard tests can be carried out at the microscopic scale: single fibre test to obtain the Young's modulus along the fibre longitudinal direction (ASTM D3379 [25]) and matrix tensile test (ASTM D638 [26]). In order to characterise the rest of the constitutive phases properties, only non-standard tests are available in the literature: pull-out [13], micro-indentation [14], fragmentation tests [15], etc.

Indeed, it is very interesting, especially from an industrial point of view, to be able to reduce the cost of experimental characterisation tests which are usually destructive procedures that must be carried out for a significant number of samples in order to get reliable results (thus leading to quite expensive experimental campaigns) [12]. Moreover, as far as concerns the characterisation of the elastic properties of the constitutive phases, a large data dispersion is obtained during experimental tests. This is due to the difficulty to properly set the experiment and to handle the microscopic constituents [14].

In this scenario, it interesting to observe that in the literature two techniques are proposed to overcome the aforementioned issues [82]: the virtual field method (VFM) and the finite element model updating (FEMU).

The VFM is an approach which allows identifying the constitutive parameters of a material by means of the principle of the virtual work, in the hypothesis of small strains [84, 85]. For instance, it is possible to assume a static test performed on a thin anisotropic plate of uniform thickness: under the hypotheses of plane stress field, specimen subjected to N concentrated forces and negligible body forces, it is possible to characterise the lamina elastic coefficients. Therefore, the VFM allows defining more complex characterisation tests able to provide more information, than standard procedures. In addition, as for the standard procedures, the VFM does not imply iterative procedures with the related typical convergence issues [82]. The VFM results to be a powerful tool for characterising anisotropic materials. In fact, many researchers continue to study and develop new approaches based on virtual fields. In [86] Gu *et al.* proposed a new test able to identify the whole set of elastic constants for an orthotropic plate. Rossi *et al.* [87–89] developed new procedures to find the most significant experimental and operative parameters that can play an important role in the measurement process, like the orientation of the fibres. In [88] Nigamaa *et al.* proposed a variant of the VFM, the Eigenfunction Virtual Field Method (EVFM), according to which the measured strains are used for generating the virtual fields. Similarly, in [90] Rahmani *et al.* presented an identification method, based on Regularized Virtual Field Method (RVFM), aimed to determine the local properties of a unidirectional composite transversally loaded.

As far as the FEMU is concerned, it combines the experimental data with FE simulations [91, 92]. It has become popular in the last 20 years, thanks to the progresses in informatics (namely hardware capacity) and to the diffusion of commercial FE software. In the framework of the FEMU, a mechanical test is chosen and it is performed on the composite specimen. According to the adopted full-field technique, a specific field (displacement or strain components) is measured over a portion (or over the whole) outer surface of the specimen. Then, the same mechanical test is simulated by a FE analysis assuming a first guess for the elastic parameters, and the same deformation field is numerically calculated [82]. The numerical and experimental results are compared by building a pertinent cost function (usually an error-estimator), which is evaluated and compared with some threshold values in order to satisfy convergence requirements. If the convergence criteria are met, the search procedure is stopped, otherwise a new set of elastic parameters is chosen and used for the next iteration.

Moreover, the FEMU approach has been improved by Rahmani *et al.* [93], who proposed an improved FEMU approach, the Regularized Model Updating (RMU), based on micromechanics concepts and which adds some mathematical constraints in order to speed up the convergence of the algorithm and improve the accuracy of the solutions. In [94] the authors proposed an identification procedure based on the natural frequencies of a composite panel. In this procedure, the moduli of the constitutive phases are evaluated

and particular attention was put on the effect of the noise on the experimental data and on the influence of the boundary conditions, modelled as extension springs whose stiffness was evaluated by the FEMU procedure. The method reported in [95] allows to measure all the 21 elastic coefficients of a completely anisotropic medium. In this case, seven static mechanical tests are required on a single L-shaped specimen.

Other approaches were successfully used for linear elastic characterisastion, such as the constitutive equation gap method [96], the equilibrium gap method [96, 97], the reciprocity gap method [98], and the constitutive compatibility method [99]. All these approaches, reviewed in [100, 101], were mostly used for isotropic materials, hence they are not discussed here.

Finally, it is interesting to briefly analyse the comparison between the standard ASTM tests, VFM and FEMU techniques, as done in [82]. Of course, the number of tests to be carried out is the highest in the case of standard ASTM tests, according to which the stress/strain states are quite simple. Accordingly, their sensitivity to different elastic parameters is often uncoupled. The higher complexity of testing configurations adopted by VFM and FEMU allows for a significant reduction in the number of tests required to completely characterise the material. Conversely the sensitivity analysis is harder than in the case of ASTM tests. Finally, the computational complexity is low for standard ASTM tests and VFM technique, which allows for a direct calculation of elastic coefficients after an evaluation of stress and strain field, while the FEMU approach requires iterative procedures that are often time consuming. However, the VFM is based on the assumption of constant stiffness matrix terms and its generalisation to the characterisation of the non-linear material behaviour is anything but trivial.

1.2.2 Identification of the parameters tuning the viscoelastic behaviour

Composite materials are characterised by a dynamical behaviour that is strongly affected by damping [102]. Accordingly, a proper characterisation of the damping capability of the material, at each relevant scale, is a challenging task [28]. This problem is more difficult than that of the elastic properties characterisation essentially because of the non-linear nature of the viscoelastic behaviour of the matrix, in terms of time response, which influences the damping capability of the composite at all characteristic scales.

From an experimental point of view, two methods are commonly used: the direct method and the indirect one. On the one hand, the direct techniques are based on the measurement of the dissipated energy per load cycle, which can be evaluated from the area of an hysteresis loop [29]. On the other hand, the indirect methods allow estimating the dissipated energy from the analysis of the spectrum response: free vibration-decay, resonant-dwell, bandwidth and impedance methods are some of the experimental techniques used for damping characterisation [30].

As stated above, the damping capability of the composite at the macroscopic scale can be directly related to the viscoelastic properties of its microscopic constituents [103, 104]. Nowadays, the so-called Dynamical Mechanical Analysis (DMA) [105–107] represents an useful method to characterise the material properties of reinforced polymers in terms of thermal, elastic and viscoelastic behaviours [108].

The DMA test is performed by applying harmonic loads to the specimen. By measuring the sample response, it is possible to compute an apparent modulus that can be used to estimate the viscoelastic material parameters of the specimen. In the case of a

composite multilayer plate wherein the lamina has an isotropic transverse behaviour [28], the identification process has to be carried out three different times, e.g. by considering a symmetric angle-ply stack, to determine the longitudinal and transversal Young's moduli as well as the in-plane shear modulus. In particular, the ply orientation θ must be set equal to 0°, 90° and 45° respectively, to determine the longitudinal E_L, transversal E_T and shear G_{LT} moduli. In this way, it is possible to compute an apparent modulus E_x, that can be used to estimate the viscoelastic behaviour of the specimen, as

$$\frac{1}{E_x} = \frac{1}{E_L} \cdot cos^4(\theta) + \left(\frac{1}{G_{LT}} - \frac{2 \cdot \nu_{LT}}{E_L} \right) \cdot sin^2(\theta) \cdot cos^2(\theta) + \frac{1}{E_T} \cdot sin^4(\theta). \tag{1.4}$$

Unfortunately, when high modulus composite materials are investigated, the DMA technique provides less accurate results [108] compared to the ASTM three-points bending test [17]. Indeed, the DMA test provides an apparent modulus giving only an average approximation of the plate flexural stiffness which group both structural and material aspects. However, the DMA test does not allow to extract information about microscopic properties.

From the engineer's viewpoint it is more interesting to look for those tests which allow identifying material properties at all relevant scales and which are not limited by the size of the composite sample or by the geometrical and material properties of the constitutive phases composing it. The formulation of a suitable inverse problem for material properties characterisation is a widely studied topic in the literature [109–111]. In this background, Barkanov *et al.* [112] proposed an inverse technique based on modal analysis and on the response surface method to characterise the nonlinear behaviour of the viscoelastic core layer in sandwich panels. Elkhaldi *et al.* [113] worked on the viscoelastic parameters identification for a sandwich panel where a generalised Maxwell model is considered and a gradient-based algorithm is used to solve the associated inverse problem. Cortés *et al.* [114] developed an identification strategy to characterise the parameters of the fractional derivative model representing the viscoelastic behaviour of a sandwich beam. In all these works the goal is the minimisation of the error between the predicted Frequency Response Function (FRF) and the measured one. Ledi *et al.* [115] proposed an identification method for frequency-dependent material properties of viscoelastic sandwich beams able to take into account for the behaviour of the interface between layers.

As it can be inferred from the aforementioned works, the damping capability related to the viscoelastic behaviour of the constitutive phases (mostly that of the matrix) can be characterised by exploiting the information restrained in the dynamic response of the structure. The strategy presented in Chapter 4 follows this trend and represent a generalisation of the above works by extending the identification procedure to the lower scale, i.e. to the viscoelastic behaviour of the constitutive phases.

As far as the numerical implementation of the viscoelastic behaviour, different material laws are available and in the literature. A common approach is to enrich the existent models with more parameters. Classical linear viscoelastic material models are: (a) the Maxwell's model, (b) the Kelvin-Voigt model, (c) the Maxwell-Kelvin model, (d) the power law, (e) the Prony's series and, finally, the generalised Kelvin model [116].

The Maxwell's model yields totally unrecoverable viscous flow plus recoverable elastic deformation

$$\dot{\varepsilon}(t) = \frac{\sigma(t)}{\tau E_0} + \frac{\dot{\sigma}(t)}{E_0}, \tag{1.5}$$

where τ is the time constant of the material and E_0 the Young's modulus.

A Kelvin-Voigt yields totally recoverable deformation with no unrecoverable viscous flow

$$\sigma(t) = \tau E_0 \dot{\varepsilon}(t) + E_0 \varepsilon(t), \tag{1.6}$$

where the deformation does not recover instantaneously.

The Maxwell-Kelvin model is a four-parameter model, where Maxwell and Kelvin models are placed in series and the resulting compliance $D(t)$ reads

$$D(t) = \frac{1}{E_1} + \frac{t}{\tau_1 E_1} + \frac{1}{E_2}\left[1 - exp\left(-\frac{t}{\tau_2}\right)\right], \tag{1.7}$$

where the first index is related to the Maxwell's model parameters and the second index concerns the Kelvin-Voigt model parameters.

The short-term deformation of polymers can be described with the power law, in which the stiffness can be represented as

$$E(t) = At^{-n}, \tag{1.8}$$

where the parameters A and n are adjusted with experimental data.

Although the short-term creep and relaxation of polymers can be well-described by the power law, as the time becomes longer, a more refined model becomes necessary. The Prony's series allows describing the required long-term behaviour, in terms of stiffness:

$$E(t) = E_{\text{inf}} + \sum_{i=1}^{n} E_i \mathrm{e}^{-\frac{t}{\tau_i}}, \tag{1.9}$$

where τ_i are the relaxation times, E_i the relaxation moduli and E_{inf} the static Young's modulus.

However, the choice to increase the number of parameters into the viscoelastic law leads to a drastically increase of the computational time, as described in [117]. The implementation of more efficient material laws is, thus, of paramount importance and the fractional derivative approach could represent a sound alternative, as outlined in [29]. In particular, from the experimental point of view, it is observed that the stress is proportional to the fractional derivative of order α (fractional exponent):

$$\sigma(t) = \frac{G}{\Gamma(1-\alpha)} \int_0^t \frac{\dot{\varepsilon}}{(t-\tau)^{\alpha}} d\tau = G D_0^{\alpha}(t), \tag{1.10}$$

where $D_0^{\alpha}(t)$ is the fractional derivative operatore relative to the Riemann-Liouville formulation, $0 \leq \alpha \leq 1$ and $G \in \Re_+^*$. It is noteworthy that the elastic behaviour is reached when $\alpha = 0$ (Hooke's law) and, on the other hand, the visco-anelastic law is obtained with $\alpha = 1$ (Newton's law).

The physical meaning of the fractional-derivative model has been shown with the molecular model of Rouse [118], for dilute solutions of polymers. A polymer molecule is composed by chains of atoms in which the relative forces are modelled with springs. Moreover, the polymer molecules are surrounded by a Newtonian fluid at temperature T: every polymer molecule shows a velocity composed by the fluid speed and the velocity due to the relative motion between different molecules. By following the proposed Rouse's

model, it is possible to find a relationship between stress and strain rate, defined by a fractional derivative model, in the time domain:

$$\sigma(t) = \nu_s \varepsilon(\dot{t}) + \left[\frac{3}{2}(\nu_0 - \nu_s) nkT\right]^{1/2} D^{1/2}\varepsilon(t), \tag{1.11}$$

where ν_s and ν_0 are the polymer and the fluid viscosity, respectively, T is the temperature, n the number of molecular chains and k the Boltzmann's constant. Therefore, it is possible to consider that the numerical implementation of a fractional-derivative law is physically justified from a molecular model.

This model is able to well describe the viscoelastic behaviour of composites, which is history-dependent. As described in [29], a significant number of fractional-derivative viscoelastic models have been developed to describe the mechanical response of eterogeneous materials such as elastomers and polymers [119, 120]. Indeed, classical rheological models previously introduced can be written in terms of fractional derivatives: the Kelvin-Voigt [121], Maxwell [122] and Zener [123, 124] to obtain creep and relaxation functions. Rabotnov *et al.* developed an hereditary theory representing a generalised fractional-derivative rheological model [125]. The Rabotnov's theory is widely used to describe the behaviour of the polymers, metals and concrete. Bagley and Torvik derived the fractional-derivative law in the frequency domain to describe the behaviour of polymers and elastomers [126].

Some examples of application of this model can be found in the literature: Krasnobrizha*et al.* [117] proposed a model to describe the hysteresis behaviour of woven composite using a collaborative elastoplastic damage model, based on fractional derivatives; Meral *et al.* [127] used the fractional-derivative model to describe the viscoelastic behaviour of soft biological tissues; Fukunaga *et al.* [128] applied the fractional-derivative operator to describe the behaviour of viscoelastic materials under large strain.

1.2.3 Identification of the composite behaviour under uncertainty

As outlined in [31], the uncertainties can be classified in three main categories: aleatory (variability of structural parameters), epistemic (lack of adequate information about the system) and prejudicial (absence of stochastic characterisation of the structural system). Composite structures are affected by the three forms of uncertainty and the characterisation of the parameters tuning the variability law becomes of prime importance.

A lot of efforts has been put in the development of robust identification methods in presence of noise. Regarding the identification procedures available in the literature, various methods have been developed over the last decades [101]. Some of them explicitly require full-field measurements to be available [129]. The FEMU was the first proposition [130–132]. Least squares errors were considered with no special emphasis on their weighting. Other types of gaps were introduced. In elasticity, different variational principles were considered [100, 133]. The constitutive equation error, which was initially introduced for the verification of numerical models [134], was also used for identification purposes [135–137]. The reciprocity gap [98, 138, 139] considers only surface measurements to determine various types of defects in the bulk material of the analysed domain. Non-iterative methods such as the VFM [140] and the equilibrium gap method [141–145] were introduced to calibrate elastic parameters and damage models.

In the majority of aforelentioned studies, the uncertainty characterising the measurement was not explicitly accounted for. Optimal extractors, namely, the least sensitive to measurement uncertainties were introduced for the choice of virtual fields [146], the estimation of fracture mechanics parameters [147], or the identifiability of load and contrast fields in micro-cantilevers [148]. Specific weighting based on global Digital Imagine Correlation (DIC) uncertainty was also proposed for the identification of elastic properties [149]. Roux and Hild [150] extended this optimality feature by analysing each of the aforementioned identification methods in view of their sensitivity to measurement uncertainty and by formulating an optimal criterion. In particular, an unified framework was proposed to recast the identification procedures described above. The main difference is the metric used to measure the distance between measured and computed displacement fields. In this unified framework, the spectral sensitivity of all these identification methods has been assessed and a comparison between the sensitivity of all these methods to measurement uncertainty has been performed. In [150], the optimality of the identification is defined as its least sensitivity to measurement noise. It was proven that the metric based on the inverse covariance matrix of the measured displacements minimises the Mahalanobis distance: it corresponds to weighted FEMU.

Moreover, Roux and Hild observed that the constitutive law could be relaxed to better account for the measured data [151]: in this way, the identification appears as a compromise between a constitutive law describing a material and noise corrupting the measurements.

The previously described identification procedures consider, however, only the effects of noise on the characterisation process.

Composites are multi-phase, heterogeneous materials that can be tailored to obtain the required engineering properties offering, thus, many unique advantages in terms of mechanical properties, compared to conventional materials. However, the manufacture of composites involves complex processes, which are often difficult to control, thus potentially leading to a considerable scatter in their mechanical properties; this distinguishes composites from other common engineering materials [152]. Uncertainty in the performance of composite structures can be broadly addressed through material, geometric and structural considerations [153–155].

The influence of the manufacturing process on the composite material property uncertainty is multi-faceted and is often not traced explicitly. The material properties variability is significantly influenced by the relative amounts of the constituent elements (fibres and matrix), i.e. fibre volume fraction, rich resin regions, lack of appropriate curing, porosity of the matrix, alignment of fibres, adequate bonding between fibres and matrix, temperature effects, etc. [156–160]. Yushanov and Bogdanovich [161] highlighted that uncertainty in fibre curvature and layer arrangement, associated with manufacturing processes such as thermal treatment, filament winding, braiding, etc. are also important in estimating the appropriate material properties. The uncertainty in these parameters propagates to the macroscopic scale and translates into the variability of stiffness and strength properties affecting the overall structural response. All the above factors complicate the definition and quantification of uncertainty in design and assessment of such structures.

Uncertainty at the assembly level is associated with different joining techniques, joint types and machining aspects. Furthermore, the interaction between tooling and composite lay-up processes may contribute to geometrical variability [156, 160]. For example, if the laminate is cured at high temperature, then the tooling and lay-up might have different

thermal coefficients of expansion resulting in residual stresses and distortions [158]. Finally, the inherent random nature of various load types and classes, environmental factors such as temperature variation and permeability, and the imperfections and misalignments arising from boundary conditions further contribute to the nature and level of uncertainty which needs to be accounted for in modelling and predicting the response of composite structures.

Experimental methods that are commonly used to characterise the uncertainty require a huge number of standard ASTM tests, which are really expensive [32]. Moreover, these tests are only suited to evaluate mesoscopic uncertainties, in terms of material and geometrical properties of the lamina without providing any information about the variability characterising the properties of the constitutive phases at the microscopic scale.

In order to get statistical representative results, the aforementioned tests must be performed a huge number of times. Of course, this implies significant costs (and time) and the variability results (e.g. mean and standard deviation of material properties) are strongly affected by the (human) errors introduced to carry out the experimental campaign, especially for those tests conducted at the microscopic scale. To this purpose, Sepahvand *et al.* developed the inverse stochastic method based on the general polynomial chaos (gPC) [162–168] to identify uncertain lamina elastic parameters from experimental modal data. Further examples of probabilistic methods are the parametric probabilistic approach [33] and the Bayesian inference techniques wherein all information are included into a prior distribution model [34–37]. However, in the case of composite structures, the uncertainty affecting the ply elastic behaviour is strictly related to the variability of the elastic properties of the constitutive phases. To the best of the author's knowledge, the aforementioned probabilistic techniques have never been extended to the identification of the variability parameters characterising the elastic properties of the microscopic constituents of the composite.

Concerning the state-of-the-art of the approaches combining optimisation and uncertainty, three specific research areas can be identified in the literature, as outlined in [169]: reliability-based optimisation (RBO), robust design optimisation (RDO) and model updating. The RBO technique concerns the solution of an optimisation problem in which the main goal is to design for safety by considering extreme events: common objective functions are defined by the structural weight and the constraints are both deterministic and probabilistic (e.g. probability of failure of the structure) [170–173]. The RDO method is usually implemented in order to minimise the influence of stochastic variations on the mean design [174]. Finally, the typical goal of the model updating technique is to reduce the differences between model prediction and data from tests [132, 175]. In this context, the MSIS proposed in this thesis and presented in Chapter 5 (in a slightly different formulation to deal with uncertainty) can be considered as a model updating technique that allows identifying the elastic properties of the composite (and the related uncertainty) at each scale. This information can be later used in the framework of both RBO and RDO approaches.

1.3 Conclusions

This bibliographic study has highlighted peculiarities of the (multi-scale) characterisation of the composite material behaviour. Composite materials show a complex behaviour, that is manly due to their inherently heterogeneous nature at the microscopic scale: the constitutive phases are the main responsible for the anisotropic behaviour at the upper

scales (i.e. ply-level and laminate-level). In this context, the characterisation of the material properties, at each pertinent scale, is of paramount importance in order to correctly predict the macroscopic response of the composite.

In particular, this thesis is focused on the development of a general MSIS well-suited for the characterisation of both the elastic and the viscoelastic behaviours of the composite, eventually in presence of uncertainty, at each pertinent scale, starting from non-destructive tests. Regarding the characterisation of the elastic properties, standard and non-standard tests are commonly used in the literature, but they are not able to provide the full-set of 3D elastic properties. Moreover, VFM and the FEMU techniques have recently been developed to identify the 3D set of elastic properties of the elementary ply. However, all these techniques and methods have never been generalised to characterise the elastic behaviour of the microscopic constituents with non-destructive tests.

As far as the viscoelastic behaviour of the composite is concerned, three main techniques are available in the literature: the estimation of the dissipated energy through the evaluation of the hysteresis loop; the DMA test, that is able to identify only the mesoscopic properties of a particular specimen; the solution of an inverse problem based on the experimental dynamic response of the specimen, which has been investigated only for sandwich composite plates (by considering a simple isotropic viscoelasticity behaviour for the elastomeric layer).

As far as the identification of the parameters describing the variability of the elastic properties is concerned, three approaches are proposed in the literature to overcome the main restrictions affecting both standard and non-standard (destructive) tests, which are expensive and that produce non-reliable results at the microscopic scale. In particular, they are: (a) the inverse stochastic method (based on the general polynomial chaos and on the macroscopic modal data), (b) the parametric probabilistic approach and (c) the Bayesian inference technique. Although their interesting features and the great potential behind each method, these techniques have never been generalised to the identification of the uncertainty of the microscopic material properties starting from non-destructive macroscopic tests.

Starting from the analysis of the advantages and shortcomings characterising each of the aforementioned techniques, three different declinations of the developed MSIS will be presented in Chapters 3, 4 and 5 in order to give a contribution in the field of inverse problems applied to the identification of the composite material behaviour.

Chapter 2

Optimisation Methods and Algorithms

2.1 Introduction

Optimisation methods and algorithms have been attracted the interest of researchers and companies from several decades. Often, the word "optimisation" is excessively and improperly used in different contexts. In this Chapter, the general features of optimisation are discussed and the word "optimisation" is intended in the sense of mathematical programming.
The Chapter is split into two main parts. The first one introduces a brief literature survey on optimisation methods, both deterministic algorithms and meta-heuristics. The second part presents the special genetic algorithm used in this work.
The Chapter is structured as follows. In Section 2.2 a possible classification of optimisation methods is given. In Section 2.3 the main features of deterministic algorithms used to solve constrained non-linear programming problems are briefly recalled. Section 2.4 focuses on the generalities of meta-heuristics and, in a second time, on genetic algorithms (GAs). Section 2.5 briefly recalls the main features of the original GA used in this thesis initially presented [1], while Section 2.6 presents the last version of the general, multi-purpose GA presented in [176]. Finally, Section 2.7 ends the Chapter with some conclusions and perspectives.

2.2 Classification of optimisation methods

Roughly speaking, *optimisation* can be defined as the selection of the best element (according to a given criterion) from a set of available alternatives [177]. Before proceeding with the discussion, some main concepts must be introduced.

The aim of optimisation is to minimise an assigned *objective function* (or *cost function*) f depending on several (sometime a huge amount of) parameters. Those parameters that cannot be set to a constant value are called *optimisation variables* or *design variables*. Design variables are usually collected in the array $\mathbf{x} \in \mathbb{R}^n$ and constitute the unknowns of the optimisation problem, so the dependence of f on $\mathbf{x}$ is made clearer by the notation $f(\mathbf{x})$.

In practical engineering applications, an optimisation problem is usually subject to m_e *equality constraints*, in the form of $h_i(\mathbf{x}) = 0$, $i = 1, ..., m_e$, and/or m_i *inequality*

constraints, in the form $g_j(\mathbf{x}) \leq 0$, $j = 1, ..., m_i$. Optimisation constraints formalise some physical or technological requirements, depending on the problem at hand. A point $\mathbf{x}^*$ meeting the set of constraints is called *feasible*. The choice of the mathematical form of the objective/constraints functions and of the design variables set is called *modelling*.

From a mathematical viewpoint, the optimisation problem is classically stated in the form of a constrained minimisation problem as follows:

$$\begin{aligned} &\min_{\mathbf{x}} \quad f(\mathbf{x}), \\ &\text{subject to:} \\ &\begin{cases} g_i(\mathbf{x}) \leq 0, \ i = 1, \ldots, m_i, \\ h_j(\mathbf{x}) = 0, \ j = 1, \ldots, m_e, \\ \mathbf{x}_{\text{LB}} \leq \mathbf{x} \leq \mathbf{x}_{\text{UB}}. \end{cases} \end{aligned} \tag{2.1}$$

In Eq. (2.1), $\mathbf{x}_{\text{LB}}$ and $\mathbf{x}_{\text{UB}}$ are the lower and upper bounds on the design variables, respectively. Problem (2.1) is conventionally referred as a *Constrained Non-Linear Programming Problem* (CNLPP).

Usually, the solution of problem (2.1) cannot be derived in a closed form (apart some very special cases) and a suitable optimisation algorithm must be used in order to carry out the solution search. The choice of the optimisation algorithm is influenced by several factors:

- the nature of design variables;
- the presence of constraint functions;
- the nature of both objective and constraint functions, i.e. continuity, convexity, linearity, etc.

Accordingly, optimisation algorithms can be classified by taking into account the previous criteria: a possible classification, taken from [178], is proposed in Fig. 2.1.

The first classification criterion is the presence of optimisation constraints. Although engineering problems often involve several constraints, unconstrained optimisation theory is fundamental because constrained problems are typically solved by reducing them to equivalent unconstrained ones.

The second criterion focuses on the linearity: if objective and constraints functions are linear functions of the design variables $\mathbf{x}$, then the optimisation problem is linear. Linear Programming constitutes an important branch of optimisation methods. The peculiarity of linear programming problems is that the only information exploited by the algorithm is related, at most, to the gradient of objective/constraint functions (in fact, the Hessian matrix is identically null).

The third criterion is related to the convexity. Convexity is extremely important in optimisation problems because it brings information about the nature of the optimum solution that the algorithm is searching for. The notion of convexity applies to both sets and functions. An optimisation problem is *convex* if the following conditions are met:

- the objective function is convex;
- the equality constraint functions are linear;

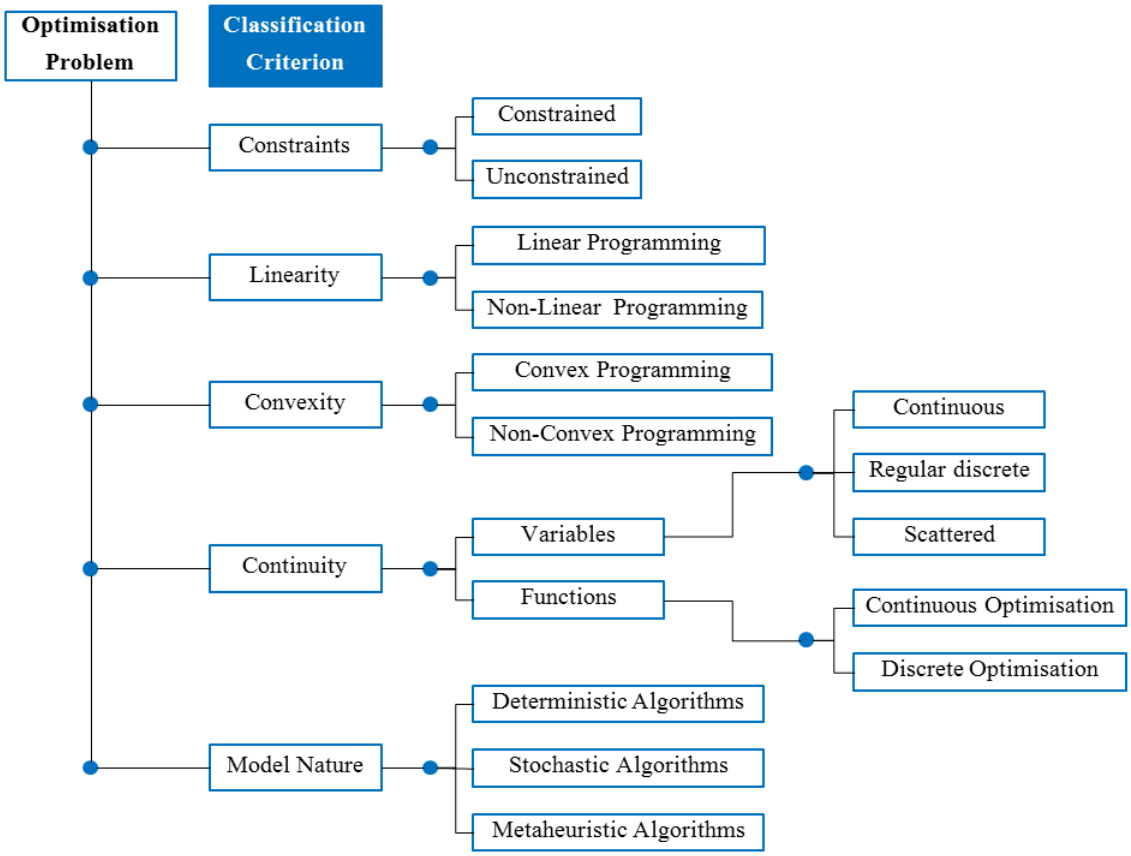

Figure 2.1 – Classification of optimisation algorithms.

- the inequality constraint functions are convex (i.e. $g_j(\mathbf{x})$ is convex $\forall j = 1, ..., m_i$).

A point $\mathbf{x}^*$ is a *global minimiser* if $f(\mathbf{x}^*) \leq f(\mathbf{x})$ for all $\mathbf{x}$ in the feasible domain. Accordingly, $f(\mathbf{x}^*)$ is the global minimum (also called global optimum or global solution). Alternatively, if $f(\mathbf{x}^*) \leq f(\mathbf{x})$ only in a neighbourhood of $\mathbf{x}^*$, $\mathbf{x}^*$ is called *local minimiser* and $f(\mathbf{x}^*)$ is the local minimum (or local optimum or local solution). It can be shown that, when f is convex, any local minimiser is a global minimiser and, if f is also differentiable, then any stationary point $\mathbf{x}^*$ is a global minimiser [178]. On the other hand, it is noteworthy that almost all real-world engineering problems are intrinsically non-convex. Therefore, it is not surprising that searching the global solution is prohibitive for several problems from a computational viewpoint.

Another criterion for classifying optimisation algorithms is related to the continuity. An optimisation problem is continuous only when objective/constraint functions are continuous and, meanwhile, the set of design variables is continuous in $\mathbb{R}^n$ (or, at least, in a subset of $\mathbb{R}^n$). The discontinuous nature of a problem can come from either functions or the variables set. If the variables are discrete (regularly or scattered, i.e. without a fixed step length), suitable algorithms should be employed to solve the related optimisation problem.

Finally, the information available about the model is important to determine which algorithm is the most suited for solving the optimisation problem. When the model is completely known and the optimisation variables as well as objective and constraint functions are continuous, deterministic algorithms are the best choice. However, it could happen that some quantities are characterised by uncertainty. In this case, stochastic

algorithms are the most suited. A special class of algorithms, deserving a particular attention, is referred as *meta-heuristics* [179]. The main feature of these algorithms is the insertion of a random component to perform the solution search. The randomness allows for an efficient exploration of the computational domain and, therefore, meta-heuristics are particularly recommended in case of non-convex optimisation problems. Moreover, meta-heuristics are the only possible solution when the optimisation problem is characterised by discontinuous design variables and/or objective/constraint functions. Nevertheless, an exhaustive overview on all the variants of optimisation algorithms is out of the scopes of this work.

The inverse problems faced in this thesis are non-convex. To deal with this kind of problems, both deterministic and meta-heuristic algorithms have been used, constituting, hence, a hybrid strategy. In the following sections, some basic information about the adopted deterministic and meta-heuristics algorithms are given.

2.3 Deterministic Methods for CNLPP

2.3.1 Generalities on Deterministic Methods

Deterministic methods exploit the information provided by the model to update the design variables array from $\mathbf{x}_k$ to $\mathbf{x}_{k+1}$, where the subscrpit k denotes the current iteration. Deterministic algorithms constitute a well-established research field in the literature (refer, for instance, to [180] and [59]). In the following, the expression "deterministic" and "gradient-based" can be confused: this means that the basic information for updating the design variables relies on the knowledge of the gradient (of both objective and constraint functions).

Before discussing the main features of constrained optimisation, a brief recall of the fundamentals of unconstrained optimisation is needed. When dealing with unconstrained optimisation, there are essentially two families of strategies for generating the iterate $\mathbf{x}_k$: *line search* methods and *trust region* methods [178].

- *Line search methods.* Firstly a suitable *descent direction* direction $\mathbf{p}_k$ is chosen for the objective function f. Secondly, the following mono-dimensional optimisation problem is solved

$$\min_{s>0} \; f(\mathbf{x}_k + s\mathbf{p}_k) \tag{2.2}$$

  in order to determine a suitable *step length* s. The algorithms available in the literature mainly differ because of the different choice of the descent direction and also for the strategy to update the step length s.
  Regarding the descent direction, four different choices are available: the steepest descent direction $\mathbf{p}_k = -\nabla f(\mathbf{x}_k)$ (i.e. the anti-gradient), the Newton direction $\mathbf{p}_k = -\left[\nabla^2 f(\mathbf{x}_k)\right]^{-1} \nabla f(\mathbf{x}_k)$ (needing the computation of the second derivatives of the function at each iteration), the quasi-Newton iteration $\mathbf{p}_k = -\mathbf{B}_k^{-1}\nabla f(\mathbf{x}_k)$ (where the matrix $\mathbf{B}_k$ is a suitable approximation of the Hessian matrix) and the conjugate direction. As far as the calculation of the step length is concerned, several algorithms/methods are available in literature: the Armijo's algorithm, the cubic interpolation method, the golden section search method, etc. The interested reader is adressedd to [178] for a deeper insight into the matter.

- *Trust-region methods.* In trust-region methods, firstly the *ball radius* (or *trust-region radius*), Δ_k, is chosen, then the search direction is calculated. Since the search direction is unknown at the beginning of the iteration, it is preferable to talk about ball radius instead of step length. A quadratic approximation of the original problem is solved within the trust region, in order to determine the following iterate. Provided a suitable technique for updating Δ_k during iterations, the possibilities for the search direction are the same as the aforementioned line search algorithms (except for the conjugate gradient method, that has not an equivalent formulation in the trust region framework). An important remark concerning trust-region algorithms is their sensitivity to poorly scaled models. A model is poorly scaled when the sensitivity of the objective function with respect to the design variables can significantly vary. Line search algorithms are, in general, more robust than trust-region methods and they can intrinsically guarantee for *invariance*, i.e. non-sensitivity to poorly scaled models.

As stated above, algorithms developed for unconstrained optimisation are of paramount importance because, with minor modifications, they can be used to solve the CNLPP, which is often transformed into an equivalent unconstrained problem [178].

2.3.2 Optimality Conditions for CNLPP

In the following, the two basic theorems for constrained optimisation are recalled. Given a CNLPP in the form of Eq. (2.1), the functional L, also called Lagrangian of problem (2.1), can be defined as:

$$L(\mathbf{x}, \boldsymbol{\lambda}, \boldsymbol{\mu}) = f(\mathbf{x}) + \boldsymbol{\lambda}^{\boldsymbol{T}}\mathbf{g}(\mathbf{x}) + \boldsymbol{\mu}^{\boldsymbol{T}}\mathbf{h}(\mathbf{x}), \tag{2.3}$$

where $\boldsymbol{\lambda}$ and $\boldsymbol{\mu}$ are the arrays of Lagrange multipliers for inequality constraints ($\lambda_i \geq 0,\ \forall i = 1, ..., m_i$) and equality constraints ($\mu_j,\ \forall j = 1, ..., m_e$), respectively.

Theorem 2.3.1 ***First-order necessary conditions.***
Assume that

1. $\mathbf{x}^*$ *is a local solution of problem (2.1);*
2. *the functions f, g_i and h_j are continuously differentiable;*
3. *the LICQ (Linear Independence Constraint Qualification) condition holds at $\mathbf{x}^*$, i.e. the gradient of each equality and inequality constraint function must be linearly independent.*

Then, two Lagrange multipliers arrays $\boldsymbol{\lambda}^* \geq \mathbf{0}$ and $\boldsymbol{\mu}^*$ exist and the following conditions, known as Karush-Kuhn-Tucker (KKT) conditions, are met:

$$\begin{cases} \nabla_x L(\mathbf{x}^*, \boldsymbol{\lambda}^*, \boldsymbol{\mu}^*) = \mathbf{0}, \\ \lambda_i^* g_i(\mathbf{x}^*) = 0,\ \forall i = 1, \ldots, m_i, \\ h_j(\mathbf{x}^*) = 0,\ \forall j = 1, \ldots, m_e. \end{cases} \tag{2.4}$$

In Eq. (2.4), ∇_x is the gradient operator with respect to the design variables $\mathbf{x}$. The point $(\mathbf{x}^*, \boldsymbol{\lambda}^*, \boldsymbol{\mu}^*)$ is named KKT point.

Theorem 2.3.2 ***Second-order sufficient conditions.***
Let the functions f, g_i and h_j be twice continuously differentiable. Suppose $(\mathbf{x}^*, \boldsymbol{\lambda}^*, \boldsymbol{\mu}^*)$ is a KKT point and suppose the Hessian of the Lagrangian $\nabla^2 L(\mathbf{x}^*, \boldsymbol{\lambda}^*, \boldsymbol{\mu}^*)$ is positive definite. Then $\mathbf{x}^*$ is a strict local solution of problem (2.1).

For the proof of the aforementioned theorems, the reader is addressed to [59,178,180].

2.3.3 Deterministic algorithms for CNLPPs

The deterministic algorithms used in this manuscript rely on the well-known *fmincon* optimisation toolbox implemented into the MATLAB package [181]. For the sake of brevity, in this Section only the Sequential Quadratic Programming (SQP) and the Active Set (AS) algorithms are discussed.

SQP and AS algorithms can be presented together. Indeed, AS is just a particular SQP method wherein constraints are handled in a more effective way. Therefore, the main steps described here below are shared by both SQP and AS methods.
The main idea behind the SQP method is to approximate the CNLPP at hand in a sequence of Quadratic Programming (QP) problems. The conditions to be met for a QP problem are:

- the objective function f is a *quadratic function* of the design variables;
- equality (h_j) and inequality (g_i) constraints are *linear functions* of the design variables.

A solution can always be provided by using QP techniques or, at least, it can be proven that the solution does not exist. The shortcoming of such a method is related to the computational burden which depends on nature of both the objective function and the constraint ones and on the number of optimisation constraints, as well. An extensive amount of books and articles on this topic can be found in the literature [178,182,183].

A general overview of the SQP algorithm is given in Fig. 2.2. Once the CNLPP has been stated in the form of Eq. (2.1), a suitable initial guess should be provided. The Lagrange multipliers are initialised and the iteration index k is set to 0. Then, the Lagrangian functional is evaluated through Eq. (2.3). The gradients of objective and constraint functions are needed for the following steps: they can be analytically provided or numerically evaluated (e.g. through a finite-difference scheme). Hence, the Hessian matrix of the Lagrangian is approximated (through a suitable formula) to be used, together with the previously computed gradients, to set up the local QP subproblem:

$$\begin{aligned} \min_{\mathbf{d}} \;\; Q_k(\mathbf{d}) = \min_{\mathbf{d}} \;\; & \frac{1}{2}\mathbf{d}^T \mathbf{H}^{\mathbf{BFGS}}{}_k \mathbf{d} + \nabla f_k^T \mathbf{d}, \\ & \text{subject to:} \\ & \overline{\mathbf{A}}_k \mathbf{d} \leq \mathbf{b}_k. \end{aligned} \tag{2.5}$$

In Eq. (2.5), the Hessian matrix $\mathbf{H}$ has been approximated by means of the *BFGS* formula [178]. $\mathbf{d}$ is the array of design variables for the subproblem and represents the search direction for the k-th iteration of the SQP algorithm. It is noteworthy that, being subproblem (2.5) a QP problem, optimisation constraints should be in linearised form. Therefore, the optimisation constraints of the original problem (2.1) are linearised, as

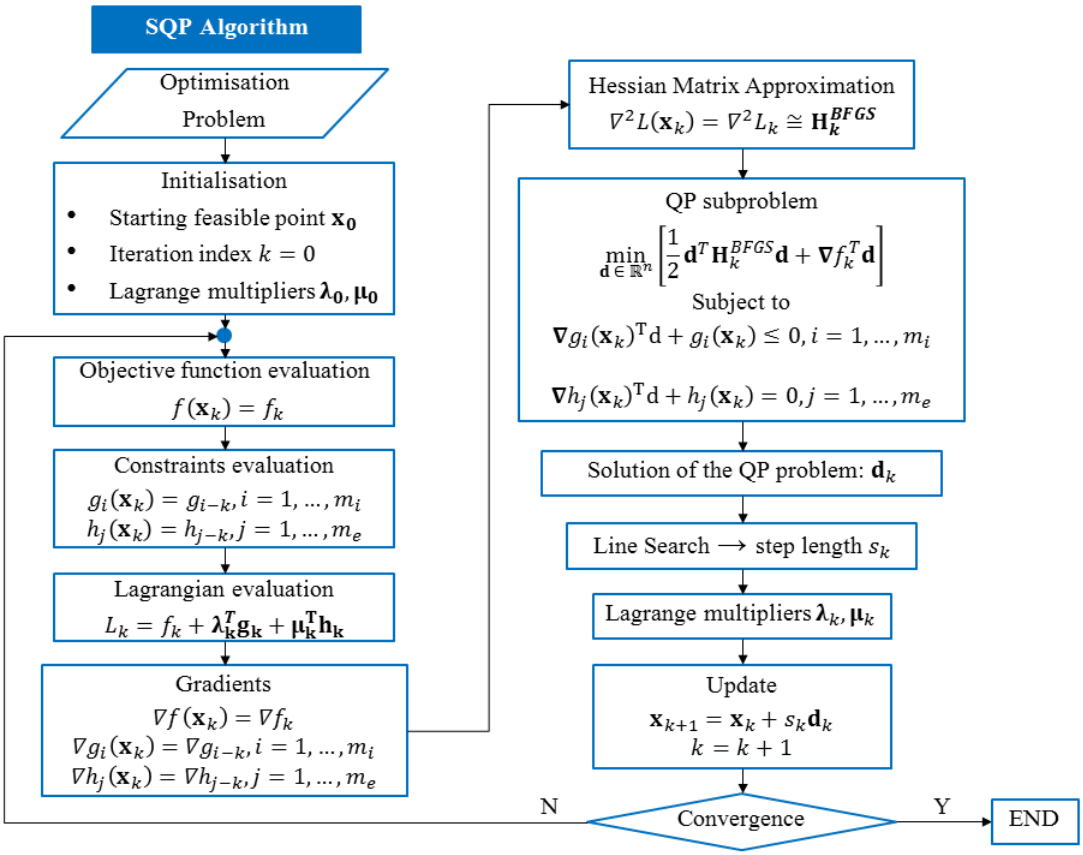

Figure 2.2 – Overview of the SQP algorithm.

shown in Fig. 2.2, and their gradients are collected in the matrix $\overline{\mathbf{A}}_k$. Without going into details, the assembly technique implemented to get matrix $\overline{\mathbf{A}}_k$ constitutes the main difference between SQP and AS methods. More precisely, for AS algorithm only those inequality constraints that are violated give a contribution to the matrix $\overline{\mathbf{A}}_k$ (equality constraints are always included). Analogously, the coefficients of the constraints first-order approximation are collected into the array $\mathbf{b}_k$. The QP subproblem (2.5) is solved thanks to standard techniques [178]. For AS method, some internal iterations could be needed to check if the active-set of optimisation constraints has been correctly evaluated and, eventually, the matrix $\overline{\mathbf{A}}_k$ is updated.
As previously remarked, the solution is the descent direction $\mathbf{d}_k$ along wich the correct step s_k must be computed. At the end of this phase, Lagrange multipliers are updated and, finally, the new iterate $\mathbf{x}_{k+1}$ can be evaluated. Different stopping criteria are considered for SQP/AS algorithms [181]:

- *Maximum number of iterations:* $k + 1 = K_{max}$;
- *Small Objective function improvement:* $|f(\mathbf{x}_{k+1}) - f(\mathbf{x}_k)| < \sigma_f$, with $0 < \sigma_f << 1$;
- *Negligible change of variables values:* $|\mathbf{x}_{k+1} - \mathbf{x}_k| < \sigma_x$, with $0 < \sigma_x << 1$;
- *Norm of the Lagrange function gradient close to* 0: $||\nabla L(\mathbf{x}_{k+1})|| < \sigma_\nabla$, with $0 < \sigma_\nabla << 1$.

If one among these convergence criteria is met, the algorithms stops. Of course, the latter set of criteria makes sense only if the objective function and the imposed constraints

are dimensionless. For a deeper insight into SQP algorithms, the reader is addressed to [178, 181].
When compared to the SQP method, the AS algorithm can tolerate some iterations outside the feasible region in solving constrained optimisation problems. This fact allows for an efficient exploration of the feasible domain (especially its boundary) in CNLPPs.

2.4 Meta-heuristics for CNLPPs

2.4.1 Generalities on Meta-heuristics

Meta-heuristics can be defined as "global" optimisation methods for non-convex CNLPPs making use of several empirical rules, which are inspired by a precise natural phenomenon. The word "global" must be interpreted in the sense that a meta-heuristic allows for a better exploration of the domain if compared to deterministic methods, because it acts on a population of points within the design domain rather than on a single point. However, a meta-heuristic *can* find only a pseudo-optimal solution (probably in the neighbourhood of the global optimum) but there is no guarantee to actually find it.
In the literature one can find several types of meta-heuristics. A short list is given here below.

- Evolution Algorithms (EAs) [184–186] are a particular class of algorithms that imitate the principles of natural evolution. The main EAs are:

  1. Fogel's Evolutionary Programming (FEP) [187] that is an exploring search technique within a space of finite-state machines;
  2. Glover's Scatter Search Algorithm (GSSA) [188] that, starting from an initial population of reference points, creates a new generation of offspring through weighted linear combinations;
  3. Genetic Algorithms (GAs) that have been initially introduced by Holland [189, 190] and which are based on both Natural Selection and genetics (GAs are presented in the next Section).

- Bacteriologic algorithms (BAs) [191] are inspired by evolutionary ecology and, more particularly, by bacteriologic adaptation.

- Gaussian or Natural Adaptation algorithms (NAAs) [192] rely on a certain theorem valid for all regions of acceptability and all Gaussian distributions: the NAAs efficiency is defined as information divided by the work needed to get the information [192]. Because the NAA maximises the average fitness rather than the fitness of the individual, the landscape is smoothed such that valleys between peaks may disappear.

An useful and common term often used for all the evolution-based systems cited beforehand is *Evolution Programs* (EPs).

The idea of evolution programming is not new and many researchers studied and dealt with this topic in the last sixty years. Several EPs have been conceived and developed for many different problems. However, despite EPs can be formulated to deal with a given problem, and even though they can differ for several features, all EPs share a common

principle: a population of individuals undergoes a certain number of transformations and, during this evolution, individuals "fight" to survive.

Among the methods based on *swarm intelligence* it is possible to include the following algorithms:

- the Ant Colony Optimisation (ACO) method [193] uses many ants (or agents) to explore the solution space and find locally productive areas;
- the Particle Swarm Optimisation (PSO) strategy [194] makes use of a population (swarm) of candidate solutions (particles) moving in the search space: the movement of the particles is influenced both by their own best-known position and swarm global best-known position;
- the Intelligent Water Drops (IWD) algorithm [195] is an optimisation algorithm inspired from natural water drops which change their environment to find the near-optimal or optimal path to their destination.

Other meta-heuristics, falling within the class of stochastic optimisation methods, are Simulated Annealing (SA) [196] and Tabu Search (TS) [197] algorithms.

Nevertheless, the aim of this Section is nor to discuss about the different features characterising each meta-heuristic, neither to discuss about any philosophical and/or conceptual difference between the various algorithms available in the literature. Rather, in the followings the attention is focused on a special class of EPs: the GAs.

2.4.2 Generalities on Genetic Algorithms

During the last sixty years, GAs have known an impressive development and have gained an increasing popularity. There is a huge literature on GAs: the interested reader is adressedd to the fundamental works of Holland [189], Goldberg [190], Michalewicz [186], Renders [198] and the independent contribution of Rechenberg [199].

GAs were introduced and studied for the first time by Holland and his co-workers and students, see [189, 190]. GAs are search algorithms based, on the one hand, on the Darwinian concept of the Natural Selection and, on the other hand, on genetics. In a certain sense, GAs make their own the concept of the *Survival of the Fittest* by using a pseudo-random exchange of information in order to create an exploration algorithm having some features of the Natural Selection. Moreover, GAs effectively (and smartly) handle the information obtained through the exploration of the domain in order to generate new and more efficient individuals which represent the result of the Natural Evolution.

GAs make use of a vocabulary taken from genetics. The *population* evolving along the generations is composed of *individuals* and each individual is composed of *chromosomes*. Chromosomes constitute the individual's *genotype*. Very often, in standard GAs, the individual has a genotype made of a single-chromosome, i.e. a *haploid* individual. Each chromosome is made of *genes* arranged in a linear succession: each gene controls the inheritance of a particular character and it is located in a precise position within the chromosome (such positions are called *loci*). For more details on *haploidy*, *diploidy*, *dominance* and other similar topics related to GAs, the reader is addressed to [190, 200].

In a standard GA, the information restrained in the individual's genotype is generally coded by means of an alphabet of cardinality $k = 2$ (i.e. standard GAs use a *binary* alphabet). Each genotype codes a particular *phenotype*, i.e. the physical expression of the

individual's genotype whose meaning is defined externally by the user. Therefore, each individual represents a potential solution for the problem at hand.
In organisms, the phenotype includes physical characteristics, like eyes color, hair color, etc., whilst in the framework of GAs the phenotype represents the set of all possible values (real, discrete, etc.) that the design variables can take.

The evolution of a population along the generations corresponds to a search through a space of potential solutions. This search requires a balance among two features: the exploration of the whole domain and the exploitation of the information related to the best solutions (i.e. best individuals) within this space [190].

2.4.3 The standard GA

According to [186, 190], a standard GA is characterised by the following five features:

1. a genetic representation of the potential solution to a given problem;
2. a strategy to create an initial population of potential solutions;
3. a cost function that plays the role of the environment (ranking solutions in terms of their *fitness*) together with a selection operator that chooses, according to a certain criterion, the individuals involved into the reproduction process;
4. genetic operators that alter the composition of the individuals (i.e. standard crossover and mutation operators);
5. parameters governing the behaviour of the GA (population size, crossover probability, mutation probability, etc.) to be set by the external user.

The general architecture of a standard GA is illustrated in Fig. 2.3

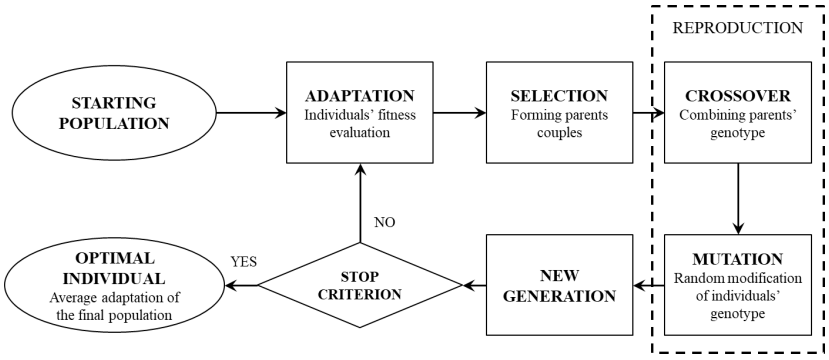

Figure 2.3 – General flowchart of a standard GA.

Adaptation and selection operators

As stated above, the starting population, composed of N_{ind} individuals, is randomly generated. Once the phenotype has been determined and translated into the genotype, objective and constraint functions can be evaluated (for all the individuals).

The role of the *adaptation operator* is to provide a unique measure of the individual's adaptation. In this phase, a suitable *fitness function* is defined. This is a scalar function that, depending on the value of both objective and constraint functions for the generic

individual, can vary in the range [0, 1], where 0 corresponds to the *worst* individual (within the current population), while 1 is assigned to the *best* one. The definition of the fitness function is not unique and several choices are possible [190].

The role of the *selection operator* is to form the $N_{ind}/2$ couples of parents for the reproduction phase on the basis of their fitness values. The basic concept is that the fitter individuals (i.e. individuals characterised by high values of the fitness function) have a high probability to be chosen for the reproduction phase. The selection criterion aims at mimicking this simple natural phenomenon: the most adapted individuals (with respect to the surrounding environment) will live longer than the less adapted ones, thus they have an increased probability to reproduce. In practice, the previously defined fitness function is employed to assign to each individual a probability of selection and, then, the effective selection is done through an *ad hoc* criterion.

An easy way to realise a selection operator consists of using a random process known as *roulette-wheel* selection. The roulette-wheel selection operator is built as follows: at each individual corresponds a portion of the wheel equal to the ratio of its fitness to the total fitness of the population. Generally speaking, the k-th individual occupies a portion of the wheel proportional to the ratio:

$$p_k = \frac{\mathrm{fit}_k}{\sum_{i=1}^{N_{ind}} \mathrm{fit}_i} \ , \tag{2.6}$$

where fit_k is the fitness of the k-th individual. p_k represents also the selection probability of the k-th individual. The selection operator simply works by turning the roulette-wheel. Of course, according to this scheme, the individuals which have an increased probability to take part to the reproduction phase (and hence to pass their traits to the next generation) are those characterised by high values of the fitness function. Since the size of the population is constant and equal to N_{ind}, the wheel must be turned exactly N_{ind} times to form the couples of parents for the reproduction phase.

The reproduction phase: crossover and mutation operators

The next step of the process is the reproduction phase which takes place on each couple of individuals by means of two operators: *crossover* and *mutation*.

The crossover operator carries out, concretely, the creation of new individuals. In particular, the crossover operator acts at the gene-level. For each individual composing the generic couple, every single gene of each chromosome is randomly cut, with a probability p_{cross}, in one ore more locations (of course, the cut is done at the same position for each homologous gene of the couple genotype). At this point two new individuals are created by mixing and crossing the information restrained in the parents' genotype.
At the end of the crossover phase, for each couple, two new individuals are obtained through the recombination of the genetic information restrained into the parents' genotype.

Then, the mutation operator gains the scene. Such an operator randomly acts, with a probability p_{mut} (which takes a very low value), at the level of the gene for the generic individual. In particular, the mutation operator works on the single bit of the chain, by switching it from 0 to 1 or vice-versa. The mutation operator aims at increasing the *biodiversity* among the individuals composing the population. In addition, it can be noticed that such a process represents a pure random search in the design space.

Indeed, mutation operator plays also the role of a *second-order adaptation mechanism* within the whole genetic search process, see [190] for more details. It is noteworthy that, introducing (and increasing) biodiversity by means of the mutation mechanism is an aspect of outstanding importance: through the biodiversity it is possible to avoid a premature convergence of the algorithm towards local minima and/or pseudo-optimal solutions, a phenomenon often called *genetic drift*.

Finally, if the the stopping criterion defined by the user (typically a given number of iterations) is satisfied, the GA provides the optimal solution together with a number of pseudo-optimal or near-optimal solutions due to the "average adaptation" of the final population.

A summary of the advantages and drawbacks of GAs is listed here below.

Advantages of GAs

- GAs can deal with non-convex problems because of their intrinsic capability of exploring the design domain. Moreover, they work on a population of points and not on a single point in the design space.
- GAs are *zero-order methods*, i.e. they only need the evaluation of objective and constraint functions, without any further information. This fact allows for dealing with discontinuous problems, wherein the discontinuity could occur in terms of function or in terms of variables nature (discrete/scattered variables can be easily handled as well as continuous ones).
- The use of probability-based rules instead of deterministic ones does not mean that GAs act completely randomly. The information about the behaviour of the objective function and constraints is suitably stored and exploited along the iterations.

Drawbacks of GAs

- Real-world engineering problems, especially those of the structural domain, need an important computational effort. One single objective function evaluation could require a significant amount of time. The solution to this issue is to promote systems providing a reliable, but still computationally cheap, approximation of the objective function.
- GAs are not effective when decisions problems are faced.
- A GA is sensitive to the setting of its intrinsic parameters, namely the crossover and mutation probabilities, the size of the population, the choice of the selection operator, etc.

2.5 The Genetic Algorithm BIANCA

This Ph.D. thesis makes use of the GA ERASMUS [176] which is an improved version of the GA BIANCA (*Biologically Inspired ANalysis of Composite Assemblages*), initially developed by Montemurro [1]. Therefore, before introducing the GA ERASMUS described in Section 2.6, it is necessary to present some basic features of the GA BIANCA.

As suggested by its name, BIANCA was developed mainly to deal with the optimisation of composite structures. The first version of BIANCA (which was implemented in

FORTRAN language) was based on the structure of the standard GA described above. In particular, this GA has been generalised by Montemurro [1] in order to deal with **a wide class of optimisation problems**: it has been formulated in order to outperform the capabilities of standard GAs available in the literature. In particular, a new general representation of the individual genotype and new genetic operators was developed, thus making BIANCA able to deal with a new class of optimisation problems: the optimisation of *engineering modular systems*. Moreover, this algorithm implements also a very general (i.e. problem-independent) constraint handling technique, called *Automatic Dynamic Penalisation* (ADP) strategy [1, 201].

The most important feature of BIANCA is the capability of dealing with engineering modular systems. A modular system is whatever system constituted of several elementary and repetitive unit entities (the modules) which have certain intrinsic parameters. In particular, each module is characterised by the same vector of unknows which can take different values for each module (in the most general case of different modules). A typical example of a modular system is a composite laminate, in which the module is represented by the single ply that is characterised by the orientation angle, the thickness, the material properties, etc. It is noteworthy that the optimisation of modular systems has been considered as a prohibitive problem for decades. The most important challenge is related to the fact that, when optimising a modular system, there is no criterion to *a priori* define the optimum number of modules. Therefore, the number of modules should be included among the optimisation variables together with the constitutive parameters of each module. However, as discussed in [1, 176], when the optimisation problem of a modular system is stated in the most general sense, the resulting CNLPP is defined over a space with non-constant dimension. Roughly speaking, the problem is characterised by a *variable number of optimisation variables*. For a modular system, the associated CNLPP can be formalised as

$$
\begin{aligned}
&\min_{\mathbf{x}} \;\; f(\mathbf{x}, n_c), \\
&\text{subject to:} \\
&\begin{cases}
g_i(\mathbf{x}, n_c) \leq 0, \;\; i = 1, \ldots, m_i(n_c), \\
h_j(\mathbf{x}, n_c) = 0, \;\; j = 1, \ldots, m_e(n_c), \\
\mathbf{x}_{\mathrm{LB}} \leq \mathbf{x} \leq \mathbf{x}_{\mathrm{UB}}, \\
\mathbf{x}_{\mathrm{LB}}, \;\; \mathbf{x}, \;\; \mathbf{x}_{\mathrm{UB}} \in \mathbb{R}^{n(n_c)},
\end{cases}
\end{aligned}
\tag{2.7}
$$

where the dependence of the number of both design variables and constraints on the number of modules n_c has been made explicit.
It is noteworthy that, being the number of modules included among the design variables, the classical concept of design domain for problem (2.7) can be generalised and reinterpreted as a *multi-verse* of design spaces on which the algorithm acts simultaneously [176]. This multi-verse is thus populated by points representing modular systems made of different numbers of modules: consequently, each space within this multi-verse has a different dimension. As a consequence, the number of unknowns of the CNLPP of Eq. (2.7) is different for distinct points. For more details the interested reader is addressed to [176].

2.5.1 The structure of the individual's genotype

In order to deal with problem (2.7) and to develop an appropriate tool for performing the solution search, an optimisation strategy inspired by a more rigorous interpretation of the Natural Selection was developed in the Montemurro's Ph.D. thesis [1]. More precisely, the advantage of the intrinsic capability of "algorithmic adaptation" of GAs was fully exploited to this purpose. Basically, a richer and well-structured encoding of the genetic information represents the necessary preamble for building an improved GA able to deal with optimisation problems of modular systems.

According to the metaphor adopted by GAs, each point in the design space corresponds to an individual and its genotype is composed of chromosomes and genes [186,190]. As stated above, a standard GA performs the reproduction phase on a couple of individuals selected within the population according to a certain criterion. However, standard reproduction operators (i.e. crossover and mutation) are not suited to deal with optimisation problems of modular systems because the number of optimisation variables encoded within the individual genotype is constant and cannot change during iterations.

Moreover, in classical GAs, the Darwinian concept of *natural selection* is not properly implemented. In fact, this concept is strictly related to that of *species*: during a sufficiently long time interval, the selection, by operating on a certain number of individuals, can lead to the appearance of new species, which fit better to the surrounding environment.

In particular, a GA wherein individuals and species evolve simultaneously has been conceived in [1]: in this way the real natural selection is more closely synthetically reproduced by the numerical algorithm.

In this framework, the first step is the translation of the concept of species in the context of GAs. To achieve this task, the structure of the individual's genotype is changed: chromosomes and genes must be organised in such a way that different species can be clearly identified.

In agreement with the paradigm of Nature, within BIANCA the species is identified by the number of chromosomes of the individual's genome. Therefore, individuals having a genotype made of different number of chromosomes belong to different species.

Considering the previous aspects, in [1] the individual's genotype has been generalised though it is still represented by a binary array, as shown in Fig. 2.4. In this picture, the quantity $(g_{ij})^k$ represents the j-th gene of the i-th chromosome of the k-th individual. Letter e stands for empty location, i.e. there is no gene at this location, while n^k is the k-th individual chromosomes number (which identifies also the species to which such an individual belongs to).

It is evident that a GA that allows for evolving simultaneously (and independently) species and individuals must be characterised by genetic operators allowing the reproduction between individuals belonging to different species.

To this purpose , the classical reproduction phase has been generalised by introducing new operators called *Chromosome Shift*, *Chromosome Reorder*, *Chromosome Number Mutation* and *Chromosome Addition-Deletion*. A complete description of these new operators and their role in the reproduction phase is given in [1].

$(g_{11})^k$	$(g_{12})^k$	...	$(g_{1m})^k$	n^k
$(g_{21})^k$	$(g_{22})^k$	...	$(g_{2m})^k$	
...	...	...	...	
...	...	...	...	
$(g_{n1})^k$	$(g_{n2})^k$	...	$(g_{nm})^k$	
e	e	e	e	

Figure 2.4 – Structure of the individual's genotype with variable number of chromosome in BIANCA [1].

2.6 The ERASMUS algorithm

The GA BIANCA has been originally coded in FORTRAN environment in order to foster computational speed.

However, the individual's genotype structure presented in Section 2.5 is suited only for dealing with optimisation problems of modular systems characterised by a single type of modularity.

A modular system is characterised by different types of modularity when the constitutive modules can be regrouped in different sets: within each set, the modules are characterised by the same vector of unknowns (i.e. the module design variables). An example of modular system showing different types of modules is given in Fig. 2.5. In the fuselage section,

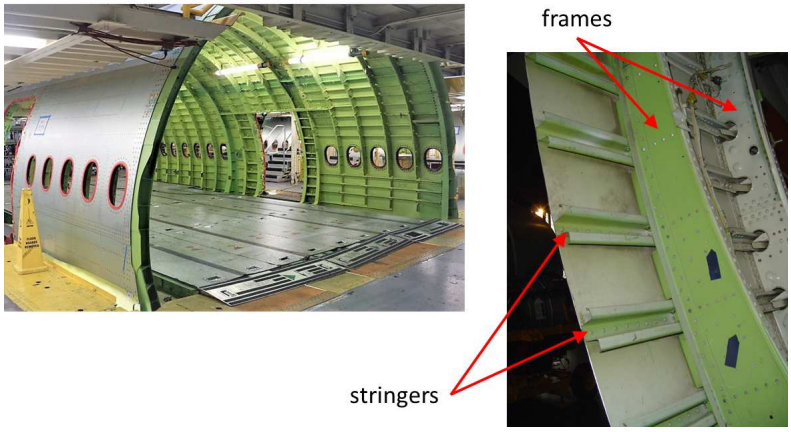

Figure 2.5 – An example of modular structure (a fuselage section) with two types of modules: stringers and frames

for example, there are two families of modules: the stringers and the frames. Of course, each kind of module is characterised by different types of design variables.

When a system presents more than one type (or class) of modularity, the structure of the individual's genotype must be generalised in order to integrate the variable number of modules for each modularity class.

To this purpose a very general derivative-free optimisation algorithm has been developed by Montemurro and his co-workers [176]: the ERASMUS (*EvolutionaRy Algorithm for optimiSation of ModUlar Systems*) code. Its main objective is the generalisation of both the structure of the individual and the genetic operators initially introduced in BIANCA

to the case of modular systems with different classes of modularity. As far as the new structure of the individual's genotype is concerned, it has been enriched to consider different kinds of modules. This task has been carried out by means of the *structured variables* in MATLAB and of the *lists* in PYTHON, as illustrated in Fig. 2.6.

Without loss of generality, let N_m be the number of different types of modules for the

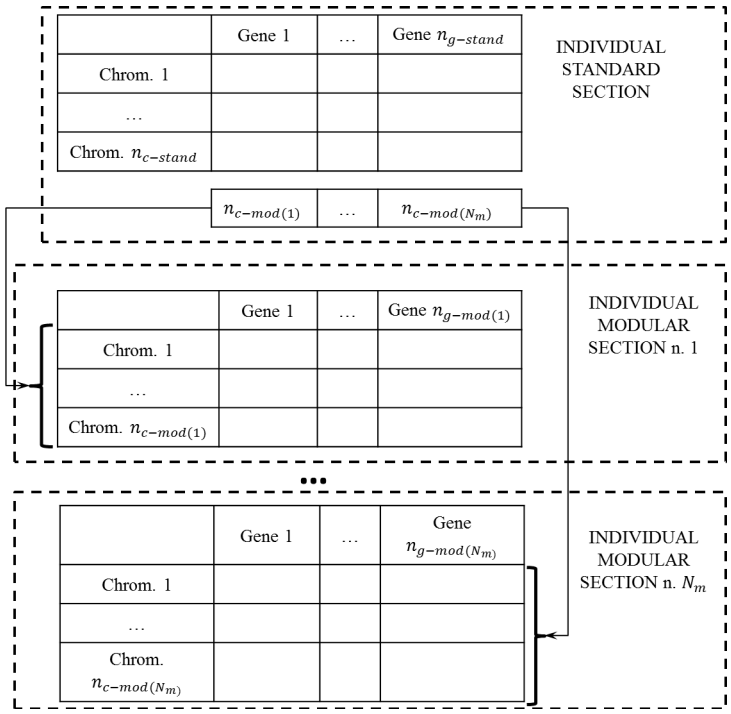

Figure 2.6 – The general individual's genotype structure in ERASMUS

problem at hand. Each individual (i.e. a point in the design space) is characterised by a genome composed of $N_m + 1$ *sections* having a precise hierarchy.

The first section (i.e. the *standard section*) is linked to the non-modular part of the problem and its genotype is split in two parts. The first one is composed of a fixed number ($n_{c-stand}$) of chromosomes and each chromosome is made of $n_{g-stand}$ genes. The second part is composed of only one chromosome having N_m genes which can be related (or not) to the values of some genes of the first part. This first section undergoes the action of the standard GA operators (refer to Section 2.4).

As shown in Fig. 2.6, each gene belonging to the mono-chromosome structure of the *standard section* is related to the number of modules $n_{c-mod(k)}$ of the generic k-th *modular section*, ($k = 1, \ldots, N_m$). Accordingly, each one of the remaining N_m modular sections is characterised by a genotype composed of $n_{c-mod(k)}$ chromosomes and $n_{g-mod(k)}$ genes. Naturally, the reproduction between species is allowed only for the modular sections.

The main features of the ERASMUS tool are listed here below.

Improved Capabilities of ERASMUS

- ERASMUS can handle optimisation problems of modular systems with different types of modularity.
- Selection: two known techniques of selection are included, i.e. roulette wheel and tournament.

- Standard reproduction operators: the main genetic operators are crossover and mutation, acting, with a certain probability, on each gene of the individual's genotype, i.e. independently on each design variable.
- Additional genetic operators: the *elitism* operator is used to preserve the best individual at each generation.
- Handling multiple populations: the need to simultaneously explore different regions of the design space, as well as the search of optima responding to distinct design criteria require the introduction of multiple populations evolving simultaneously. A classical *ring-type migration* operator has been introduced in order to allow exchange of information between populations evolving through parallel generations.
- Stop criteria: maximum number of generations reached or test of convergence, i.e. no improvements of the mean fitness of the population after a given number of cycles.
- ERASMUS has no limitations in terms of constraints handling thanks to the implemented ADP strategy [201].
- Representation of information: a new structure of the individual's genotype adapted and extended to represent the concept of *species*.
- New genetic operators of crossover allowing the reproduction among individuals belonging to different species.
- New mutation operators allowing the evolution of the different species.

2.7 Conclusions

Some optimisation tools have been discussed. As the domain of optimisation is wide, the purpose of this Chapter is just to introduce the main features of some optimisation algorithms and to explain why they are important. Classification criteria for optimisation problems have been provided, as well, and the attention has been focused on deterministic and meta-heuristic algorithms for the solution of CNLPPs. The most remarkable aspect of this discussion is that the choice of the optimisation algorithm should be carefully addressed according to the problem at hand.

Thus, when the optimisation problem is non-convex, the use of meta-heuristics is a possible answer to solve it: this kind of optimisation algorithms allow to explore widely the research domain, decreasing the possibility to find a local minimum, instead of the global one. However, the computational cost related to the use of meta-heuristics is expensive. For this reason, in order to speed up the optimisation process, in this work the use of the hybrid meta-heuristic - deterministic tools is proposed. The optimisation process is always split in two steps. During the first step, the domain is explored through the ERASMUS algorithm and, when a profitable zone is identified, the best individual provided by the meta-heuristic algorithm is used as initial guess for the second optimisation step which is carried out by a deterministic algorithm.

Chapter 3

Characterisation of composite elastic properties by means of a multi-scale two-level inverse approach

3.1 Introduction and main motivations of the study

The article reported in this Chapter has been published in *Composite Structures*. It deals with the problem of characterising the elastic properties of a composite material at both mesoscopic (ply-level) and microscopic (constitutive phases-level) scales. In particular, this Chapter presents the first version of the MSIS. In its first version the MSIS is able to identify, at each pertinent scale, the elastic properties of the composite, by using the data resulting from non-destructive experimental techniques.

The MSIS is here tested on a multilayer plate where the elementary lamina is a fibre-reinforced undirectional pre-preg. The non-destructive test is a harmonic test.

In order to prove the effectiveness of the MSIS, the experimental test has been replaced by a numerical analysis carried out on a reference configuration of the multilayer plate. Therefore, the information restrained in the *reference* macroscopic dynamic response of the composite is used into the inverse problem formulation. In this background, the multi-scale identification problem is split into two interdependent sub-problems which are stated, at both levels, as CNLPPs. At the first level, the goal is the characterisation of the lamina properties by minimising the distance between the numerical and the reference harmonic responses of the composite, subject to suitable constraints on the laminate natural frequencies and on the positive definiteness of the lamina stiffness tensor.

The goal of the second-level inverse problem is the identification of the elastic properties of both fibre and matrix by minimising the distance between the effective elastic properties evaluated through a homogenisation process and those provided by the first-level inverse problem. Of course, also in this case suitable thermodynamic constraints are considered in order to avoid an ill-posed problem. The MSIS for the elastic case is based on the strain energy homogenisation method of periodic media [75,116,176,202]. For both levels of the optimisation procedure the GA ERASMUS coupled with the *fmincon* tool of the MATLAB optimisation toolbox have been used to perform the solution search.

3.2 Characterisation of composite elastic properties by means of a multi-scale two-level inverse approach

Composite Structures 204 (2018) 767–777

Contents lists available at ScienceDirect

Composite Structures

journal homepage: www.elsevier.com/locate/compstruct

Characterisation of composite elastic properties by means of a multi-scale two-level inverse approach

Lorenzo Cappelli[a], Marco Montemurro[a,*], Frédéric Dau[a], Laurent Guillaumat[b]

[a] Arts et Métiers ParisTech, Institut de Mécanique et d'Ingénierie (I2M) de Bordeaux CNRS UMR 5295, F-33400 Talence, France
[b] Arts et Métiers ParisTech, Laboratoire angevin de mécanique, procédés et innovation (LAMPA), F-49100 Angers, France

ARTICLE INFO

Keywords:
Composite material
Homogenisation
Optimisation
Harmonic analysis
Inverse problems
Identification

ABSTRACT

This work deals with the problem of characterising the elastic properties of a composite material at both mesoscopic (ply-level) and microscopic (constitutive phases-level) scales. This goal is attained by means of an adequate multi-scale identification strategy (MSIS) which aims at identifying the constitutive properties, at each relevant scale, by exploiting the information restrained in the macroscopic dynamic response of the composite. In this background, the multi-scale identification problem is split into two interdependent sub-problems which are stated, at both levels, as constrained minimisation problems. At the first level the goal is the characterisation of the lamina properties by minimising the distance between the numerical and the reference harmonic responses of the composite. The second level problem aims at identifying the elastic properties of both fibre and matrix by minimising the distance between the effective elastic properties evaluated through a homogenisation process and those provided by the first-level inverse problem. The MSIS is based on a special global hybrid optimisation tool and on the strain energy homogenisation method of periodic media. Its effectiveness is proven through a meaningful benchmark.

1. Introduction

Nowadays, composite materials are widely used in several fields, from automotive applications to aerospace ones. This is mainly due to their high stiffness/mass and strength/mass ratios when compared to steel or aluminium alloys. Furthermore, engineers are continuously looking for strategies that allow increasing performances, building integrated and lighter structures, designing complex geometry and providing stiffness and strength where needed.

Nevertheless, in order to properly conceive complex and optimised solutions, it is mandatory to characterise the full set of the composite material properties at each pertinent scale. One of the main issues of composite materials is related to the difficulty of characterising the full set of elastic properties at the lower scales, i.e. microscopic (that of the constitutive phases) and mesoscopic (the lamina level) ones.

Indeed, it is very interesting, especially from an industrial point of view, to be able to reduce the cost of experimental characterisation tests which are usually destructive procedures. Such tests must be carried out on a significant number of samples in order to get reliable results (thus leading to quite expensive experimental campaigns) [1]. Moreover, as far as concerns the characterisation of the elastic properties of the constitutive phases, a large data dispersion is obtained during micro-scale experimental tests, due to the difficulty to properly set the experiment and to handle the microscopic constituents [2].

Concerning the experimental (destructive) tests, they can be divided into meso and micro-scale characterisation tests. The most important meso-scale tests are: (1) the tension test for flat specimens (ASTM D3039 [3]); (2) three/four points bending test (ASTM D790 [4]); (3) compression tests (shear loading methods ASTM D3410 [5]; (4) end loading methods ASTM D695 [6]; (5) combined loading methods ASTM D6641 [7]); (6) shear tests (in-plane shear tests ASTM D5379 [8]-D7078 [9]-D3518 [10], out-of-plane - interlaminar shear tests ASTM D2344 [11]-D5379).

Nevertheless, ASTM standard tests conducted at the lamina level are not able to provide the full set of 3D elastic properties: only the in-plane material properties together with an approximated value of the out-of-plane shear moduli can be retrieved through these tests.

Conversely, only few standard tests can be carried out at the microscopic scale: single fibre test to obtain the Young's modulus along the fibre longitudinal direction (ASTM D3379 [12]) and matrix tensile test (ASTM D638 [13]). In order to characterise the rest of the constitutive phases properties, only non-standard tests are available in literature: pull-out [14], micro-indentation [2], fragmentation tests [15], etc.

* Corresponding author.
E-mail addresses: marco.montemurro@ensam.eu, marco.montemurro@u-bordeaux.fr (M. Montemurro).

https://doi.org/10.1016/j.compstruct.2018.08.007
Received 20 May 2018; Received in revised form 9 July 2018; Accepted 4 August 2018
Available online 06 August 2018
0263-8223/

When looking at the determination of the elastic properties of the microscopic phases, the limitations related to ASTM tests and/or unconventional destructive tests become more important. On the one hand, ASTM tests can provide information (with a high level of dispersion) only about the Young's modulus along fibre axis and matrix in-plane properties. The rest of the elastic properties (especially those of the fibre) cannot be retrieved by means of ASTM tests. On the other hand, also unconventional destructive tests, often used to characterise the matrix-fibre interface properties, present some major shortcomings: the experimental set-up is quite complex and, even when the experiment is properly realised, the obtained results show a significant dispersion (results are very sensitive to boundary conditions and edge effects related to the experimental set-up), see [16].

In order to go beyond the main restrictions imposed by destructive tests, the research activity here presented focuses on the development of a multi-scale identification strategy (MSIS), based on non-destructive tests, able to characterise the elastic properties of the composite at each relevant scale, namely microscopic and mesoscopic ones.

The main idea behind this approach is quite simple: the proposed MSIS aims at identifying the full set of elastic properties at both lamina-level and constitutive phases-level starting from the analysis of the *macroscopic* dynamic response of a multilayer plate. In particular, the macroscopic dynamic behaviour can be easily obtained by means of non-destructive modal tests: the information restrained in the harmonic spectrum response of the specimen can be then exploited to carry out the multi-scale characterisation process.

It is noteworthy that the utilisation of identification strategies exploiting the information restrained in a macroscopic modal analysis is not new. This kind of approach has already been applied in literature [17–21] for characterising the elastic properties of the constitutive lamina. An assessment of these approaches is available in [22,23]. Most of these techniques, e.g. that proposed in [24], make use of an optimisation tool (generally a gradient-based algorithm) in order to minimise the difference between the measured dynamic response (typically a given set of natural frequencies) and the numerical one calculated via a finite element (FE) model of the structure.

However, to the best of the authors' knowledge, this approach has never been generalised to characterise the material and geometrical features of the microstructure of composite materials.

Indeed, in the context of the proposed approach, the material characterisation problem is split into two distinct (but related) sub-problems. The first level of the procedure focuses on the transition from macroscopic scale to mesoscopic one and aims at minimising the distance between the *reference* harmonic response of the structure and its numerical counterpart: the goal is to search for the elastic properties of the constitutive ply minimising this distance. The second step focuses on the transition from mesoscopic scale to microscopic one: the goal is the determination of both geometrical and elastic properties of the constitutive phases meeting the lamina elastic properties resulting from the first-level inverse problem.

The MSIS is characterised by several original features. On the one hand, it relies on a special hybrid optimisation tool to perform the solution search, i.e. an in–house code made by the union of a special genetic algorithm (GA) (able to deal with problems characterised by a *variable number of design variables* [25]) and of a classical gradient-based one. On the other hand, the link between the two identification problems (stated at different scales) is ensured by a general numerical homogenisation scheme: the one utilising volume-averaged stresses determined on a suitable representative volume element (RVE) of the material in the framework of the strain energy method of periodic media [26].

The paper is structured as follows: the problem and the MSIS are introduced in Section 2. The mathematical formulation of the inverse problem at the ply-level and the related numerical aspects are discussed in Section 3, while the micro-scale characterisation problem as well as the numerical homogenisation scheme (and the related FE model) are discussed in Section 4. The numerical results of the MSIS are illustrated and discussed in Section 5. Finally, Section 6 ends the paper with some conclusions and perspectives.

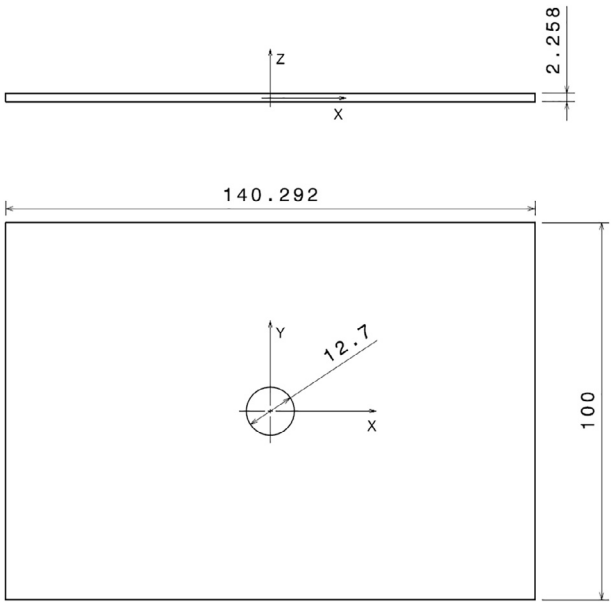

Fig. 1. Geometry of the multilayer composite plate (sizes in [mm]).

2. Multi-scale identification of composite elastic properties

2.1. Problem description

The multi-scale inverse approach presented in this study is applied to a reference multilayer composite plate made of unidirectional laminae whose geometry is illustrated in Fig. 1.

The constitutive ply is made of carbon-epoxy fibre Hexcel $T650/F584$ pre-impregnated tapes, with a fibre volume fraction $V_f = 0.555$: the material properties of the constitutive phases composing the ply (taken from [27]) are listed in Table 1. As it can be noticed, the fibre has a transverse isotropic behaviour, while the matrix is isotropic.

The reference laminate is constituted of eight identical plies (i.e. same material and thickness) arranged according to the following stack $[0°/-45°/45°/90°]_S$. The thickness of the lamina is $t_{ply} = 0.28225$ mm. The orientation angle of the generic ply is positive according to counter-clockwise rotation around the z-axis: x-axis indicates the 0° orientation.

The analysis presented in this work constitutes a numerical validation of the MSIS: the *reference response* of the structure (at each scale) is determined by means of a multi-scale numerical analysis on the reference configuration of the laminate described above.

In particular, as described in Section 5.1, the reference material properties of the constitutive phases are used in order to calculate, on the one hand, the *reference effective elastic properties* of the lamina at the mesoscopic scale and, on the other hand, the *reference harmonic response* and the *reference natural frequencies* of the multilayer plate (macroscopic scale).

Concerning the microscopic scale the following hypotheses apply:

Table 1
Micro-scale reference material properties for the fibre $T650/35-3K$ and the matrix $F584$ (taken from [27,28]).

Fibre properties	Matrix properties					
E_1^f [MPa]	E_2^f [MPa]	ν_{12}^f	ν_{23}^f	G_{12}^f [MPa]	E_m [MPa]	ν_m
276000.0	17300.0	0.250	0.428	11240.0	4140.0	0.350

- the material of both constitutive phases has a linear elastic behaviour;
- perfect bonding condition at the fibre-matrix interface is considered;
- the damping capability of both phases is disregarded.

As far as mesoscopic and macroscopic scales are concerned, the following assumptions are made:

- the constitutive lamina has an elastic orthotropic behaviour;
- perfect bonding condition at the interface between two consecutive plies;
- the damping properties of the ply are neglected;
- the laminate kinematic is described in the framework of the first-order shear deformation theory (FSDT).

2.2. The multi-scale identification strategy

The main goal of the MSIS is to find the material properties of the considered structure at each relevant scale by exploiting the information restrained in the macroscopic dynamical response of the composite. The reference response can be provided either by a non-destructive harmonic test or by a numerical harmonic analysis conducted on a reference structure. This latter is the case considered in the present study: the reference configuration of the multilayer plate as well as the reference dynamical results are presented in Section 5.

In this background, the problem of characterising the elastic properties of the composite at different scales can be split into two distinct (but related) *inverse problems*.

- **First-level inverse problem**. This phase involves the transition from macroscopic scale (laminate-level) to mesoscopic one (ply-level): the goal is to characterise the ply elastic properties (the design variables of this phase) minimising the distance between the numerical harmonic response of the multilayer plate and the reference one.
- **Second-level inverse problem**. This step focuses on the transition from mesoscopic scale to microscopic one (that of the constitutive phases): the goal is to find the optimum value of elastic properties of both fibre and matrix (the optimisation variables of this phase) meeting the set of the lamina elastic properties provided by the first-level problem. In this second phase, the link between the two scales is ensured by means of a homogenisation analysis performed on the numerical model of the RVE of the material in order to compute the effective elastic properties of the ply.

The general architecture of the two-level MSIS is shown in Fig. 2.

3. Mathematical formulation of the first-level inverse problem

3.1. Optimisation variables, objective function and constraints

As stated above, the first-level inverse problem concerns the macroscopic/mesoscopic scale transition. The aim of this phase is to characterise the elastic properties of the constitutive lamina. In this background, the identification problem is formalised as a classical inverse problem. The goal is to find the set of elastic properties of the ply (in the most general 3D case) minimising the distance between the reference dynamic response of the structure and that provided by the numerical model of the structure.

According to the general hypotheses recalled in Section 2, the constitutive ply has a linear elastic orthotropic behaviour. However, taking into account the fibres arrangement, only six parameters must be identified during this step. As illustrated in Fig. 6, the considered RVE is characterised by five planes of orthogonal symmetry implying the following relationships: $E_2 = E_3$, $G_{12} = G_{13}$ and $\nu_{12} = \nu_{13}$.

Therefore, all the meso-scale material parameters can be collected into the vector of design variables $\mathbf{x}^{\mathrm{I}}$ as follows:

$$\mathbf{x}^{\mathrm{I}} = \{E_1, E_2, G_{12}, G_{23}, \nu_{12}, \nu_{23}\}. \tag{1}$$

It is noteworthy that the ply elastic properties cannot get arbitrary values, rather they have to satisfy a set of existence constraints in order to ensure the positive definiteness of the lamina stiffness tensor:

$$\begin{aligned} g_1^{\mathrm{I}}(\mathbf{x}^{\mathrm{I}}) &= \left|\nu_{12}\right| - \sqrt{\tfrac{E_1}{E_2}} < 0, \\ g_2^{\mathrm{I}}(\mathbf{x}^{\mathrm{I}}) &= \left|\nu_{23}\right| - \sqrt{\tfrac{E_2}{E_3}} < 0, \\ g_3^{\mathrm{I}}(\mathbf{x}^{\mathrm{I}}) &= 2\cdot\nu_{12}\cdot\nu_{13}\cdot\nu_{23}\cdot\tfrac{E_3}{E_1} + \nu_{12}^2\cdot\tfrac{E_2}{E_1} + \nu_{23}^2\cdot\tfrac{E_3}{E_2} + \nu_{13}^2\cdot\tfrac{E_3}{E_1} - 1 < 0. \end{aligned} \tag{2}$$

Moreover, the lamina elastic constants vary within the design space defined in Table 2, i.e. by introducing appropriate lower and upper bounds for each design variable. The lower and upper bounds are chosen equal to the 80% and the 120% of the reference material properties at meso-scale respectively (given in Table 4). Only the lower and upper bounds of the optimisation variable ν_{23} are set equal to the 85% and the 115% of the corresponding reference value, respectively.

Concerning the expression of the first-level objective function, an error estimator of the least-squares type has been chosen:

$$\Phi^{\mathrm{I}}(\mathbf{x}^{\mathrm{I}}) = \frac{1}{N_p\cdot N_s}\sum_{q=1}^{N_p}\sum_{r=1}^{N_s}\left[\left(\frac{f_r - f_r^{\mathrm{ref}}}{f_r^{\mathrm{ref}}}\right)^2 + \left(\frac{H_{r,q}(\mathbf{x}^{\mathrm{I}}) - H_{r,q}^{\mathrm{ref}}}{H_{r,q}^{\mathrm{ref}}}\right)^2\right]. \tag{3}$$

In the previous equation, f_r is the r-th sampled frequency, while $H_{r,q}$ is the fast Fourier transform (FFT) of the frequency response function (FRF) determined at the q-th sample point of the multilayer plate and evaluated at the r-th sampled frequency. Of course, f_r^{ref}, $H_{r,q}^{\mathrm{ref}}$ are the same quantities evaluated on the reference configuration of the laminate.

N_s and N_p are the number of sampled frequencies and of sample points over the laminate plate (where the FRF is computed/measured), respectively.

In order to get a numerical harmonic spectrum really close to the reference one (and also to match the reference natural frequencies), a set of constraints on the laminate eigenfrequencies is considered:

$$g_{3+j}^{\mathrm{I}}(\mathbf{x}^{\mathrm{I}}) = \left|\frac{f_{jn} - f_{jn}^{\mathrm{ref}}}{f_{jn}^{\mathrm{ref}}}\right| - \epsilon_j \leqslant 0, \quad j = 1, \ldots, n_f. \tag{4}$$

In Eq. (4), n_f is the overall number of natural frequencies involved in the analysis (i.e. in the frequency range used for the determination of the FRF), whilst f_{jn} and f_{jn}^{ref} are the numerical and reference j-th eigenfrequency, respectively. ϵ_j is a user-defined tolerance on the relative error for each natural frequency: in this study a maximum relative error equal to 0.005 has been considered.

Finally, the first-level inverse problem can be stated as a classical constrained non-linear programming problem (CNLPP):

$$\begin{aligned} &\min_{\mathbf{x}^{\mathrm{I}}} \Phi^{\mathrm{I}}(\mathbf{x}^{\mathrm{I}}), \\ &\text{subject to:} \\ &g_j^{\mathrm{I}}(\mathbf{x}^{\mathrm{I}}) \leqslant 0, \quad j = 1, \ldots, n_f + 3. \end{aligned} \tag{5}$$

3.2. The macroscopic finite element model

A picture of the FE model of the multilayer plate at the macroscopic scale together with the applied loads and boundary conditions (BCs) is illustrated in Fig. 3. Such a FE model (developed within ANSYS® environment [29]) is built by using ANSYS® SHELL281 layered shell elements with eight nodes and six degrees of freedom (DOFs) per node. The kinematic model is that of the first-order shear deformation theory (FSDT) [30].

The choice of shell elements is due to the aspect ratio (between the

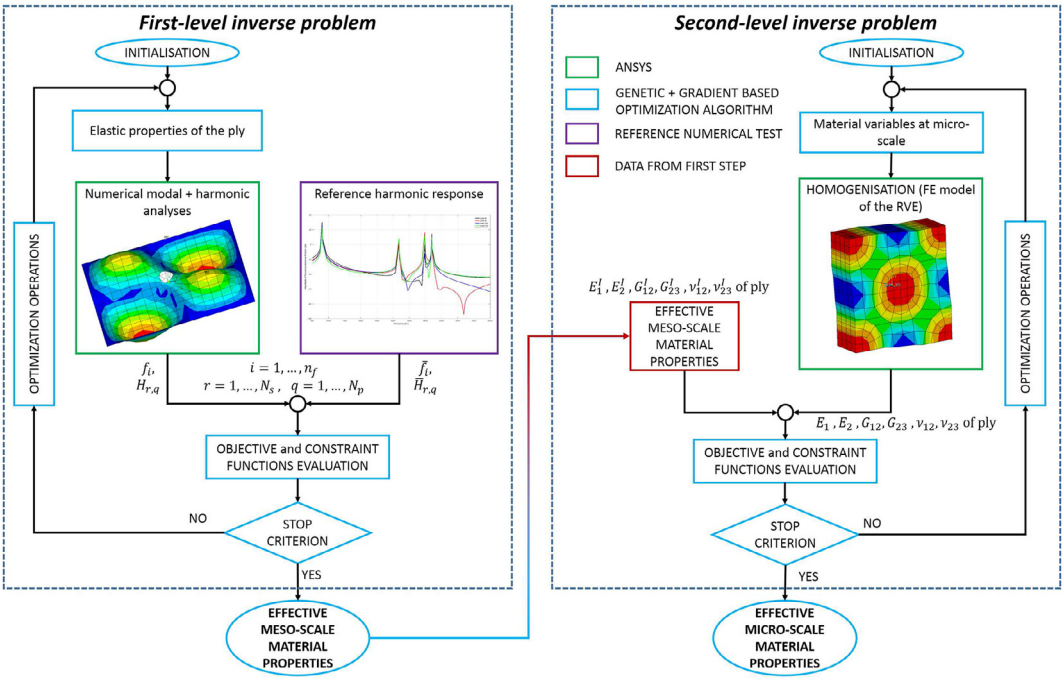

Fig. 2. The overall architecture of the MSIS.

Table 2
First-level inverse problem: design variables lower and upper bounds.

Ply elastic properties	Lower bound	Upper bound
E_1 [MPa]	124022.7	186034.1
E_2 [MPa]	6558.3	9837.4
ν_{12}	0.232	0.348
ν_{23}	0.433	0.586
G_{12} [MPa]	3069.7	4604.5
G_{23} [MPa]	2626.2	3939.3

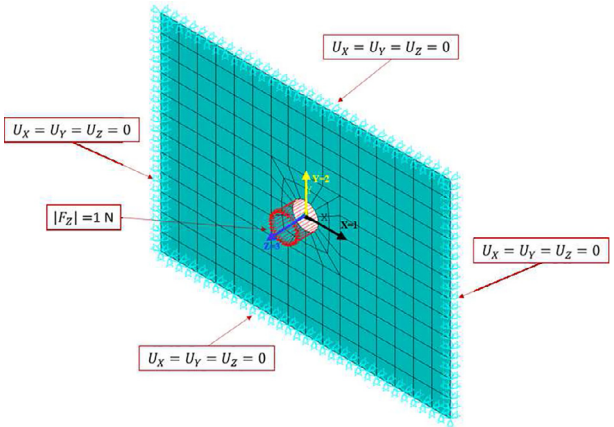

Fig. 3. FE model of the multilayer plate and the related BCs.

shortest edge length and the overall thickness) of the multilayer plate whose value, $AR = 44.29$, is in the range [20, 100] whereby the FSDT is well-suited to describe the laminate mechanical response.

During the optimisation process of the first step of the MSIS, two FE analyses are invoked for each point in the design space: firstly a modal analysis (eigenvalue analysis) to extract the first n_f natural frequencies and, secondly, a linear harmonic analysis in order to determine the harmonic response of the laminate. This latter is obtained by measuring the displacement u_z in each one of the q sample nodes of the mesh, at

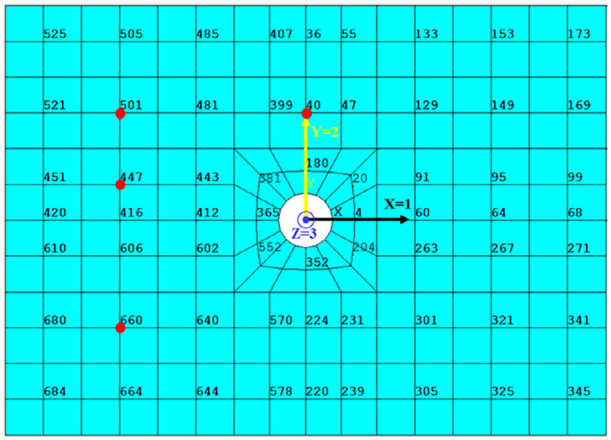

Fig. 4. Location of the sample points over the laminate used for harmonic displacements evaluation (the FRF related to nodes highlighted in red is shown in Fig. 9).

every sampled frequency f_r, as depicted in Fig. 4.

Subsequently, the FRF for each sample point is obtained by evaluating the ratio between the FFT of the displacement $u_{zq}(f_r)$ and that of the applied force $F_z(f_r)$, namely

$$H_{r,q} = \frac{u_{zq}(f_r)}{F_z(f_r)}. \tag{6}$$

It is noteworthy that, before starting the optimisation process two sensitivity studies (not reported here for the sake of brevity) have been conducted. The first one focused on the sensitivity of the system response with respect to the mesh size: it was observed that a mesh having 4176 DOFs, is sufficient to properly evaluate both the eigenfrequencies and the FRF of the laminate in each sample point. Conversely, the second sensitivity analysis aimed at investigating the influence of the number of sample points N_p on the overall FRF of the multilayer plate. It has been observed that an overall number of $N_p = 62$ sample points is sufficient to properly evaluate the global FRF of the structure.

Finally, as far as the linear harmonic analysis is concerned, the FFT of the structure in each sample point has been evaluated in the frequency range [500, 6000] Hz wherein $N_s = 82$ sampled spectrum frequencies have been considered, according to the strategy detailed in Section 5.

3.3. The numerical strategy

Problem (5) is highly non linear and non-convex in terms of both objective and constraint functions. Its non-linearity is mainly related to the expression of both objective and constraint functions, see Eqs. (2)–(4).

For inverse problems, the uniqueness of solution is not *a priori* guaranteed: the set of parameters matching a given *observed state* may not be unique. Nevertheless, no proved theoretical rules exist in literature [31,32] to define the number of data points N_p for a given number of unknowns (n) that have to be identified. Generally, the inverse problem is stated as a CNLPP and it can be viewed as an *over-determined system of equations* [31,32]. Since more observation points than parameters exist (N_p is usually much greater than n) there are more equations than unknowns. If an optimal point exists, of course it may be not unique, thus implying the existence of many combinations of parameters that result to be equivalent optimal solutions for the CNLPP at hand.

Considering all these aspects and according to the practice always employed in literature, in this work a number of observed states (i.e. sample points N_p) greater than two times the number of design variables n has been considered. As previously stated, the number of sample points has been inferred by means of a numerical sensitivity analysis of the FRF of the plate with respect to parameter N_p: as a results $N_p = 62$ has been chosen to properly perform the optimisation calculations.

Taking into account the previous aspects, a hybrid optimization tool composed of the new version of the GA BIANCA [33], interfaced with the MATLAB *fmincon* algorithm [34], has been used.

The GA BIANCA has already been successfully applied to solve different kinds of real-world engineering problems, see for instance [33,35–37].

As shown in Fig. 5, the optimisation procedure for problem (5) is split in two phases. During the first phase, solely the GA BIANCA is used to perform the solution search. Due to the strong non-linearity of problem (5), the aim of the genetic calculation is to provide a potential sub-optimal point in the design space, which constitutes the initial guess for the subsequent phase, i.e. the local optimisation, where the MATLAB *fmincon* tool is employed to finalise the solution search. The optimisation algorithm is the *active-set* which is a Quasi-Newton method making use of an approximation of the Hessian matrix to estimate the descent direction. For more details on the active-set algorithm see [34].

For the resolution of the first-level inverse problem, both optimisation algorithms have been interfaced with the FE model of the multilayer plate. As shown in Fig. 5, for each individual at each generation, the optimisation tool performs two FE analyses: a modal analysis to extract the n_f natural frequencies followed by a linear harmonic analysis for the evaluation of the FRF of the laminate. Then, the GA elaborates the results provided by the two FE analyses in order to execute the genetic operations on the basis of the current value of both objective and constraint functions. These operations are repeated until the GA BIANCA meets the user-defined convergence criterion.

The number of design variables and that of constraint functions is six and $n_f + 3$, respectively. The generic individual of the GA BIANCA represents a potential solution for the problem at hand. The genotype of the individual for problem (5) is characterised by only one chromosome composed of six genes, each one coding a component of the vector of design variables, see Eq. (1).

4. Mathematical formulation of the second-level inverse problem

4.1. Optimisation variables, objective function and constraints

As stated previously, the second-level inverse problem is focused on the transition from mesoscopic scale to microscopic one. The main purpose of this step is the characterisation of the elastic properties of the constitutive phases (i.e. fibre and matrix) by minimising the distance between the effective elastic properties of the constitutive lamina (determined numerically) and the reference ones (i.e. the optimum values) resulting from the first-level inverse problem, which represent the *reference response* for this phase.

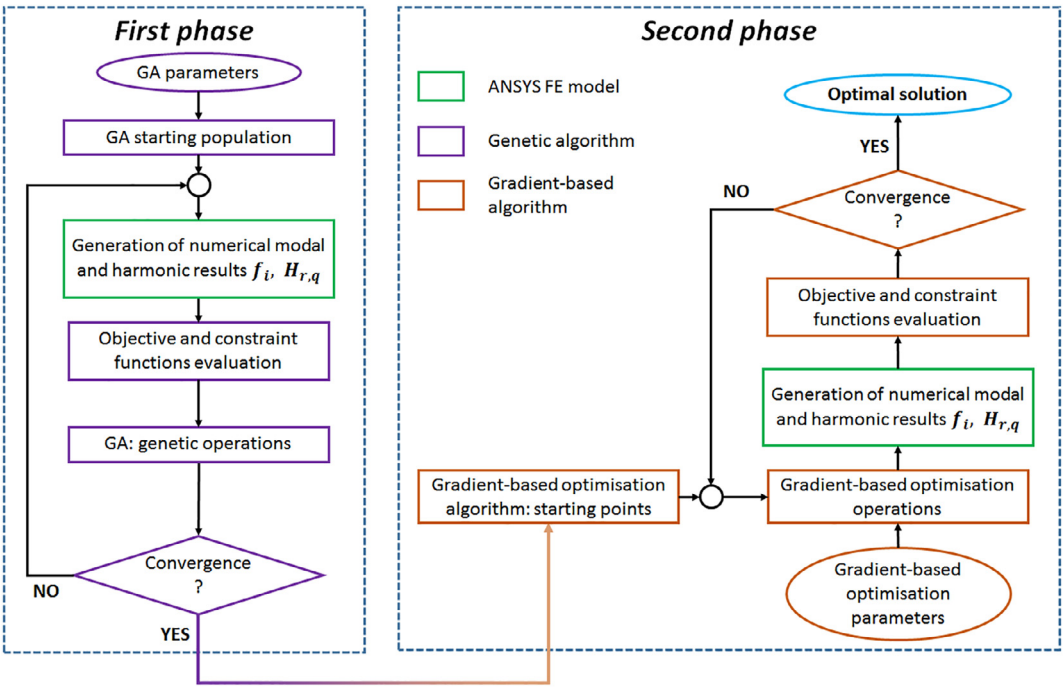

Fig. 5. Two-phases optimisation scheme for the first-level inverse problem.

Of course, the effective elastic properties of the lamina must be evaluated by means of a suitable homogenisation procedure. To this purpose, a FE model of the RVE of the composite is built in order to carry out the numerical homogenisation calculations which allow determining the equivalent meso-scale ply properties as a function of those of the constitutive phases. It is noteworthy that both geometrical and material parameters of the constitutive phases affect the equivalent material properties of the constitutive layer. Nevertheless, in the following the fibre volume fraction is set *a priori*, thus it is not considered among the design variables because it is always a reliable datum (always provided by the supplier in the specification sheet).

Considering the general hypotheses described in Section 2.1, the fibre has a linear elastic transverse isotropic behaviour while, the matrix has a linear elastic isotropic behaviour: only seven material parameters need to be identified. Therefore, these quantities are collected into the vector $\mathbf{x}^{\mathrm{II}}$ as follows:

$$\mathbf{x}^{\mathrm{II}} = \{E_1^f,\, E_2^f,\, G_{12}^f,\, \nu_{12}^f,\, \nu_{23}^f,\, E_m,\, \nu_m\}. \tag{7}$$

Similarly to the first-level inverse problem, the constitutive elastic properties cannot assume arbitrary values, but they have to fulfil a set of existence constraints to guarantee the positive definiteness of the fibre and matrix stiffness tensors:

$$\begin{aligned}
g_1^{II}(\mathbf{x}^{II}) &= \left|\nu_{12}^f\right| - \sqrt{\frac{E_1^f}{E_2^f}} < 0,\\
g_2^{II}(\mathbf{x}^{II}) &= |\nu_{23}^f| - 1 < 0,\\
g_3^{II}(\mathbf{x}^{II}) &= \frac{E_1^f}{E_2^f}\cdot(2\cdot\nu_{23}^f\cdot{\nu_{12}^f}^2 + 2\cdot{\nu_{12}^f}^2) - 1 < 0,\\
g_4^{II}(\mathbf{x}^{II}) &= \nu_m - \tfrac{1}{2} < 0,\\
g_5^{II}(\mathbf{x}^{II}) &= -\nu_m - 1 < 0.
\end{aligned} \tag{8}$$

Furthermore, the components of the design variables vector can take values within the design space defined in Table 3, in which appropriate lower and upper bounds for each design variable are assigned. The lower and upper bounds are chosen equal to the 80% and the 120% of the reference material properties at micro-scale (given in Table 1), respectively.

Moreover, regarding the objective function expression, an error estimator of the least-square type has been chosen:

$$\begin{aligned}
\Phi^{II}(\mathbf{x}^{II}) = \frac{1}{6}\Bigg[&\left(\frac{E_1 - E_1^{\mathrm{I}}}{E_1^{\mathrm{I}}}\right)^2 + \left(\frac{E_2 - E_2^{\mathrm{I}}}{E_2^{\mathrm{I}}}\right)^2 + \left(\frac{G_{12} - G_{12}^{\mathrm{I}}}{G_{12}^{\mathrm{I}}}\right)^2 + \left(\frac{G_{23} - G_{23}^{\mathrm{I}}}{G_{23}^{\mathrm{I}}}\right)^2\\
&+ \left(\frac{\nu_{12} - \nu_{12}^{\mathrm{I}}}{\nu_{12}^{\mathrm{I}}}\right)^2 + \left(\frac{\nu_{23} - \nu_{23}^{\mathrm{I}}}{\nu_{23}^{\mathrm{I}}}\right)^2\Bigg].
\end{aligned} \tag{9}$$

In the previous equation, superscript "I" indicates the optimum value of the generic ply elastic property provided by the first-level inverse problem.

Also in this case, the second-level inverse problem can be formalised as a classical CNLPP:

Table 3
Second-level inverse problem: design variables lower and upper bounds.

Micro-scale elastic properties	Lower bound	Upper bound
E_1^f [MPa]	220800.0	331200.0
E_2^f [MPa]	13840.0	20760.0
ν_{12}^f	0.200	0.300
ν_{23}^f	0.343	0.514
G_{12}^f [MPa]	8992.0	13488.0
E_m [MPa]	3312.0	4968.0
ν_m^f	0.280	0.420

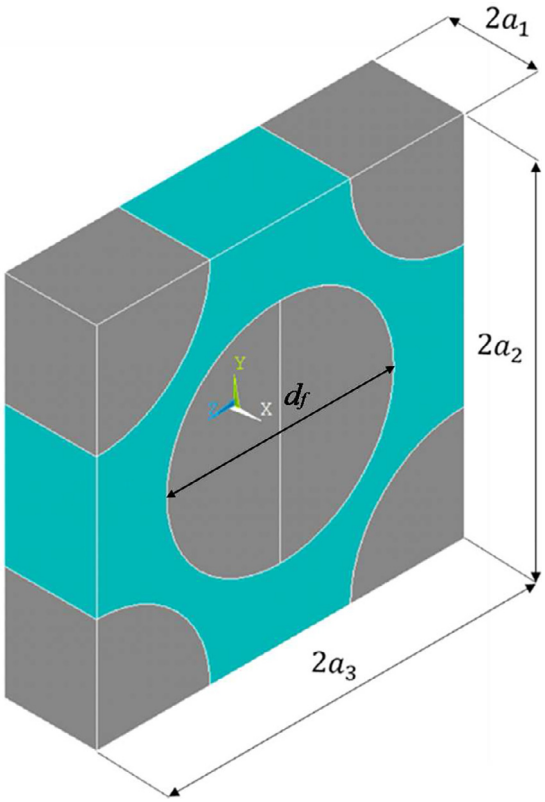

Fig. 6. The reference RVE.

$$\begin{aligned}
&\min_{\mathbf{x}^{II}} \Phi^{\mathrm{II}}(\mathbf{x}^{II}),\\
&\text{subject to:}\\
&g_j^{II}(\mathbf{x}^{II}) \leqslant 0, \quad j = 1,\ldots,5.
\end{aligned} \tag{10}$$

4.2. The microscopic finite element model and the homogenisation strategy

The link between the microscopic and mesoscopic scales is represented by a homogenisation phase, performed on the RVE of Fig. 6. The lamina effective elastic properties are computed by means of the well-known strain energy homogenisation technique of periodic media described in [26]. This homogenisation scheme has proven to be an efficient numerical homogenisation procedure able to determine the equivalent material properties of different heterogeneous materials characterised by complex RVE topologies. The strain energy homogenisation technique of periodic media based on volume averaged stresses has already been used in other works, see [35,38–40].

The main hypothesis of this technique is that the repetitive unit of the periodic structure and the corresponding volume of the homogeneous solid undergo the same deformation having, hence, the same strain energy. At the mesoscopic scale (i.e. at the ply level), the heterogeneous medium is then replaced by an equivalent homogeneous anisotropic virtual material characterised by a set of elastic properties determined during the homogenisation phase. Of course, these properties depend upon the geometrical and material parameters of the RVE.

In this study, the real random micro-structure of the lamina (which is usually characterised by misalignments of the fibres, porosity, damaged zones, etc.) is not taken into account and the topology of the RVE is described by a perfect hexagonal array, as shown in Fig. 6.

The FE model of the RVE has been realised within the commercial FE code ANSYS®. A 20-nodes solid element (SOLID186) with three DOFs per node has been used. The model together with its structured

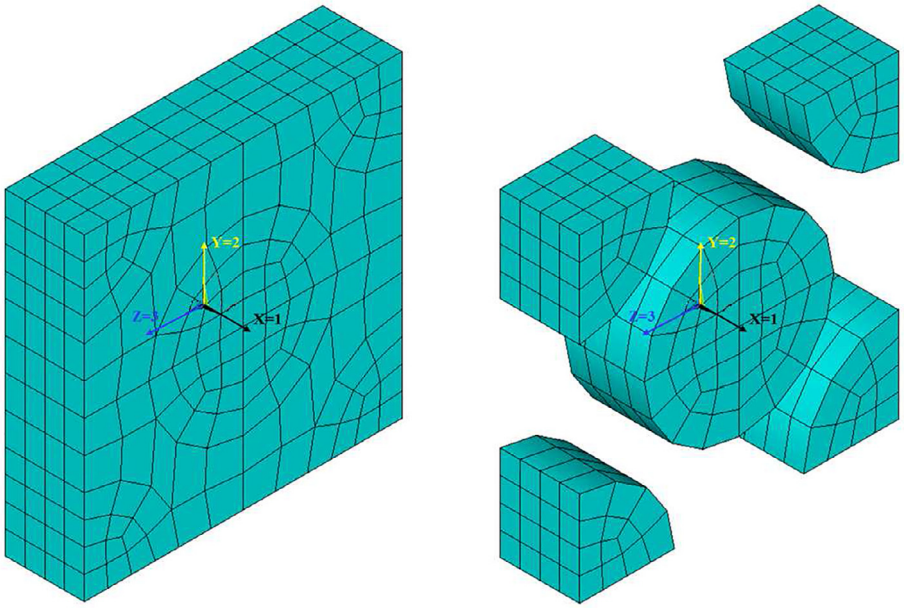

Fig. 7. FE model of the RVE, micro-scale.

mesh is illustrated in Fig. 7. Finally, a sensitivity study (not reported here for the sake of brevity) on the proposed FE model with respect to the mesh size has been conducted: it was observed that a mesh having 19551 DOFs is sufficient to properly evaluate the set of homogenised elastic properties at the mesoscopic scale.

In order to evaluate the components of the stiffness matrix [C] of the lamina, the RVE is submitted to an average strain field ε_{ij}^0 (tensor notation). The six components of the average strain are applied by considering the classical periodic boundary conditions (PBCs) on the RVE [26].

$$\begin{aligned} &u_i(a_1, x_2, x_3) - u_i(-a_1, x_2, x_3) = 2\cdot a_1\cdot\varepsilon_{i1}^0, \quad -a_2 \leqslant x_2 \leqslant a_2, -a_3 \leqslant x_3 \leqslant a_3,\\ &u_i(x_1, a_2, x_3) - u_i(x_1, -a_2, x_3) = 2\cdot a_2\cdot\varepsilon_{i2}^0, \quad -a_1 \leqslant x_1 \leqslant a_1, -a_3 \leqslant x_3 \leqslant a_3,\\ &u_i(x_1, x_2, a_3) - u_i(x_1, x_2, -a_3) = 2\cdot a_3\cdot\varepsilon_{i3}^0, \quad -a_1 \leqslant x_1 \leqslant a_1, -a_2 \leqslant x_2 \leqslant a_2,\\ &i = 1, 2, 3. \end{aligned} \tag{11}$$

The PBCs, shown in Eq. (11), result in a complex strain field inside the RVE. The applied average strains always meet the following condition (V denotes the RVE volume):

$$\bar{\varepsilon}_{ij} = \frac{1}{V}\cdot\int_V \varepsilon_{ij}\, dV = \varepsilon_{ij}^0. \tag{12}$$

For the homogeneous material at the upper scale, the relationship between average stress and strain (Voigt's notation) is:

$$\bar{\sigma}_\alpha = C_{\alpha\beta}\cdot\bar{\varepsilon}_\beta, \quad \alpha, \beta = 1, \ldots, 6. \tag{13}$$

In the previous equation the Einstein's summation convention on repeated indexes is tacitly assumed. The components of the stiffness matrix [C] are determined by solving six static analyses on the RVE and by imposing the previous PBCs, where only one component at time of the strain ε_β^0 is different from zero for each one of the six problems. For all the static analyses the volume-averaged value of the generic component of the stress field $\bar{\sigma}_\alpha$ can be easily computed and the stiffness matrix of the ply can be calculated one column at time:

$$\begin{aligned} C_{\alpha\beta} = \frac{\bar{\sigma}_\alpha}{\varepsilon_\beta^0} = \frac{1}{V\cdot\varepsilon_\beta^0}\cdot\int_V \sigma_\alpha(x_1, x_2, x_3)\, dV, \quad \alpha, \beta = 1, \ldots, 6;\ \varepsilon_\gamma^0 = 0, \quad \gamma\\ = 1, \cdots, 6, \quad \gamma \neq \beta. \end{aligned} \tag{14}$$

The engineering moduli of the constitutive lamina at the mesoscopic scale can be calculated starting from the components of the compliance matrix [S] = [C]$^{-1}$. For more details on the homogenisation procedure, the interested reader is addressed to [26].

4.3. The numerical strategy

Problem (10) is a non-convex CNLPP in terms of both constraint and objective functions, see Eqs. (8) and (9).

Concerning problem (10), the number of variables is equal to *seven*. The existence of the optimum solution may not be unique because the number of *observed states* is lower than that of design variables to be identified. Therefore, the transition from mesoscopic to microscopic scale is governed by non-bijective relationships which can give rise to a significant amount of equivalent optimum solutions for the problem at hand.

In order to find a solution for the second-level inverse problem, the two-step optimisation procedure is adapted to the transition from mesoscopic scale to microscopic one, as illustrated in Fig. 8.

For the resolution of the second-level inverse problem, the optimisation algorithm has been interfaced with the FE model of the RVE at micro-scale, to perform the numerical homogenisation. As stated above, the optimisation tool invokes the FE model of the material RVE on which six static analyses are performed: the PBCs allow determining the components of the ply stiffness tensor, for each individual at each generation.

Then, the optimisation tool elaborates the results provided by the FE analyses in order to execute the optimisation operations on the basis of the current values of both objective and constraint functions (both for the GA and the gradient algorithm). These operations are repeated until the user-defined convergence criterion is satisfied.

Concerning the GA, the genotype of the individual for problem (10) is characterised by only *one* chromosome composed of *seven* genes, each one coding a component of the vector of design variables of Eq. (7).

5. Numerical results

5.1. Determination of the harmonic response for the reference configuration

Before launching the optimisation process, the reference harmonic response must be determined. The geometry as well as the material properties of the reference configuration have been introduced in Section 2. The reference harmonic response is calculated by performing

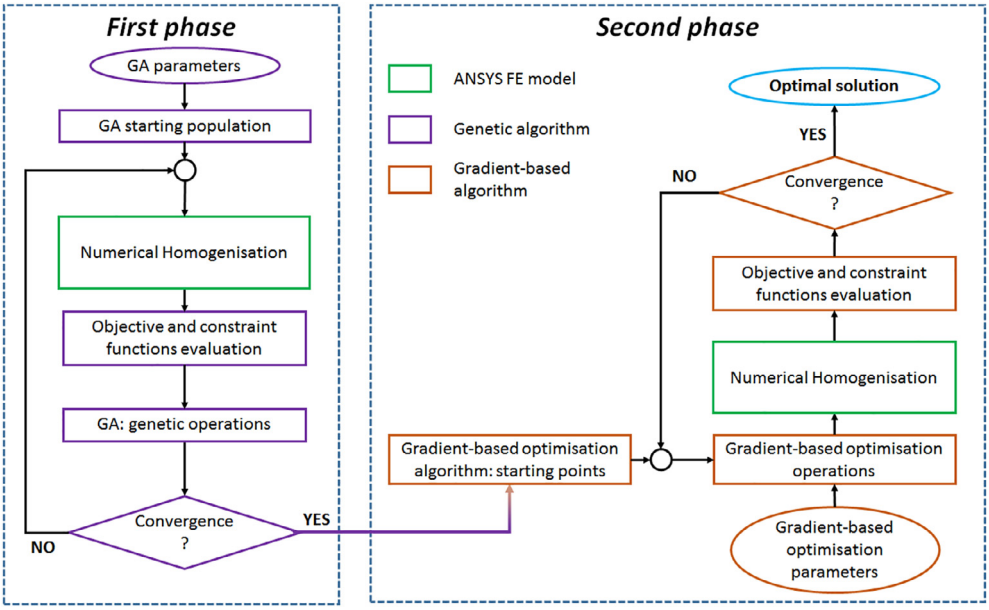

Fig. 8. Optimisation scheme for the second-level inverse problem.

Table 4
Reference values of the lamina material properties.

Ply properties						
E_1 [MPa]	E_2 [MPa]	ν_{12}	ν_{23}	G_{12} [MPa]	G_{23} [MPa]	ρ [kg/m^3]
s155028.4	8197.9	0.290	0.510	3837.1	3282.8	1770.0

two successive analyses (modal analysis followed by a linear harmonic one) on the macroscopic FE model of the multilayer plate discussed in Section 3. Of course, at the macroscopic scale both the reference FRF of the laminate and the set of reference natural frequencies have been calculated by using the geometrical properties of the reference structure and by considering the ply elastic properties listed in Table 4. These material parameters are obtained by means of a preliminary homogenisation analysis through the FE model of the RVE of the composite (see Section 4) in which the reference values of Table 1 for the elastic properties of both fibre and matrix are used.

The frequency samples used for the determination of the structure FRF vary between $f_{LB} = 500$ Hz and $f_{UB} = 6000$ Hz. $n_f = 8$ natural frequencies falls in this interval: they are extracted to evaluate the optimisation constraints of Eq. (4). Their reference values are listed in Table 5. The FRF of the multilayer plate is divided according to the sampling sequence summarised in Table 6. It must be noticed that the sampling intervals used for the definition of the FRF and, hence, of the objective function of the first-level inverse problem of Eq. (3), have been properly parametrized in terms of the current value of the

Table 5
Reference natural frequencies.

Nat. freq.	Value [Hz]
f_{1n}^{ref}	760.98
f_{2n}^{ref}	1847.19
f_{3n}^{ref}	1997.35
f_{4n}^{ref}	2966.36
f_{5n}^{ref}	3770.59
f_{6n}^{ref}	3856.76
f_{7n}^{ref}	4605.93
f_{8n}^{ref}	5061.77

Table 6
Sampling sequence for FRF calculation ($\delta = 1$ Hz).

Frequency intervals [Hz]	N. of sampled spectrum points
$\left[1-\frac{f_{1n}^{\text{ref}}-f_{LB}}{f_{1n}^{\text{ref}}}\right]f_{1n} < f < f_{1n}-\delta$	6
$f_{1n}+\delta < f < f_{2n}-\delta$	10
$f_{2n}+\delta < f < f_{3n}-\delta$	10
$f_{3n}+\delta < f < f_{4n}-\delta$	10
$f_{4n}+\delta < f < f_{5n}-\delta$	10
$f_{5n}+\delta < f < f_{6n}-\delta$	10
$f_{6n}+\delta < f < f_{7n}-\delta$	10
$f_{7n}+\delta < f < f_{8n}-\delta$	10
$f_{8n}+\delta < f < \left[1-\frac{f_{UB}-f_{8n}^{\text{ref}}}{f_{8n}^{\text{ref}}}\right]f_{8n}$	6

structure natural frequencies f_{jn}, $(j = 1, ..., n_f)$. Moreover, since damping is neglected, a small range of frequencies in the neighbourhood of each natural frequency f_{jn} (by considering a "small" interval of length $\delta = 1$ Hz centred at each natural frequency) has been excluded from the sampling sequence. The exciting nodal force has a value $F_z = 1\,N$.

Finally, as discussed in Section 3, the FRF is calculated at each one of the 62 reference points defined over the laminate, as illustrated in Fig. 4.

5.2. Results of the first-level inverse problem (meso-scale)

In this section, the results of the first-level inverse problem are shown and discussed. After carrying out a statistic analysis in order to evaluate the effect of the optimisation parameters on the optimum solutions, according to [38], the main parameters tuning the behaviour of both the GA and the active-set algorithm (used to carry out global and local optimisation, respectively) are set as listed in Tables 7 and 8.

For this first case, the GA makes use of two populations with 60 individuals evolving along 130 generations. The exchange of information among populations is performed through a ring-type operator every 10 generations, with a probability which is automatically evaluated by the GA itself. Moreover, concerning the constraint-handling technique for the first-level inverse problem, the Automatic Dynamic Penalisation (ADP) method has been considered, see [41].

Table 7
Genetic algorithm parameters (for both first-level and second-level inverse problems).

Parameters	First-level	Second-level
N. of individuals	120	140
N. of populations	2	2
N. of iterations	130	130
Crossover probability.	0.85	0.85
Mutation probability.	0.06	0.07
Isolation time	10	10

Table 8
Gradient-based algorithm parameters (for both first-level and second-level inverse problems).

Parameters	Value
Solver algorithm	Active-set
Max function evaluation	10000
Tolerance on the objective function	10^{-15}
Tolerance on the gradient norm	10^{-15}

The choice of using multiple populations of small size, i.e. with a small number of individuals, is motivated by the fact that here the goal is to find the global minimum (for the objective function of the problem at hand) without increasing too much the computational effort. Indeed, the exchange of information between best individuals belonging to different populations (through the use of the ring-type operator), and hence the possibility of crossing them, allows the GA for exploring the feasible design domain and for handling the genetic information in the best way. More details about the use of multiple populations can be found in [25]. For the first-level inverse problem, the single numerical harmonic analysis (which must be performed for each individual at each iteration) needs about 30 s to be executed (on an Intel® Xeon® 2.70 GHz CPU with two processors and with a RAM of 128 GB), which implies an overall time of about 8.3 days to get an optimum solution.

The optimum solutions found at the end of both the genetic calculation and the local gradient-based optimisation are summarised in Table 9, whilst the values of the eigenfrequencies for the optimum solution are given in Table 10.

The FRF of the optimum solution evaluated in four different nodes (nodes 40, 447, 501 and 660 according to Fig. 4) are illustrated in Fig. 9.

As it can be easily inferred from the analysis of these results, the ply elastic properties of the optimum solution are in good agreement with the reference data: the absolute percentage difference ranges from 0% for G_{12} to 5.78% for ν_{23}. This is a quite expected result because, due to the kinematic model at the basis of ANSYS shell elements (first-order shear deformation theory), the effect of ν_{23} on both the displacement field and the natural frequencies is negligible. The plate is not thick enough to observe a significant influence of ν_{23} on its dynamic response.

Table 9
Optimum solution of the first-level inverse problem provided by the GA and the gradient-based algorithm; the percentage difference between the solution and the ply reference data are given in parentheses.

Meso-scale elastic properties	Reference data	GA results	Gradient-based results
E_1 [MPa]	155028.4	153846.0 (−0.762)	155027.5 (-6.45×10^{-04})
E_2 [MPa]	8197.9	8103.3 (−1.15)	8197.7(-1.95×10^{-03})
ν_{12}	0.290	0.284 (−1.94)	0.290 (3.45×10^{-03})
ν_{23}	0.510	0.480 (−5.76)	0.480 (−5.78)
G_{12} [MPa]	3837.1	3906.9 (1.82)	3837.1 (0)
G_{23} [MPa]	3282.8	3291.1 (0.254)	3282.5 (-7.62×10^{-03})

Table 10
First eight natural frequencies for the optimum solution of the first-level inverse problem; for each value, the percentage difference with respect to the reference counterpart is indicated in parentheses.

Nat. freq.	f_{in}^{ref} [Hz]	f_{in} [Hz]
f_{1n}	760.98	760.97 (3.51×10^{-04})
f_{2n}	1847.19	1847.18 (3.82×10^{-04})
f_{3n}	1997.35	1997.34 (3.83×10^{-04})
f_{4n}	2966.36	2966.34 (3.99×10^{-04})
f_{5n}	3770.59	3770.57 (4.20×10^{-04})
f_{6n}	3856.76	3856.74 (4.23×10^{-04})
f_{7n}	4605.93	4605.91 (4.27×10^{-04})
f_{8n}	5061.77	5061.74 (4.58×10^{-04})

Nevertheless, both the eigenfrequencies and the FRF, in all sample points, are very well estimated. The numerical results found at the end of the optimisation perfectly match the reference data with an absolute percentage difference ranging from 3.51×10^{-4}% (for the 1-*th* mode) to 4.58×10^{-4}% (for the 8-*th* mode).

Finally, the utilisation of the active-set method really improves the quality of the pseudo-optimal solution provided by the GA: the value of the objective function decreases from 4.29×10^{-4}, at the end of the genetic calculation to 6.00×10^{-7}, at the end of the local optimisation.

5.3. Results of the second-level inverse problem (micro-scale)

The second-level inverse problem is solved by considering a fibre volume fraction $V_F = 0.555$ [27] and a fibre diameter equal to $d_f = 6.8\,\mu$m [42].

The RVE dimensions are obtained as follows:

$$a_3 = \frac{d_f}{4}\sqrt{\frac{2\pi}{V_f}}, \quad a_2 = a_3, \quad a_1 = a_2/4. \tag{15}$$

The parameters tuning the behaviour of both the GA and the active-set algorithm for the second-level inverse problem are listed in Tables 7 and 8. As in the case of the first-level inverse problem, the Automatic Dynamic Penalisation (ADP) method has been considered for handling constraints [41]. As far as the second-level inverse problem is concerned, the optimisation process is faster: about 2.3 days are required to find a solution because the set of 6 static analyses to be conducted on the composite RVE needs only 6 s (and they must be performed for each point in the design space).

The optimum solutions of the second-level problem found at the end of both the genetic calculation and the local gradient-based optimisation are summarised in Tables 11 and 12.

As it can be easily inferred from the analysis of these results, the elastic properties of the constitutive phases for the optimum solution are in agreement with the reference data. In particular, Young's and shear moduli for both fibre and matrix are estimated with a very good accuracy: the absolute percentage difference ranges from 0.254% for E_1^f to 5.56% for E_2^f.

Conversely, the estimation of the Poisson's ratio (for both phases) is characterised by a higher discrepancy: the maximum absolute percentage difference is 13.4% on ν_{23}^f. However, this is a quite expected result because, as stated above, the Poisson's ratio ν_{23} of the lamina has a negligible influence on the laminate dynamic response. Indeed, the related sensitivity of both objective and constraint functions of the first-level problem to the variable ν_{23} is not significant at all. Therefore, the relatively small absolute percentage error on ν_{23} at the end of the first-level inverse problem (5.78%) is amplified when looking for the optimum solution of the second-level inverse problem in terms of Poisson's ratios of both fibre and matrix (the associated optimisation problem is non-linear).

Finally, the quality of the optimum solution of the second-level

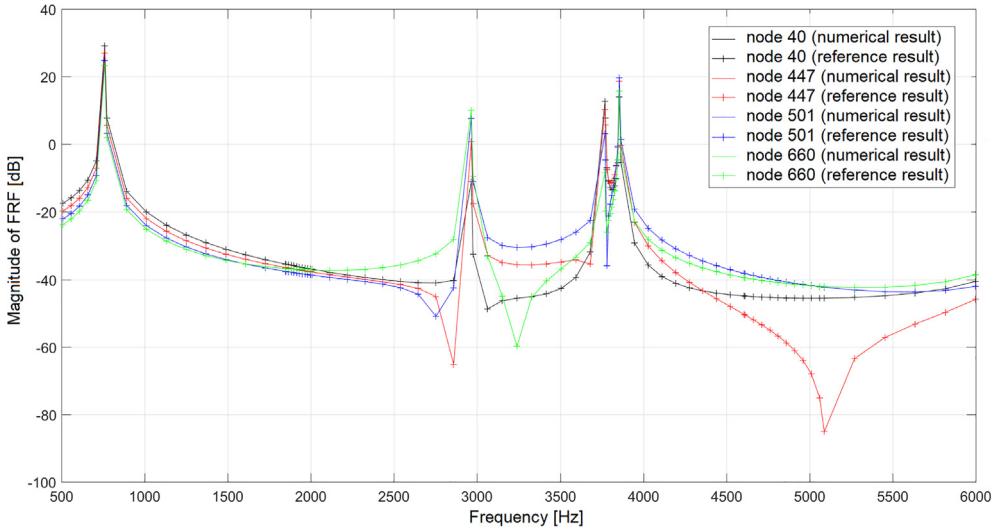

Fig. 9. Example of FRF for both optimum and reference solutions evaluated at nodes 40, 447, 501 and 660.

Table 11
Optimum solution of the second-level inverse problem provided by both the GA and the active-set algorithm; the percentage difference between the solution and the reference material properties are given in parentheses.

Micro-scale elastic properties	Reference data	GA results	Gradient-based results
E_1^f [MPa]	276000.0	276701.0 (0.254)	276701.0 (0.254)
E_2^f [MPa]	17300.0	18277.5 (5.65)	18262.1 (5.56)
ν_{12}^f	0.250	0.274 (9.76)	0.275 (9.83)
ν_{23}^f	0.428	0.487 (13.6)	0.486 (13.4)
G_{12}^f [MPa]	11240.0	10807.1 (−3.85)	10780.7 (−4.09)
E_m [MPa]	4140.0	4108.4 (−0.763)	4108.4 (−0.763)
ν_m	0.350	0.315 (−9.99)	0.315 (−9.99)

Table 12
Ply material properties at the end of the first-level inverse problem (used as target values) and those related to the optimum solution resulting from the second-level inverse problem; the percentage differences are indicated in parentheses.

Ply elastic properties	First-level problem results	Optimum results
E_1 [MPa]	155027.5	155392.0 (0.235)
E_2 [MPa]	8197.7	8170.8 (−0.328)
ν_{12}	0.290	0.290 (0.0)
ν_{23}	0.480	0.480 (0.0)
G_{12} [MPa]	3837.1	3837.2 (2.87×10^{-3})
G_{23} [MPa]	3282.5	3289.0 (0.196)

inverse problem is very good: the objective function value is 2.0519×10^{-5} at the end of the local gradient-based optimisation.

6. Conclusions and perspectives

In this work a multi-scale identification strategy (MSIS) able to characterise the elastic properties of composite materials, at each characteristic scale, is presented. The MSIS is characterised by several original features that make it a very general methodology for characterising the elastic properties of anisotropic media.

In the context of the MSIS, the problem of characterising the elastic properties of the composite at different scales is split into two distinct (but related) *inverse problems*. The first-level inverse problem involves the transition from macroscopic scale (laminate-level) to mesoscopic one (ply-level): the goal is to characterise the ply elastic properties minimising the distance between the numerical harmonic response of the multilayer plate and the reference one. Conversely, the second-level inverse problem focuses on the transition from mesoscopic scale to microscopic one (that of the constitutive phases): the goal is to find the optimum value of elastic properties of both fibre and matrix matching the set of the lamina elastic properties provided by the first-level problem.

The overall identification process relies on a single non-destructive harmonic test performed at the macroscopic scale. The MSIS makes use of the strain energy homogenisation technique of periodic media to carry out the scale transition (from microscopic to mesosocopic one) as well as of a hybrid optimisation tool to perform the solution search for both first-level and second-level inverse problems.

The effectiveness of the MSIS is evaluated through a numerical benchmark: a multilayer plate made of unidirectional carbon/epoxy pre-preg plies $T650/F584$, whose elastic properties are taken from literature, is considered as a reference structure and its harmonic response has been taken as a reference one.

At the mesoscopic scale (ply-level) the results of the identification process are very good: the maximum absolute percentage error is observed on the ply transverse Poisson's ratio ν_{23} and is about 5.78%. At the microscopic scale (constitutive phases-level) all elastic properties are identified with a good level of accuracy, except the fibre and matrix Poisson's ratios: those of the fibre, i.e. $\nu_{12}^f$and ν_{23}^f, are affected by a absolute percentage error of about 10% and 14%, respectively, whilst that of the matrix, ν^m, is characterised by a percentage error of about 10%.

On the one hand, the relatively small error on the transverse Poisson's ratio of the lamina is due to the very low sensitivity of the objective function to this material property (the laminate is not thick enough). On the other hand, this error propagates at the lower scale and affect the Poisson's ratios of both fibre and matrix for which the percentage error is amplified (the problem is non-linear).

Nevertheless, thanks to the proposed multi-scale identification approach, it is possible to retrieve both longitudinal and transversal effective properties of the constitutive phases of the RVE and this task cannot be easily performed by means of standard ASTM tests. Moreover, such a result has been obtained by using a unique macroscopic non-destructive harmonic test.

The proposed strategy constitutes just a "first attempt": the methodology must be generalised and improved in order to catch the true behaviour of the material of the constitutive phases at the microscopic scale. To this purpose, research is ongoing in order to include into the MSIS the following aspects: on the one hand, the viscoelastic behaviour

of both fibre and matrix in order to validate the effectiveness of the approach by means of a comparison with experimental harmonic tests; on the other hand, the variability effects induced by the manufacturing process, e.g. local variation of the fibre volume fraction, misalignments of fibres, variation of the plies orientation angles, etc.

Of course, the integration of the viscoelastic behaviour of the matrix at the microscopic scale has three main consequences:

- the equivalent elastic properties of the constitutive lamina at the mesoscopic scale will depend upon the frequency;
- since the ply elastic properties depends upon the frequency, the problem of determining the structure natural frequencies becomes a non-linear eigenvalue problem, thus a suitable iterative method must be foreseen to perform the related modal analysis;
- the harmonic response of the laminate, at the macroscopic scale, will be strongly affected by the matrix viscoelastic behaviour; in particular, the eigenfrequencies values reduce (when compared to the undamped modal analysis) and the amplitude of the FRF take a finite value (instead of an infinite one) when the frequency of the applied load/displacement is equal to the generic damped natural frequency.

In this context, the MSIS presented in this work can be used, on the one hand, to characterise the parameters of the law tuning the matrix viscoelastic behaviour and, on the other hand, to select the mathematical model which fits best the true viscoelastic behaviour, for a given frequency range

Finally, thanks to the versatility of the proposed MSIS, it is possible to characterise the geometrical features of the RVE of the composite material: the parameters defining the shape of the inclusion or its volume fraction can be easily integrated among the optimisation variables, without altering the overall architecture of the identification methodology. On the other hand, also geometric parameters of the laminate (mesoscopic scale) can be included among the unknowns to be identified, e.g. the orientation angles and the thickness of each lamina. Research is ongoing on these aspects as well.

Acknowledgements

This research work has been carried out within the project FULLCOMP (FULLy analysis, design, manufacturing, and health monitoring of COMPosite structures), funded by the European Union Horizon 2020 Research and Innovation program under the Marie Skodowska-Curie grant agreement No. 6421211.

Appendix A. Supplementary data

Supplementary data associated with this article can be found, in the online version, athttps://doi.org/10.1016/j.compstruct.2018.08.007.

References

[1] Adams FD, Carlsson AL, pipes RB. Experimental characterization of advanced composite materials. 3rd ed. CRC Press LLC; 2003.
[2] Maurin R, Davies P, Baral N, Baley C. Transverse properties of carbon fibres by nano-indentation and micro-mechanics. Appl Compos Mater 2018;15:61–73.
[3] ASTM International, West Conshohocken, PA, ASTM D3039/D3039M-17. Standard Test Method for Tensile Properties of Polymer Matrix Composite Materials; 2017.
[4] ASTM International, West Conshohocken, PA, ASTM D790-17. Standard test methods for flexural properties of unreinforced and reinforced plastics and electrical insulating materials; 2017.
[5] ASTM International, West Conshohocken, PA, ASTM D3410/D3410M-16. Standard test method for compressive properties of polymer matrix composite materials with unsupported gage section by shear loading; 2016.
[6] ASTM International, West Conshohocken, PA, ASTM D695-15. Standard test method for compressive properties of rigid plastics; 2015.
[7] ASTM International, West Conshohocken, PA, ASTM D6641/D6641M-16e1. Standard test method for compressive properties of polymer matrix composite materials using a combined loading compression (CLC) test fixture; 2016.
[8] ASTM International, West Conshohocken, PA, ASTM D5379/D5379M-12. Standard test method for shear properties of composite materials by the V-notched beam method; 2012.
[9] ASTM International, West Conshohocken, PA, ASTM D7078/D7078M-12. Standard test method for shear properties of composite materials by V-notched rail shear method; 2012.
[10] ASTM International, West Conshohocken, PA, ASTM D3518/D3518M-13. Standard test method for in-plane shear response of polymer matrix composite materials by tensile test of a laminate; 2013.
[11] ASTM International, West Conshohocken, PA, ASTM D2344/D2344M-16. Standard test method for short-beam strength of polymer matrix composite materials and their laminates; 2016.
[12] ASTM International, West Conshohocken, PA, ASTM D3379-75(1989) e1. Standard test method for tensile strength and young's modulus for high-modulus single-filament materials (Withdrawn 1998); 1975.
[13] ASTM International, West Conshohocken, PA, ASTM D638-14. Standard test method for tensile properties of plastics; 2014.
[14] Nairn JA. Analytical fracture mechanics analysis of the pull-out test including the effects of friction and thermal stresses. Adv Compos Lett 2000;9(6):373–83.
[15] Feih S, Wonsyld K, Minzari D, Westermann P, Lilholt H. Testing procedure for the single fiber fragmentation test, Vol. No. 1483(EN), Denmark. Risoe-R: Forskningscenter Risoe; 2004.
[16] Young TJ. Characterisation of interfaces in micro- and nano-composites. University of Surrey; 2012. [Ph.D. thesis].
[17] Lee C, Kam T. Identification of mechanical properties of elastically restrained laminated composite plates using vibration data. J Sound Vib 2006;295:999–1016.
[18] Xing L, Zhidong G, Zengshan L, Lu L. A new stress-based multi-scale failure criterion of composites and its validation in open hole tension tests. Chin J Aeronaut 2014;27(6):1430–41.
[19] Andy V, Brian CN, Stepan L, Dirk V. Multi-scale modelling strategy for textile composites based on stochastic reinforcement geometry. Comput Methods Appl Mech Eng 2016;310:906–34.
[20] Furtado S, Araujo A, Silva A. Inverse characterization of vegetable fibre-reinforced composites exposed to environmental degradation. Compos Struct 2018;189:529–44.
[21] Zhou X-Y, Gosling PD, Ullah Z, Kaczmarczyk L, Pearce C. Exploiting the benefits of multi-scale analysis in reliability analysis for composite structures. Compos Struct 2016;155:197–212.
[22] Pedersen P. Identification techniques in composite laminates. NATO ASI Ser E Appl Sci 1999;361:443–52.
[23] Pedersen P, Frederiksen PS. Identification of orthotropic material modul by a combined experimental/numerical method. Measurement 1992;10(3):113–8.
[24] Mota Soares CM, Moreira de Freitas M, Aro AL, Pedersen P. Identification of material properties of composite plate specimens. Compos Struct 1993;25:277–85.
[25] Montemurro M. Optimal design of advanced engineering modular systems through a new genetic approach. Paris VI, France: UPMC; 2012. [Ph.D. thesis],http://tel.archives-ouvertes.fr/tel-00955533.
[26] Barbero E. Finite element analysis of composite materials. CRC Press, Taylor and Francis Group; 2007.
[27] Soutis C, Beaumont PWR, editors. Multi-scale modelling of composite material systems. The art of predictive damage modelling, Woodhead Publishing Series in Composites Science and Engineering New York: Elsevier; 2005.
[28] Corporation Hexcell. Hexply 2016;F584.
[29] Ansys. ANSYS Mechanical APDL Basic Analysis Guide. Release 15.0, ANSYS Inc, Southpointe, 275 Technology Drive, Canonsburg, PA 15317; 2013.
[30] Jones RM. Mechanics of composite materials. McGraw-Hill; 1975.
[31] Sun N-Z. Inverse problems in groundwater modelling. Boston 6 of Theory and Applications of Transport in Porous Media; Kluwer Academic Publishers.
[32] Tarantola A. Inverse problem theory: methods for data fitting and model parameter estimation. New York: Elsevier; 1988.
[33] Costa G, Montemurro M, Pailhs J. A general hybrid optimization strategy for curve fitting in the non-uniform rational basis spline framework. J Optim Theory Appl 2018;176(1):225–51.
[34] The MathWorks Inc. 3 Apple Ill Drive, Natick, MA 01760-2098, Optimization Toolbox User's Guide; 2017.
[35] Montemurro M, Catapano A, Doroszewski D. A multi-scale approach for the simultaneous shape and material optimisation of sandwich panels with cellular core. Compos Part B: Eng 2016;91:458–72.
[36] Montemurro M, Catapano A. Variational analysis and aerospace engineering: mathematical challenges for the aerospace of the future. In: Springer Optimization and Its Applications, Springer International Publishing, 2016, Ch. A new paradigm for the optimum design of variable angle tow laminates, 1st ed., vol. 116, pp. 375–400.https://doi.org/10.1007/978-3-319-45680-5.
[37] Montemurro M, Catapano A. On the effective integration of manufacturability constraints within the multi-scale methodology for designing variable angle-tow laminates. Compos Struct 2017;161:145–59.
[38] Montemurro M, Nasser H, Koutsawa Y, Belouettar S, Vincenti A, Vannucci P. Identification of electromechanical properties of piezoelectric structures through evolutionary optimisation techniques. Int J Solids Struct 2012;49(13):1884–92.
[39] Catapano A, Montemurro M. A multi-scale approach for the optimum design of sandwich plates with honeycomb core, Part I: homogenisation of core properties. Compos Struct 2014;118:664–76.
[40] Catapano A, Montemurro M. A multi-scale approach for the optimum design of sandwich plates with honeycomb core, Part II: the optimisation strategy. Compos Struct 2014;118:677–90.
[41] Montemurro M, Vincenti A, Vannucci P. The automatic dynamic penalisation method (ADP) for handling constraints with genetic algorithms. Comput Methods Appl Mech Eng 2013;256:70–87.
[42] Cytec Industries Inc. THORNEL T-650/35 Pan-based fiber; 2012.

Chapter 4

Multi-scale identification of the viscoelastic behaviour of composite materials

4.1 Introduction and main motivations of the study

The second article, presented in this Chapter, has been published in *Mechanics of Materials*. It deals with the characterisation of the viscoelastic behaviour of composite materials, at each pertinent scale. To this purpose, the MSIS has been extended to efficiently exploit the information restrained into the macroscopic non-linear dynamic response of the composite specimen in order to properly identify its damping capability.

In particular, the idea is to identify the viscoelastic behaviour of the composite at both mesoscopic (lamina-level) and microscopic (constitutive phases level) scales. This objective can be achieved by solving an inverse problem, in which the identification of the parameters tuning the viscoelastic behaviour of the constitutive phases is obtained by minimising the distance between the numerical and the reference harmonic macroscopic responses of the composite subject to pertinent constraints on the natural damped frequencies as well as on the positive definiteness of the stiffness tensor of each phase.

Of course, the homogenisation procedure based on the strain energy of periodic media has been generalised to the case of viscoelastic materials in this work. More precisely, the viscoelastic behaviour of the matrix is described, in the frequency domain, by means of the Bagley-Torvik model [203] which makes use of fractional derivatives.

Nevertheless, when considering such a viscoelastic model, both modal and harmonic analyses (which are used at the macroscopic scale to assess the dynamic response of the composite) become non-linear because the stiffness tensor of the lamina depends upon the frequency. Accordingly, a suitable solver based on the non-linear Arnoldi's method (NLAM) has been implemented in the MATLAB environment and interfaced with the ANSYS software used to build the FE model of the multilayer plate.

4.2 Multi-scale identification of the viscoelastic behaviour of composite materials

Mechanics of Materials 137 (2019) 103137

Contents lists available at ScienceDirect

Mechanics of Materials

journal homepage: www.elsevier.com/locate/mechmat

Research paper

Multi-scale identification of the viscoelastic behaviour of composite materials through a non-destructive test

Lorenzo Cappelli[a], Marco Montemurro[*,a], Frédéric Dau[a], Laurent Guillaumat[b]

[a] Arts et Métiers ParisTech, Institut de Mécanique et d'Ingénierie (I2M) de Bordeaux CNRS UMR 5295, Talence F-33400, France
[b] Arts et Métiers ParisTech, Laboratoire Angevin de Mécanique, Procédés et innovAtion (LAMPA), Angers F-49100, France

ARTICLE INFO

Keywords:
Composite materials
Homogenisation
Harmonic analysis
Inverse problems
Optimisation
Viscoelasticity

ABSTRACT

The problem of characterising the viscoelastic behaviour of a composite material, at each pertinent scale, is addressed in this paper. To this purpose, a dedicated multi-scale identification strategy (MSIS), exploiting the information restrained in the macroscopic non-linear dynamic response of the composite, is developed. The MSIS aims to identify the viscoelastic behaviour of the composite at both mesoscopic (lamina-level) and microscopic (constitutive phases level) scales. This goal can be achieved by solving an inverse problem, wherein the identification of the parameters tuning the viscoelastic behaviour of the constitutive phases is obtained by minimising the distance between the numerical and the reference harmonic (macroscopic) responses of the composite; Of course, pertinent constraints on the natural damped frequencies as well as on the positive definiteness of the stiffness tensor of each phase must be provided. The MSIS relies on: (i) a general homogenisation procedure based on the strain energy of periodic media generalised to the case of viscoelastic materials; (ii) a dedicated solver to deal with the non-linear modal and harmonic analyses of the multilayer plate at the macroscopic scale; (iii) the Bagley-Torvik viscoelastic model to describe the viscoelastic behaviour of the matrix; (iv) a general hybrid optimisation algorithm able to deal with optimisation problems defined over a domain of variable dimension to solve the inverse problem. The effectiveness of the MSIS is proven through a suitable benchmark.

1. Introduction

Composite materials have a long story: they were employed by Israelites for the manufacturing of strengthen mud bricks and by the Egyptians to produce plywood (Jones, 1975). Nowadays, because of the introduction of constitutive phases with adequate mechanical properties in terms of strength, stiffness and heat transfer behaviour, high-performance engineering structures are more and more made of composite materials.

Composite structures are subjected to a wide variety of loading conditions, including both static and dynamic loads. In order to decrease the design costs related to experimental tests, accurate numerical simulations coupled to cheaper tests are required to predict the complex behaviour of the structure.

In order to carry out numerical simulations, reliable material properties have to be defined, under both static and dynamic conditions. In particular, for fibre-reinforced composites, the macroscopic behaviour depends upon that of the constitutive phases at the lower scales. For multilayer plates three characteristic scales can be identified. At the macroscopic scale the laminate is usually modelled as a homogeneous anisotropic plate whose structural response depends upon the constitutive stiffness, mass and damping matrices (membrane, bending and membrane/bending coupling behaviours). The mesoscopic scale focuses on the lamina-level: each constitutive ply is characterised by some geometric and material parameters, i.e. the orientation angle, the thickness, the position and the material properties of the ply. Of course, each one of the previous parameters is involved in the definition of the laminate stiffness and mass matrices and has a strong influence on the macroscopic response of the multilayer plate. Finally, the microscopic scale is that of the constitutive phases (e.g. fibres and matrix for fibre-reinforced composites): at this scale each phase is characterised by a given material behaviour and by a set of geometrical parameters, e.g. fibres volume fraction, fibre shape, fibres arrangement, etc.

The characterisation of the composite material properties at each relevant scale is a rather complex problem. Concerning the identification of the elastic properties, ASTM standard tests can be found in the literature: mesoscopic destructive tests (as tension ASTM International, 2017a, three/four points bending

* Corresponding author.
E-mail addresses: marco.montemurro@ensam.eu, marco.montemurro@u-bordeaux.fr (M. Montemurro).

https://doi.org/10.1016/j.mechmat.2019.103137
Received 17 April 2019; Received in revised form 19 July 2019; Accepted 29 July 2019
Available online 01 August 2019
0167-6636/

List of Acronyms

ADP	Automatic Dynamic Penalisation
ANM	Asymptotic Numerical Method
BCs	Boundary Conditions
CNLPP	Constrained non-linear programming problem
DOF	Degree Of Freedom
DMA	Dynamical Mechanical Analysis
ERASMUS	EvolutionaRy Algorithm for optimiSation of ModUlar Systems
FE	Finite Element
FFT	Fast Fourier Transform
FRF	Frequency Response Function
FSDT	First-order Shear Deformation Theory
GA	Genetic Algorithm
HERO	Hybrid EvolutionaRy-based Optimisation
IIA	Inverse Iteration algorithm
ISIM	Iterative Shift-Inverter Method
LB	Lower Bound
MSIS	Multi-Scale Identification Strategy
NLAM	Non-Linear Arnoldi's method
NLJDM	Non-Linear Jacobi-Davidson Method
PBCs	Periodic Boundary Conditions
RVE	Representative Volume Element
SEHT	Strain Energy Homogenisation Technique
UB	Upper Bound

ASTM International, 2017b and shear tests ASTM International, 2012) and few microscopic ASTM standard tests are available (to characterise the matrix ASTM International, 2014 and the fibre ASTM International, 1975 longitudinal Young's modulus, respectively). Unfortunately, the aforementioned tests are not able to provide the required 3D set of material properties.

Moreover, composite materials show also a dynamical behaviour that is strongly affected by damping properties (Mahmoudi et al., 2019). Accordingly, a proper characterisation of the damping capability of the material, at each relevant scale, is a challenging task (Suarez et al., 1986). This problem is more difficult than that of the elastic properties characterisation essentially because of the non-linear nature of the viscoelastic matrix behaviour, in terms of time response, which influences the damping capability of the composite at all characteristic scales.

From an experimental point of view, two methods are commonly used: the direct method and the indirect one. On the one hand, the direct techniques are based on the measurement of the dissipated energy per load cycle, which can be evaluated from the area of an hysteresis loop (Krasnobrizha et al., 2016). On the other hand, the indirect methods allow estimating the dissipated energy from the analysis of the spectrum response: free vibration-decay, resonant-dwell, bandwidth and impedance methods are some of the experimental techniques used for damping characterisation (Kostopoulos and Korontzis, 2003).

However, it is possible to describe the damping behaviour of a composite structure by directly looking at the viscoelastic properties (Jayendiran and Arockiarajan, 2015; Swain and Roy, 2018): nowadays, a common and useful method is the so-called Dynamical Mechanical Analysis (DMA) (Melo and Radford, 2005; Finegan et al., 2003; Chandra et al., 2003). DMA is an indirect method to characterise the material properties of reinforced polymers in terms of thermal, elastic and viscoelastic behaviours (Abedi, 2016).

The DMA test is performed by applying harmonic loads to the specimen. By measuring the sample response, it is possible to compute an apparent modulus that can be used to estimate the viscoelastic properties of the specimen. In the case of a composite multilayer plate, wherein the lamina has an isotropic transverse behaviour (Suarez et al., 1986), the identification process has to be carried out three times, e.g. by considering a symmetric angle-ply stack, to determine the longitudinal E_L, transversal E_T and shear G_{LT} moduli.

Unfortunately, when high modulus composite materials are investigated, the DMA technique provides less accurate results (Abedi, 2016) compared to the ASTM three-points bending test (ASTM International, 2017b). Indeed, the DMA test provides an apparent modulus giving only an average approximation of the plate flexural stiffness response which group both structural and material aspects. However, the DMA test does not allow to extract information about microscopic properties and only fibre-reinforced polymers can be tested.

From the engineer's viewpoint it is more interesting to look for those tests which allow to identify material properties at all relevant scales and which are not limited by the size of the composite sample or by the geometrical and material properties of the constitutive phases composing it. The formulation of a suitable inverse problem for material properties characterisation is a widely studied topic in the literature (Meng et al., 2017; Yap et al., 2019; Ghorbal et al., 2017). In this background, Barkanov et al. (2009) proposed an inverse technique based on modal analysis and on the response surface method to characterise the nonlinear behaviour of the viscoelastic core layer in sandwich panels. Elkhaldi et al. (2012) worked on the viscoelastic parameters identification for a sandwich panel where a generalised Maxwell model is considered and a gradient algorithm is used to solve the associated inverse problem. Cortés and Elejabarrieta (2006) developed an identification strategy to characterise the parameters of the fractional derivative model representing the viscoelastic behaviour of a sandwich beam. The goal is the minimisation of the error between the predicted Frequency Response Function (FRF) and the measured one. Ledi et al. (2018) proposed an identification method for frequency-dependent material properties of viscoelastic sandwich beams able to take into account for the property of the interface between layers.

As it can be inferred from the aforementioned works, the damping capability related to the viscoelastic behaviour of the matrix can be characterised by exploiting the information restrained in the dynamic response of the structure. In these works, sandwich beams/plates manufactured by interposing a viscoelastic layer between metallic ones were considered because this configuration is well suited to reduce noise and vibration. However, in multilayer plates the macroscopic damping capability is mainly related to the viscoelastic behaviour of the matrix at the microscopic scale.

This work focuses on the damping capability of multilayer plates made of unidirectional fibre-reinforced laminae. In particular, this study aims to generalise the multi-scale identification strategy (MSIS) developed in a previous study (Cappelli et al., 2018) to the case of the viscoelastic behaviour of composites. The MSIS relies on the information restrained in a non-destructive harmonic test conducted at the macroscopic scale. The idea is to exploit this information to characterise the viscoelastic behaviour of the constitutive phases at the microscopic scale.

In the context of the MSIS, the multi-scale identification problem is stated as a constrained non-linear programming problem (CNLPP). The goal is to minimise the distance between a *reference harmonic response* (that can be obtained either experimentally or numerically) and the numerical one. This function is subject to some requirements involved at different scales: (a) on the positive definiteness of the stiffness tensor of the constitutive phases (microscopic scale); (b) on the damped natural frequencies of the composite (macroscopic scale); (c) on a non-negative internal work and a non-negative dissipation rate as far as the viscoelastic model is concerned.

Nevertheless, the identification of the viscoelastic behaviour of the constitutive phases (mostly due to the matrix) at the microscopic scale is characterised by two difficulties: (a) the equivalent viscoelastic properties of the constitutive lamina at the mesoscopic scale depend

upon the frequency ; (b) since the ply material properties depend upon the frequency, the problem of determining the structure damped natural frequencies becomes a non-linear eigenvalue problem, thus a suitable iterative method must be foreseen to perform the related modal analysis. Therefore, the harmonic response of the laminate, at the macroscopic scale, is strongly affected by the matrix viscoelastic behaviour.

In this context, the MSIS presented in Cappelli et al. (2018) is generalised here to the characterisation of the parameters of the law tuning the viscoelastic behaviour of the constitutive phases, for a given frequency range. The proposed MSIS relies upon the following features: (a) an hybrid optimisation tool called HERO (*Hybrid EvolutionaRy-based Optimisation*) algorithm, see Montemurro (2018); (b) an extension of the numerical homogenisation method based on the strain energy of periodic media and on volume-averaged stresses and strains (Barbero, 2007) to the case of viscoelastic materials; (c) the Arnoldi's method (Voss, 2004; Hamdaoui et al., 2016) to solve the non-linear modal analysis for materials with frequency-dependent viscoelastic properties. The effectiveness of the MSIS for viscoelastic materials is proven on a meaningful benchmark taken from the literature.

The paper is structured as follows. The problem and the MSIS are introduced in Section 2. The mathematical formulation of the inverse problem and the related numerical aspects are discussed in Section 3. The finite element (FE) models of the composite at both microscopic and macroscopic scales are presented in Section 4. The numerical results of the MSIS are illustrated and discussed in Section 5. Finally, Section 6 ends the paper with some conclusions and perspectives.

2. Multi-scale identification of composite viscoelastic properties

2.1. Problem description

In this work, the MSIS is applied to a rectangular composite plate made of unidirectional viscoelastic plies, whose geometrical parameters are shown in Fig. 1.

The constitutive ply is made of carbon-epoxy fibre Hexcel *T*650/*F*584 pre-impregnated tapes, whose fibre volume fraction is $V_f = 0.555$. Concerning the available material properties of the constitutive phases, only the elastic properties can be found in litterature (they are taken from Soutis and Beaumont (2005)). The parameters tuning the viscoelastic response of the *F*584 matrix are set *a priori* because they are not available in Soutis and Beaumont (2005). They are set to reasonable values to give all the necessary microscopic material parameters defining the matrix behaviour. The reference material properties for both the fibre and the matrix are reported in Table 1. It is noteworthy that the viscoelastic behaviour of the *F*584 matrix is described by means of the Bagley–Torvik model (briefly discussed in Section 2.2 and taken from Bagley and Torvik (1986)).

The reference laminate is constituted of 16 identical plies with the stacking sequence $[0°/-45°/45°/90°/45°/90°/-45°/0°]_S$. The average thickness of the ply is $t_{ply} = 0.28225$ mm and the orientation angle of the lamina is defined positive according to counter-clockwise rotation around the z-axis.

The goal of this study is to provide a numerical validation of the MSIS for viscoelastic materials. To this purpose, the *reference response* of the structure is determined by means of modal and harmonic analyses performed on the reference configuration of the laminate described above. As described in Section 5.1, the *reference material properties* of the constitutive phases are implemented at the microscopic scale in order to determine the *reference effective viscoelastic properties* of the single lamina. Due to the viscoelastic behaviour of the matrix, the lamina elastic properties depend upon the frequency. This variation is determined by generalising, to the viscoelastic case, the well-known homogenisation technique for periodic media based on the strain energy (Barbero, 2007), as detailed in Section 4.1. Finally, the *reference harmonic response* and the *reference natural frequencies* of the laminate are determined, at the macroscopic scale, on a FE model of the multilayer plate making use of the reference properties provided by the homogenisation method.

In order to easily follow the flow of information throughout the manuscript, Table 2 lists all the adopted models, techniques and methods which are needed to achieve the ambitious goal of the multiscale identification of the viscoelastic behaviour of the composite.

2.2. The Bagley–Torvik viscoelastic material model

Composite structures show a dynamical behaviour that is significantly influenced by the damping capability of the matrix. The time-dependent response of materials can be classified into elastic (crystalline materials), viscous and viscoelastic. A viscoelastic material can be characterised by either a linear or a non-linear time-strain relationship and it can be in the form of a liquid (unrecoverable viscous flow) or a solid (fully recoverable viscous deformation).

From a numerical point of view, different linear viscoelastic material models are available in the literature. These models are usually implemented to fit experimental data (usually creep and relaxation tests) (Barbero, 2007; Krasnobrizha, 2015). The most common models are: (a) Maxwell model; (b) Kelvin–Voigt model; (c) Zener model; (d) power law-based models; (e) Prony series-based models; (f) generalised Kelvin model. These models differ essentially in terms of the number of parameters required to get the best possible fitting of experimental data. However, these laws are usually applied in the *α-region* of polymer creep (the characteristic time of the load application varies from seconds to years) (Barbero, 2007). Nevertheless, when looking at the frequency range characterising the application presented in this study (see Section 5.1), one can state that harmonic excitation falls in the *β-region* of polymer creep (Barbero, 2007); accordingly, a different viscoelastic model must be considered.

The effectiveness of a mathematical model in describing the viscoelastic behaviour of a given material can be seen as the ability of fitting a set of data points by using the least number of parameters tuning the model. Moreover, from a computational viewpoint and for optimisation purposes, the interest is always to have a limited number of parameters to be identified without reducing the accuracy of the model. Among the most effective mathematical representations of the viscoelasticity, the models based on fractional derivatives have been widely studied in the last three decades (Krasnobrizha, 2015). For such models, the general constitutive law reads:

$$\sigma(t) + b^m D^{\beta^m}\sigma(t) = E_0^m \varepsilon(t) + E_1^m D^{\alpha^m}\sigma(t),$$
$$\text{where } \alpha^m,\ \beta^m,\ E_0^m,\ E_1^m,\ b^m \in \mathbb{R}. \tag{1}$$

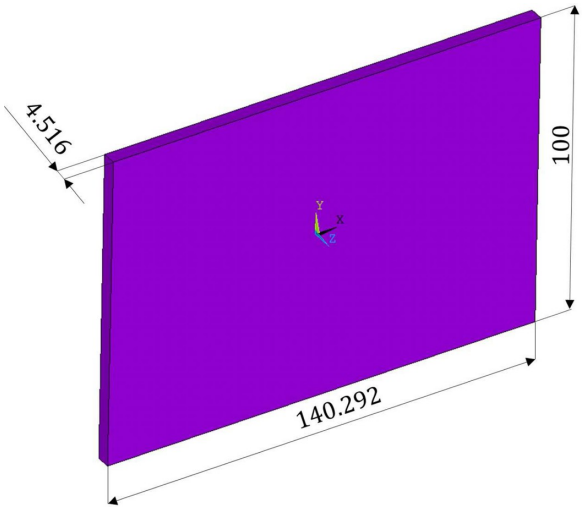

Fig. 1. Geometrical parameters of the reference composite plate (sizes in mm).

Table 1
Reference material properties for the fibre $T650/35-3K$ and the epoxy matrix $F584$ (taken from Soutis and Beaumont, 2005; Hexcell Corporation, 2016; Cappelli et al., 2018).

Fibre properties				
E_1^f [MPa]	E_2^f [MPa]	ν_{12}^f	ν_{23}^f	G_{12}^f [MPa]
276000	17,300	0.25	0.428	11240
Matrix properties				
E_0^m [MPa]	E_1^m [MPa]	b^m	$\alpha^m = \beta^m$	ν^m
4140	30	0.0053	0.5	0.35

In Eq. (1), D^α is the fractional derivative operator which represents a generalisation of the concept of derivative of a function. Consider a function $f \in L_1([a, b]) \mid a, b \in \mathbb{R}$. If $\alpha \in \mathbb{R}_+^*$, the fractional derivative of order α is defined as the fractional integral of order $n - \alpha$ derived n times (Riemann–Liouville definition - RL):

$$(D_a^\alpha f)_{RL}(x) = \frac{1}{\Gamma(1-\alpha)} \frac{d}{dx} \int_a^x \frac{f(x)}{(x-t)^\alpha} dt, \quad \text{where} \quad 0 < \alpha < 1. \tag{2}$$

The function $\Gamma(z)$, with $z \in \mathbb{R}_+^*$, is the extension of the factorial function to real numbers. The reader is addressed to Krasnobrizha (2015) and Krasnobrizha et al. (2016) for further information concerning the mathematical formulation.

The fractional derivative model has been generalised to materials presenting a reticular complex molecular structure, because the choice of $0 < \alpha < 1$ well reproduces the relaxation function of different kind of polymers, as widely discussed in Schiessel et al. (2000). The Fast Fourier Transform (FFT, whose operator is indicated as F) of the fractional derivative operator can be computed as:

$$F[(D_a^\alpha f)_{RL}(x)] = (\Omega \mathrm{i})^\alpha F[f(x)], \quad \forall\, \alpha \in \mathbb{R}_+^* \mid 0 < \alpha < 1 \wedge \forall\, x \in \mathbb{R}_+, \tag{3}$$

where Ω is the frequency and i the imaginary unit. It is noteworthy that working in frequency domain allows dealing with a very simple mathematical expression of the fractional derivative operator. Applying the FFT to Eq. (1), one obtains

$$\hat{\sigma}(\Omega) = F[\sigma(t)] = F[E^m(t)]F[\varepsilon(t)] = \hat{E}^m(\Omega)\hat{\varepsilon}(\Omega), \tag{4}$$

where the relaxation modulus $\hat{E}^m(\Omega \mathrm{i})$ reads (Bagley and Torvik, 1986)

$$\hat{E}^m(\Omega) = \frac{E_0^m + E_1^m(\Omega \mathrm{i})^{\alpha^m}}{1 + b^m(\Omega \mathrm{i})^{\beta^m}}, \tag{5}$$

that represents the Bagley–Torvik viscoelastic model. It can be observed that, when $\Omega \mapsto +\infty$, the relaxation modulus of the matrix $\hat{E}^m(\Omega) \mapsto \frac{E_1^m}{b^m}(i\Omega)^{\alpha^m - \beta^m}$ (vitreous domain). Otherwise, when $\Omega \mapsto 0$, the relaxation modulus tends to the elastic constant E_0^m. However, a reliable viscoelastic model must be characterised by a non-negative internal work and a non-negative rate of dissipation, as highlighted in Bagley and Torvik (1986). In order to ensure these thermodynamical properties, the material parameters must satisfy the following relationships:

$$0 < \alpha^m = \beta^m < 1, \; E_0^m > 0 \text{ and } E_1^m > E_0^m b^m. \tag{6}$$

Therefore, only four parameters are needed to describe the viscoelastic behaviour of the considered polymeric matrix.

2.3. The multi-scale identification strategy

The goal of the MSIS is to find the optimum value of the parameters tuning the viscoelastic behaviour of the composite, at each scale, by smartly exploiting the information restrained into the harmonic response, measured in some precise locations, of the multilayer plate.

The reference response can be obtained either by a non-destructive experimental harmonic test (e.g. performed with shaker, hammer or solenoidal excitation system) or by carrying out a numerical harmonic test on the reference structure. This work deals with the latter case: the reference configuration of the multilayer plate as well as the reference dynamical results are presented in Section 5.2.

The MSIS aims to identify the parameters defining both the elastic behaviour of the fibre and the viscoelastic behaviour of the matrix by using the information available into the dynamical response of the composite at the macroscopic scale. The proposed approach relies on some hypotheses. As far as the microscopic scale is concerned, the following assumptions are considered:

- the matrix has a viscoelastic isotropic behaviour, described by the Bagley–Torvik model, with a constant Poisson's ratio according to Luciano and Barbero (1995);
- the fibre has an elastic transversely isotropic behaviour;
- the fibre-matrix interface is perfect (i.e. perfect bonding condition between the two phases).

Regarding the mesoscopic and macroscopic scales, the following hypotheses apply:

- the constitutive lamina has a viscoelastic orthotropic behaviour with only six parameters, due to the plane of symmetries characterising the considered Representative Volume Element (RVE), as shown in Fig. 3a;
- perfect bonding condition at the interface between two consecutive plies;
- the first-order shear deformation theory (FSDT) is considered to describe the kinematics of the multilayer plate.

The general flow-chart of the *one-shot* MSIS for viscoelastic materials is shown in Fig. 2.

3. Mathematical formulation of the multi-scale inverse problem

3.1. Optimisation variables, objective function and constraints

The multi-scale identification problem considered in this work is formulated as a classical inverse problem: the goal is the determination of the material properties of the constitutive phases of the composite by minimising the euclidean distance between the reference harmonic response at macroscopic scale and that provided by the numerical simulation.

Table 2
Models, techniques and methods used in this study.

Model / Technique / Method	Role
The Bagley–Torvik model	Used to define the viscoelastic behaviour of the matrix
Strain energy homogenisation technique	Used to perform the microscopic/mesoscopic scale transition
Finite Element Method	Used to model both the RVE of the composite and the multilayer plate at microscopic and macroscopic scales, respectively
Non-Linear Arnoldi's method	Used to solve the non-linear eigenvalue problem at the macroscopic scale
GA ERASMUS	Used to perform the global search of optimal solutions for the multi-scale identification problem
Automatic Dynamic Penalisation Method	Used to handle optimisation constraints during the global search stage
fmincon tool and *active-set* algorithm	Used to perform the local search of optimal solutions for the multi-scale identification problem

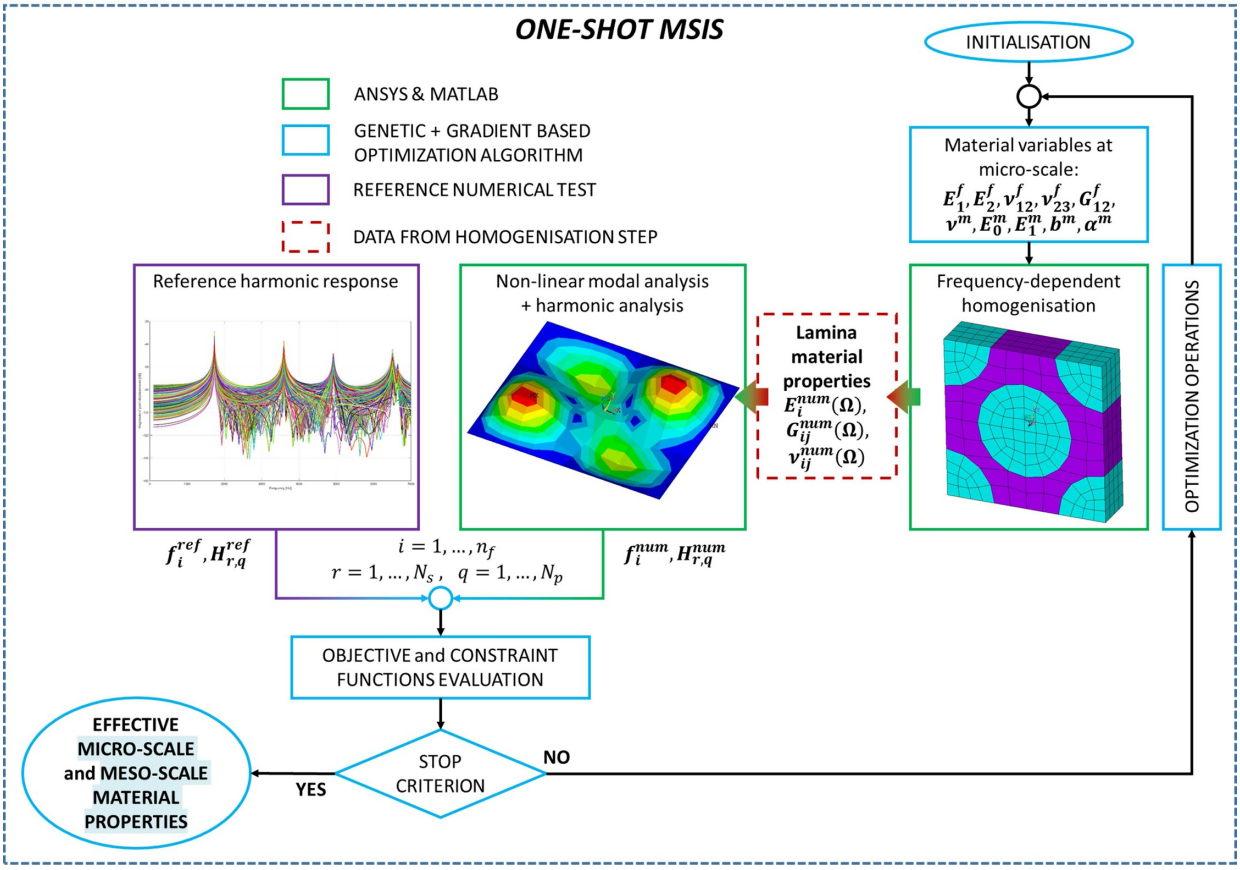

Fig. 2. Flow-chart of the *one-shot* MSIS.

According to the hypotheses introduced in Section 2, the effective elastic properties of the ply depend upon the frequency (due to the viscoelastic behaviour of the matrix) and must be computed through a suitable numerical homogenisation procedure. To achieve this task, a dedicated FE model of the RVE at the microscopic scale is built to perform the numerical homogenisation: the results are the frequency-dependent elastic constants of the lamina. In this analysis, the fibre volume fraction V_f is set up *a priori*, because usually it is a value that the manufacturer can provide reliably, as highlighted also in Cappelli et al. (2018).

Considering the behaviour of the constituent phases, as discussed in Section 2.3, the design variables of the inverse problem, i.e. the material parameters to be identified, are five elastic constants for the fibre, supposed to have a transversely isotropic behaviour and five parameters tuning the law of the isotropic viscoelastic matrix. In particular, as discussed in Cappelli et al. (2018), the fibre Poisson's coefficient ν_{23}^f is not considered among the design variables due to negligible sensitivity of the harmonic and modal responses of the plate to this parameter. Indeed, the reference plate (illustrated in Fig. 1) is very thin and ν_{23}^f does not significantly influences the macroscopic dynamical response of the structure. Accordingly, ν_{23}^f has been set to the reference value given in Table 1. Therefore, only *nine* material properties characterise the composite at the microscopic scale. They can be collected in the vector of design variables $\mathbf{x}$, as:

$$\mathbf{x} = \{E_1^f,\, E_2^f,\, G_{12}^f,\, \nu_{12}^f,\, E_0^m,\, E_1^m,\, b^m,\, \alpha^m,\, \nu^m\}. \tag{7}$$

In order to guarantee the positive definiteness of fibre and matrix stiffness tensors (Cappelli et al., 2018) and the thermodynamic requirements related to the viscoelastic behaviour of the matrix (see Section 2.2), the following set of non-linear constraints must be considered:

$$\begin{aligned}
g_1(\mathbf{x}) &= |\nu_{12}^f| - \sqrt{\frac{E_1^f}{E_2^f}} < 0,\\
g_2(\mathbf{x}) &= \frac{E_1^f}{E_2^f}\left(2\nu_{23}^f \nu_{12}^{f\,2} + 2\nu_{12}^{f\,2}\right) - 1 < 0,\\
g_3(\mathbf{x}) &= -E_1^m + E_0^m b^m < 0,\\
g_4(\mathbf{x}) &= -\alpha^m < 0,\\
g_5(\mathbf{x}) &= -E_0^m < 0,\\
g_6(\mathbf{x}) &= \nu^m - \frac{1}{2} < 0,\\
g_7(\mathbf{x}) &= -\nu^m - 1 < 0.
\end{aligned} \tag{8}$$

Table 3
Lower and upper bounds of the design variables for the multi-scale inverse problem.

Material properties	Lower bound	Upper bound
E_1^f [MPa]	220,800	331,200
E_2^f [MPa]	13,840	20,760
ν_{12}^f	0.2	0.3
G_{12}^f [MPa]	8992	13,488
E_0^m [MPa]	3312	4968
E_1^m [MPa]	24	36
b^m	0.00424	0.00636
α^m	0.4	0.6
ν^m	0.28	0.42

In order to get a numerical harmonic spectrum really close to the reference one (and also to match the reference damped natural frequencies), a set of constraints on the laminate (damped) eigenfrequencies must be integrated into the problem formulation:

$$g_{7+i}(\mathbf{x}) = \left| \frac{f_{in} - f_{in}^{\text{ref}}}{f_{in}^{\text{ref}}} \right| - \epsilon_i \leq 0, \quad i = 1, \ldots, n_f. \tag{9}$$

In Eq. (9), n_f is the number of damped natural frequencies falling in the selected frequency spectrum range (as discussed in Section 5.1), whilst f_{in} and f_{in}^{ref} are the ith computed and reference damped eigenfrequency, respectively. ϵ_i is a user-defined tolerance that establish the relative error for each eigenfrequency: here, a maximum relative error equal to 0.005 is chosen.

The microscopic material parameters vary within the design space defined in Table 3.

The objective function $\Phi(\mathbf{x})$ is defined by introducing an Euclidean distance between the reference and the numerical harmonic responses, both for real and imaginary parts. In particular, an error estimator of the least-squares type has been chosen:

$$\Phi(\mathbf{x}) = \sum_{q=1}^{N_p} \sum_{r=1}^{N_s} 2 \left(\frac{f_r - f_r^{\text{ref}}}{f_r^{\text{ref}}} \right)^2 + \left[\frac{\Re(H_{r,q}(\mathbf{x}) - H_{r,q}^{\text{ref}})}{\Re(H_{r,q}^{\text{ref}})} \right]^2 + \left[\frac{\Im(H_{r,q}(\mathbf{x}) - H_{r,q}^{\text{ref}})}{\Im(H_{r,q}^{\text{ref}})} \right]^2. \tag{10}$$

In Eq. (10), f_r is the rth sampled frequency, while $H_{r,q}$ is the FFT of the FRF determined at the qth sample point of the multilayer plate and evaluated at the rth sampled frequency. Of course, f_r^{ref}, $H_{r,q}^{\text{ref}}$ are the same quantities evaluated on the reference configuration of the laminate. $\Re(\cdots)$ and $\Im(\cdots)$ represent real and imaginary parts, whilst N_s and N_p are the number of sampled frequencies and of sample points over the laminate plate (where the FRF is computed/measured), respectively. These quantities are detailed in Sections 4 and 5.2.

Finally, the multi-scale inverse problem can be stated as a classical CNLPP:

$$\begin{aligned} &\min_{\mathbf{x}} \Phi(\mathbf{x}), \\ &\text{subject to:} \\ &g_j(\mathbf{x}) \leq 0, \quad j = 1, \ldots, 7 + n_f. \end{aligned} \tag{11}$$

3.2. The numerical strategy

Problem (11) is highly non-linear in terms of both constraint and objective functions, see Eqs. (8)–(10).

For inverse problems, the uniqueness of solution is not *a priori* guaranteed: the set of parameters matching a given *observed state* may not be unique. Nevertheless, no proved theoretical rules exist in literature (Sun, 1999; Tarantola, 1988) to define the number of data points N_p for a given number of unknowns (n) that have to be identified. Often, the inverse problem is stated as a CNLPP and it can be viewed as an *over-determined system of equations* (Sun, 1999; Tarantola, 1988). Since more observation points than parameters exist (N_p is usually much greater than n) there are more equations than unknowns. If an optimal point exists, it may be not unique, thus implying the existence of many combinations of parameters that result to be equivalent optimal solutions for the CNLPP at hand.

Considering all these aspects and according to the practice always employed in the literature, in this work a number of observed states (i.e. sample points N_p) greater than two times the number of design variables n has been considered. As explained in the next Section, the number of sample points has been inferred by means of a numerical sensitivity analysis of the FRF of the plate with respect to parameter N_p: as a results $N_p = 329$ has been chosen to properly perform the optimisation calculations.

Taking into account all of the aforementioned points, a hybrid optimisation tool composed of the genetic algorithm (GA) ERASMUS (EvolutionaRy Algorithm for optimiSation of ModUlar Systems) developed by Montemurro (2018), interfaced with the MATLAB *fmincon* algorithm (The Math Works Inc., 2017), has been used. The GA ERASMUS has already been successfully applied to solve different kinds of real-world engineering problems, see for instance (Montemurro et al., 2016; Costa et al., 2018; Montemurro and Catapano, 2016; 2017; Montemurro et al., 2019; Panettieri et al., 2019; Montemurro et al., 2018).

As shown in Fig. 2, the optimisation procedure for problem (11) is split in two phases. During the first phase, solely the GA ERASMUS is used to perform the solution search. Due to the strong non-linearity of problem (11), the aim of the genetic calculation is to provide a potential sub-optimal point in the design space, which constitutes the initial guess for the subsequent phase, i.e. the local optimisation, where the MATLAB *fmincon* tool is employed to finalise the solution search. The optimisation algorithm is the *active-set* which is a Quasi-Newton method making use of an approximation of the Hessian matrix to estimate the descent direction. For more details on the active-set algorithm see The Math Works Inc. (2017).

For the resolution of the multi-scale inverse problem, both optimisation algorithms have been interfaced with the FE models of the multilayer plate at two different scales: microscopic (constitutive phases-level) and macroscopic (laminate-level). As shown in Fig. 2, for each individual at each generation, the optimisation tool performs three different types of FE analyses:

1. an homogenisation analysis to determine the frequency-dependent equivalent elastic properties of the lamina (microscopic / macroscopic scale transition);
2. a non-linear modal analysis (by means of a suitable in-house coded solver) to extract the n_f natural frequencies;
3. a non-linear harmonic analysis for the evaluation of the FRF of the laminate.

Then, the optimisation algorithm elaborates the results provided by the two FE analyses in order to execute the optimisation operations on the basis of the current value of both objective and constraint functions. These operations are repeated until the algorithm satisfies the user-defined convergence criterion. The details of the FE analyses are given in Section 4.

The number of design variables and that of constraint functions is *nine* and $n_f + 7$, respectively. The generic individual of the GA ERASMUS represents a potential solution for the problem at hand. The genotype of the individual for problem (11) is characterised by only one chromosome composed of *nine* genes, each one coding a component of the vector of design variables, see Eq. (7).

4. Finite element models at different scales

4.1. The finite element model at the microscopic scale and the homogenisation strategy

The microscopic / macroscopic scale transition is carried out through a homogenisation step performed on the RVE shown in Fig. 3a.

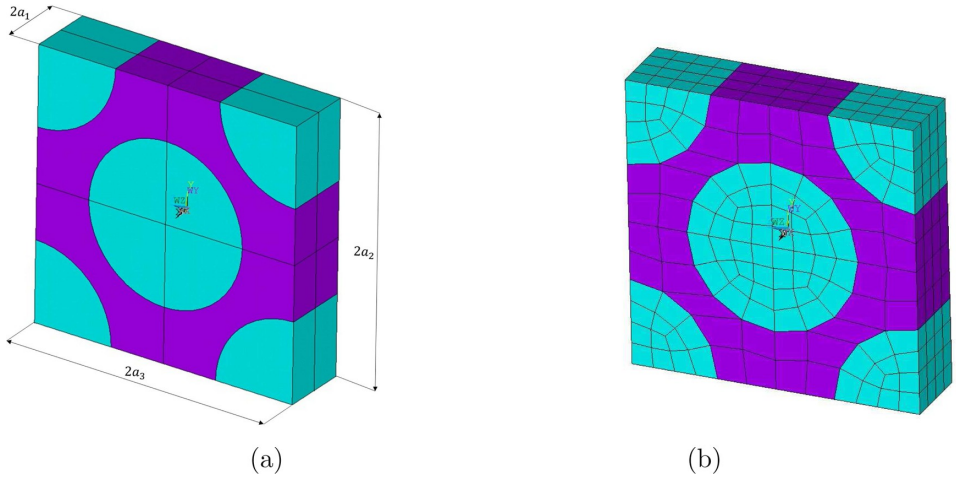

Fig. 3. (a) The reference Representative Volume element (RVE) and (b) details of the RVE mesh.

The frequency-dependent elastic properties of the ply are obtained by means of the strain energy homogenisation technique (SEHT) of periodic media (Barbero, 2007; Cappelli et al., 2018). This technique, originally introduced for elastic heterogeneous materials, can be generalised to different kinds of composites showing a general non-linear behaviour, e.g. fabrics, lattice structures, etc. This technique has already been successfully used in other works, see (Montemurro et al., 2016; 2012; Catapano and Montemurro, 2014a; 2014b): in this work, the SEHT is generalised to the case of viscoelastic materials subjected to harmonic loads. The SEHT is based on the main hypothesis that the RVE of the periodic heterogeneous material and the corresponding homogenised volume undergo the same deformation having, hence, the same strain energy. Consequently, at the ply scale, an equivalent homogeneous anisotropic material replaces the heterogeneous medium, by using the frequency-dependent stiffness tensor resulting from the homogenisation phase.

In this study, the real random micro-structure of the lamina (which is usually characterised by misalignments of the fibres, porosity, damaged zones, etc.) is not taken into account and the topology of the RVE is described by a perfect hexagonal array, as illustrated in Fig. 3a. The FE model of the RVE has been realised into the commercial FE code ANSYS®. A 20-node solid element (SOLID186) with three degrees of freedom (DOFs) per node has been used. The model together with its structured mesh is shown in Fig. 3b. A sensitivity study (not reported here for the sake of brevity) on the proposed FE model with respect to the mesh size has been conducted: it was observed that a mesh having 19551 DOFs is sufficient to properly evaluate the set of frequency-dependent homogenised elastic properties of the lamina.

The RVE is submitted to an average strain field $\bar{\varepsilon}_{ij}$ (tensor notation), to evaluate the stiffness matrix components $\bar{C}_{ij}$. The six components of the average strain tensor are applied, by means of the classical periodic boundary conditions (PBCs) as follows (Barbero, 2007; Cappelli et al., 2018):

$$\begin{aligned} &u_i(a_1, x_2, x_3) - u_i(-a_1, x_2, x_3) = 2a_1\bar{\varepsilon}_{i1}, \quad -a_2 \le x_2 \le a_2, -a_3 \le x_3 \le a_3,\\ &u_i(x_1, a_2, x_3) - u_i(x_1, -a_2, x_3) = 2a_2\bar{\varepsilon}_{i2}, \quad -a_1 \le x_1 \le a_1, -a_3 \le x_3 \le a_3,\\ &u_i(x_1, x_2, a_3) - u_i(x_1, x_2, -a_3) = 2a_3\bar{\varepsilon}_{i3}, \quad -a_1 \le x_1 \le a_1, -a_2 \le x_2 \le a_2,\\ &\text{where } i = 1, 2, 3. \end{aligned} \tag{12}$$

As stated above, the RVE is subjected to harmonic excitations, in order to compute the frequency-dependent elastic properties at the upper scale. Consequently, the internal stresses σ_α and strains ε_α, $\alpha = 1, ...,6$ (Voigt's notation) vary harmonically with different amplitudes and phases, for each RVE internal point $\mathbf{x_p}$:

$$\sigma_\alpha(f_0, \mathbf{x_p}, t) = |\sigma_\alpha(f_0, \mathbf{x_p})| \exp[(2\pi f_0 t + \varphi_{\sigma_\alpha}(f_0, \mathbf{x_p}))\mathrm{i}], \tag{13}$$

$$\varepsilon_\alpha(f_0, \mathbf{x_p}, t) = |\varepsilon_\alpha(f_0, \mathbf{x_p})| \exp[(2\pi f_0 t + \varphi_{\varepsilon_\alpha}(f_0, \mathbf{x_p}))\mathrm{i}]. \tag{14}$$

The equivalent stresses and strains at the lamina-level can be evaluated from the corresponding fields by considering an average over the RVE volume, i.e.

$$\begin{aligned} \bar{\sigma}_\alpha(f_0, t) &= \langle \sigma_\alpha(f_0, \mathbf{x_p}, t)\rangle \\ &= \frac{\exp[(2\pi f_0 t)\mathrm{i}]}{V_{\mathrm{RVE}}} \int_{V_{\mathrm{RVE}}} |\sigma_\alpha(f_0, \mathbf{x_p})| \exp[\varphi_{\sigma_\alpha}(f_0, \mathbf{x_p})\mathrm{i}]dV, \end{aligned} \tag{15}$$

$$\begin{aligned} \bar{\varepsilon}_\alpha(f_0, t) &= \langle \varepsilon_\alpha(f_0, \mathbf{x_p}, t)\rangle \\ &= \frac{\exp[(2\pi f_0 t)\mathrm{i}]}{V_{\mathrm{RVE}}} \int_{V_{\mathrm{RVE}}} |\varepsilon_\alpha(f_0, \mathbf{x_p})| \exp[\varphi_{\varepsilon_\alpha}(f_0, \mathbf{x_p})\mathrm{i}]dV. \end{aligned} \tag{16}$$

where $V_{\mathrm{RVE}} = 8a_1a_2a_3$ according to Fig. 3.

The internal RVE stresses and strains of Eqs. (13) and (14) can also be written in the Laplace–Carson (L is the related operator) space:

$$\sigma^*_\alpha(f_0, \mathbf{x_p}, f) = L[\sigma_\alpha(f_0, \mathbf{x_p}, t)] = \frac{|\sigma_\alpha(f_0, \mathbf{x_p})| \exp[\varphi_{\sigma_\alpha}(f_0, \mathbf{x_p})\mathrm{i}]}{2\pi(f - f_0)\mathrm{i}}, \tag{17}$$

$$\varepsilon^*_\alpha(f_0, \mathbf{x_p}, f) = L[\varepsilon_\alpha(f_0, \mathbf{x_p}, t)] = \frac{|\varepsilon_\alpha(f_0, \mathbf{x_p})| \exp[\varphi_{\varepsilon_\alpha}(f_0, \mathbf{x_p})\mathrm{i}]}{2\pi(f - f_0)\mathrm{i}}. \tag{18}$$

By following the same logical steps, also the average stresses and strains components of Eqs. (15) and (16) can be written in the Laplace-Carson L space:

$$\begin{aligned} \bar{\sigma}^*_\alpha(f_0, f) &= L[\bar{\sigma}_\alpha(f_0, t)] \\ &= \frac{1}{V_{\mathrm{RVE}}2\pi(f - f_0)\mathrm{i}} \int_{V_{\mathrm{RVE}}} |\sigma_\alpha(f_0, \mathbf{x_p})| \exp[\varphi_{\sigma_\alpha}(f_0, \mathbf{x_p})\mathrm{i}]dV, \end{aligned} \tag{19}$$

$$\begin{aligned} \bar{\varepsilon}^*_\alpha(f_0, f) &= L[\bar{\varepsilon}_\alpha(f_0, t)] \\ &= \frac{1}{V_{\mathrm{RVE}}2\pi(f - f_0)\mathrm{i}} \int_{V_{\mathrm{RVE}}} |\varepsilon_\alpha(f_0, \mathbf{x_p})| \exp[\varphi_{\varepsilon_\alpha}(f_0, \mathbf{x_p})\mathrm{i}]dV. \end{aligned} \tag{20}$$

In order to perform the numerical homogenisation process,

Table 4
Material properties of the fibre and the matrix used to illustrate the effectiveness of the homogenisation procedure.

Fibre properties				
E_1^f [MPa]	E_2^f [MPa]	ν_{12}^f	ν_{23}^f	G_{12}^f [MPa]
275622	20,435	0.32	0.451	10693
Matrix properties				
E_0^m [MPa]	E_1^m [MPa]	b^m	$\alpha^m = \beta^m$	ν^m
3000	30	0.0053	0.5	0.33

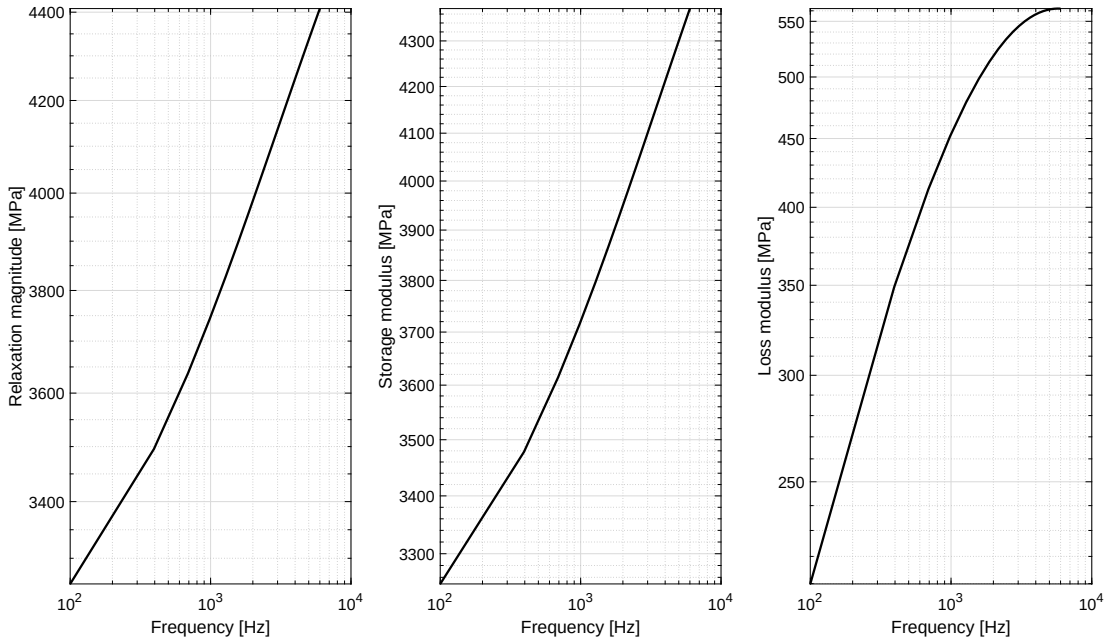

Fig. 4. Matrix Young's modulus vs. frequency (amplitude, real and imaginary parts).

harmonic analyses are required and the imposed strain field, applied through the PBCs of Eq. (12), reads:

$$\bar{\varepsilon}^*_\alpha(f_0, f) = L[\bar{\varepsilon}_\alpha(f_0, t)] = \frac{|\bar{\varepsilon}_\alpha(f_0)|}{V 2\pi(f - f_0)\mathrm{i}}, \quad \forall \ \ \alpha = 1, ..., 6, \ \text{ with}$$
$$\bar{\varepsilon}^*_\beta(f_0, f) = 0 \ \forall \ \ \beta = 1, ..., 6 \text{ and } \beta \neq \alpha. \tag{21}$$

Finally, the frequency-dependent components of the homogenised stiffness complex tensor $\bar{C}_{\alpha\beta}$ of the lamina can be evaluated as:

$$\bar{C}_{\alpha\beta}(f_0) = \frac{\bar{\sigma}^*_\alpha(f_0, f)}{\bar{\varepsilon}^*_\beta(f_0, f)} = \frac{1}{V_{\mathrm{RVE}}|\bar{\varepsilon}_\beta(f_0)|} \int_{V_{\mathrm{RVE}}} |\sigma_\alpha(f_0, \mathbf{x_p})| \exp[\varphi_{\sigma_\alpha}(f_0, \mathbf{x_p})\mathrm{i}] dV, \tag{22}$$

$$\Re[\bar{C}_{\alpha\beta}(f_0)] = \frac{1}{V_{\mathrm{RVE}}|\bar{\varepsilon}_\beta(f_0)|} \int_{V_{\mathrm{RVE}}} |\sigma_\alpha(f_0, \mathbf{x_p})| \cos[\varphi_{\sigma_\alpha}(f_0, \mathbf{x_p})] dV, \tag{23}$$

$$\Im[\bar{C}_{\alpha\beta}(f_0)] = \frac{1}{V_{\mathrm{RVE}}|\bar{\varepsilon}_\beta(f_0)|} \int_{V_{\mathrm{RVE}}} |\sigma_\alpha(f_0, \mathbf{x_p})| \sin[\varphi_{\sigma_\alpha}(f_0, \mathbf{x_p})] dV. \tag{24}$$

Even in the case of a complex stiffness tensor, the compliance matrix at a given frequency f_0 can be determined as: $\bar{\mathbf{S}}(f_0) = \bar{\mathbf{C}}^{-1}(f_0)$. Finally, the frequency-dependent lamina (complex) elastic properties can be computed from the components of the compliance matrix (Barbero, 2007).

To give an idea of the homogenisation of the frequency-dependent elastic properties of the lamina at the mesoscopic scale, an analysis is performed by considering the material properties of the constitutive phases listed in Table 4, in the frequency range $f \in [100, 6000]$ Hz.

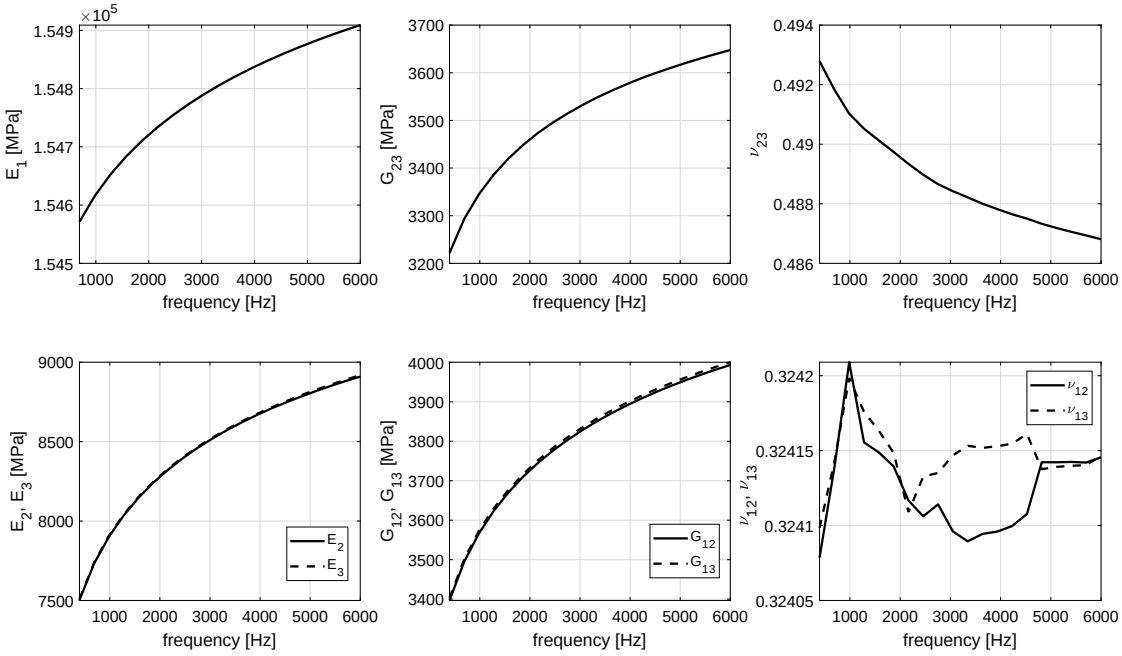

Fig. 5. Frequency-dependent elastic properties (amplitude) of the lamina resulting from the homogenisation.

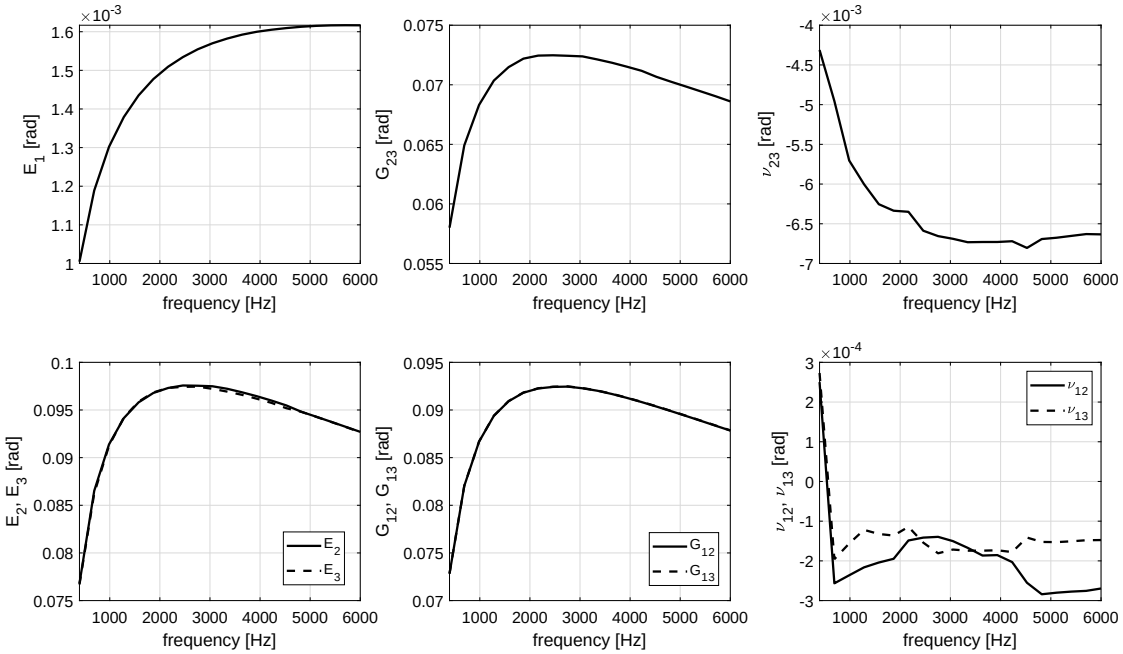

Fig. 6. Frequency-dependent elastic properties (phase) of the lamina resulting from the homogenisation.

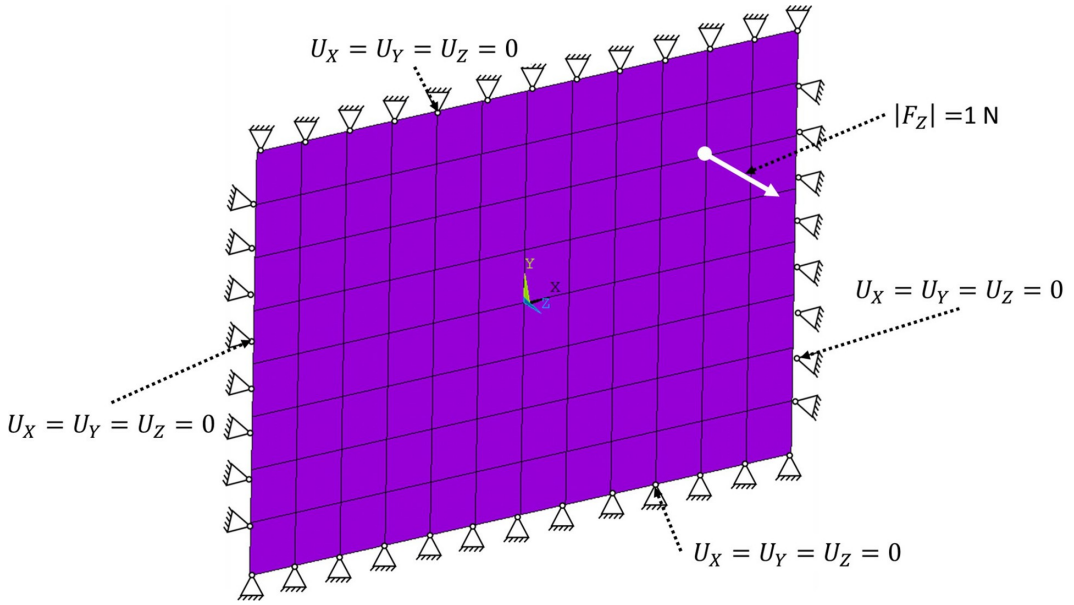

Fig. 7. FE model of the multilayer plate.

Fig. 4 illustrates the viscoelastic behaviour of the matrix, represented through the Bagley–Torvik model: the storage and the loss moduli are respectively the real and the imaginary part of the matrix Young's modulus. The trend of the engineering moduli of the lamina vs. the frequency is give in Figs. 5 and 6. As it can be easily inferred from these figures, the lamina Poisson's ratios, namely ν_{12}, ν_{13} and ν_{23}, can be considered constant with the frequency. This result is of paramount importance to reduce the required computational effort for the multiscale identification process.

4.2. The finite element model at the macroscopic scale

The FE model of the multilayer plate is built into the ANSYS® environment (Ansys, 2013) by using SHELL281 layered shell elements with eight nodes and six DOFs per node: the plate kinematics is described by the FSDT (Jones, 1975).

The laminate together with the applied excitation load and boundary conditions (BCs) is illustrated in Fig. 7: the model is characterised by 1974 DOFs and the mesh size has been chosen after a convergence study (not reported here for the sake of brevity). The choice of shell elements is due to the aspect ratio of the considered laminate ($AR = 22.14$), which is in the range [20, 100] where the FSDT gives satisfactory results.

As far as the assessment of both the constraint functions of Eqs. (8) and (9) and the objective function of Eq. (10) two macroscopic FE analyses are run for each point of the design space. Firstly, a non-linear modal analysis is performed to extract the first n_f damped natural frequencies and, secondly, a non-linear harmonic analysis is carried out to calculate the harmonic response of the plate for each sampling harmonic frequency of the chosen spectrum (Section 5.1). The *harmonic*

Table 5
Reference damped natural frequencies.

Nat. freq.	Value [Hz]
f_{1n}^{ref}	1716.34
f_{2n}^{ref}	3626.36
f_{3n}^{ref}	4758.54
f_{4n}^{ref}	6481.66
f_{5n}^{ref}	6677.52

response is obtained by measuring the displacement u_z at the generic node of the macroscopic FE model mesh, at every sampled frequency f_r, as shown in Fig. 8.

The *harmonic response* can be obtained by solving the following problem (Hamdaoui et al., 2015; Daya and Potier-Ferry, 2001; Bilasse et al., 2009):

$$[\mathbf{K}^{sys}(\Omega) - \lambda \mathbf{M}^{sys}]\{U^{sys}\} = \{f^{ext}\}, \tag{25}$$

where $\mathbf{K}^{sys}(\Omega)$, $\mathbf{M}^{sys}$, $\{U^{sys}\}$ and $\{f^{ext}\}$ are the stiffness matrix (which depends upon the pulsation $\Omega = \Re\left[\lambda^{\frac{1}{2}}\right]$ due to the viscoelastic matrix behaviour), the mass matrix, the nodal displacements vector and the external nodal forces, respectively.

The harmonic response, for each sample point, is obtained by evaluating the ratio of the FFT of the displacement along the z-axis $u_{zq}(f_r)$ to the nodal force along the same direction $F_z(f_r)$:

$$H_{r,q} = \frac{u_{zq}(f_r)}{F_z(f_r)}. \tag{26}$$

It is noteworthy that the problem of determining the structure natural frequencies becomes non-linear due to the viscoelastic behaviour of the ply. The following non-linear eigenvalue problem must be faced:

$$\begin{aligned} &[\mathbf{K}^{sys}(\Omega) - \lambda \mathbf{M}^{sys}]\{U^{sys}\} = \{0\}, \\ &\det[\mathbf{K}^{sys}(\Omega) - \lambda \mathbf{M}^{sys}] = 0, \\ &(\lambda, \{U^{sys}\}) \in \mathbb{C} \times \mathbb{C}^n. \end{aligned} \tag{27}$$

Unfortunately, the non-linear eigenvalue problem of Eq. (27) cannot be solved by means of commercial FE codes because it requires a dedicated algorithm / solver. Some research works are explicitely devoted to the implementation of a suitable algorithm for solving non-linear eigenvalue problems. As discussed in Hamdaoui et al. (2016), several algorithms are available in the literature: the asymptotic numerical method (ANM) (Daya and Potier-Ferry, 2001), the inverse iteration algorithm (IIA) Schreiber, the iterative shift-inverter method (ISIM) (Moler and Stewart, 1973), the non-linear Jacobi–Davidson method (NLJDM) (Voss, 2007) and the non-linear Arnoldi's method (NLAM) (Voss, 2004). Each method is characterised by its own advantages and drawbacks: in this work, the NLAM has been implemented into the MATLAB environment and interfaced with the FE model of the multilayer plate implemented into the ANSYS software.

In particular, the stiffness matrix of the FE model is recovered from ANSYS® and exported (and elaborated) into the MATLAB® software. The frequency-dependent stiffness matrix of the FE model can be expressed as:

$$\mathbf{K}^{sys}(\Omega) = \Re[\mathbf{K}^{sys}(\Omega)] + \mathrm{i}\Im[\mathbf{K}^{sys}(\Omega)]. \tag{28}$$

The stiffness matrix of the structure depends upon the frequency because of the viscoelastic behaviour of the ply (due to the matrix), see Eq. (22). However, this means that the numerical homogenisation method, discussed in Section 4.1, must be performed for each sampled frequency in the considered range. This would require a strong computational effort (and simulation time) which is not acceptable for optimisation purposes. This issue can be easily overcome by looking at the volume-averged stress tensor of Eq. (19) which can be expressed in the following form:

$$\bar{\boldsymbol{\sigma}}(\Omega) = \frac{1}{V_{\text{RVE}}} \int_{V_f V_{\text{RVE}}} \boldsymbol{\sigma}^f(\mathbf{x_p}) dV + \frac{1}{V_{\text{RVE}}} \int_{(1-V_f)V_{\text{RVE}}} \boldsymbol{\sigma}^m(\mathbf{x_p}) dV. \tag{29}$$

Since the Poisson's ratio of the matrix ν_m does not depend upon the frequency, the previous expression can be rewritten as:

$$\begin{aligned} \bar{\boldsymbol{\sigma}}(\Omega, \bar{\boldsymbol{\varepsilon}}) &= \frac{1}{V_{\text{RVE}}} \int_{V_f V_{\text{RVE}}} \boldsymbol{\sigma}^f(\mathbf{x_p}, \bar{\boldsymbol{\varepsilon}}) dV + \ldots \\ &+ \frac{\hat{E}^m(\Omega)}{V_{\text{RVE}}} \int_{(1-V_f)V_{\text{RVE}}} \frac{1}{1+\nu^m} \left[\boldsymbol{\varepsilon}^m(\mathbf{x_p}, \bar{\boldsymbol{\varepsilon}}) + \frac{\nu^m}{1-2\nu^m} tr[\boldsymbol{\varepsilon}^m(\mathbf{x_p}, \bar{\boldsymbol{\varepsilon}})] \right] dV, \end{aligned} \tag{30}$$

therefore, the previous equation can be rearranged in a more compact form as follows

$$\begin{aligned} &\bar{\boldsymbol{\sigma}}(\Omega, \bar{\boldsymbol{\varepsilon}}) = \mathbf{M}(\bar{\boldsymbol{\varepsilon}}) + \hat{E}^m(\Omega)\mathbf{R}(\bar{\boldsymbol{\varepsilon}}), \\ &\mathbf{M}(\bar{\boldsymbol{\varepsilon}}) = \frac{1}{V_{\text{RVE}}} \int_{V_f V_{\text{RVE}}} \boldsymbol{\sigma}^f(\mathbf{x_p}, \bar{\boldsymbol{\varepsilon}}) dV, \\ &\mathbf{R}(\bar{\boldsymbol{\varepsilon}}) \\ &\quad = \frac{1}{V_{\text{RVE}}} \int_{(1-V_f)V_{\text{RVE}}} \frac{1}{1+\nu^m} \left[\boldsymbol{\varepsilon}^m(\mathbf{x_p}, \bar{\boldsymbol{\varepsilon}}) + \frac{\nu^m}{1-2\nu^m} tr[\boldsymbol{\varepsilon}^m(\mathbf{x_p}, \bar{\boldsymbol{\varepsilon}})] \right] dV. \end{aligned} \tag{31}$$

As a consequence of Eq. (32), the equivalent frequency-dependent stiffness matrix of the homogeneous anisotropic material of the ply can be evaluated as (Voigt's notation):

$$\bar{C}_{jk} = \frac{\bar{\sigma}_j}{\bar{\varepsilon}_k} = M_{jk} + \hat{E}^m(\Omega) R_{jk}, \quad \text{where} \quad j, k = 1, \ldots, 6. \tag{32}$$

It is straightforward to verify that the global stiffness matrix of the FE model at the macroscopic scale can be decomposed as follows:

$$\mathbf{K}^{sys}(\Omega) = \mathbf{K}_0^{sys} + \hat{E}^m(\Omega)\tilde{\mathbf{K}}^{sys}, \tag{33}$$

where $\mathbf{K}_0^{sys}$ is the term related to the constant part of the ply stiffness tensor, whilst $\tilde{\mathbf{K}}^{sys}$ is the contribution related to the frequency-dependent part.

Eqs. (32) and (33) allow obtaining the frequency-dependent stiffness matrices of the material and of the structure, respectively, directly within the ANSYS® software by means of only two homogenisation analyses carried out at two arbitrary frequencies (in this case the lower and the upper bounds of the considered frequency spectrum), instead of performing an homogenisation calculation (recall that each homogenisation corresponds to six FE analyses) for each sampled frequency in the considered range. Accordingly, the computational costs of the whole optimisation process is significantly reduced (the FE analyses at both microscopic and macroscopic scales must be carried out for each

Table 6
Sampling sequence for FRF calculation.

Frequency intervals [Hz]	N. of sampled spectrum points
$\left[1 - \frac{f_{1n}^{\text{ref}} - f_{LB}}{f_{1n}^{\text{ref}}}\right] f_{1n} < f < f_{1n} - \delta_1$	11
$f_{1n} + \delta_1 < f < f_{2n} - \delta_2$	11
$f_{2n} + \delta_2 < f < f_{3n} - \delta_3$	11
$f_{3n} + \delta_3 < f < f_{4n} - \delta_4$	11
$f_{4n} + \delta_4 < f < f_{5n} - \delta_5$	11
$f_{5n} + \delta_5 < f < \left[1 - \frac{f_{UB} - f_{5n}^{\text{ref}}}{f_{5n}^{\text{ref}}}\right] f_{8n}$	11
$f_{1n} - \delta_1 < f < f_{1n} + \delta_1$	6
$f_{2n} - \delta_2 < f < f_{2n} + \delta_2$	6
$f_{3n} - \delta_3 < f < f_{3n} + \delta_3$	6
$f_{4n} - \delta_4 < f < f_{4n} + \delta_4$	6
$f_{5n} - \delta_5 < f < f_{5n} + \delta_5$	6

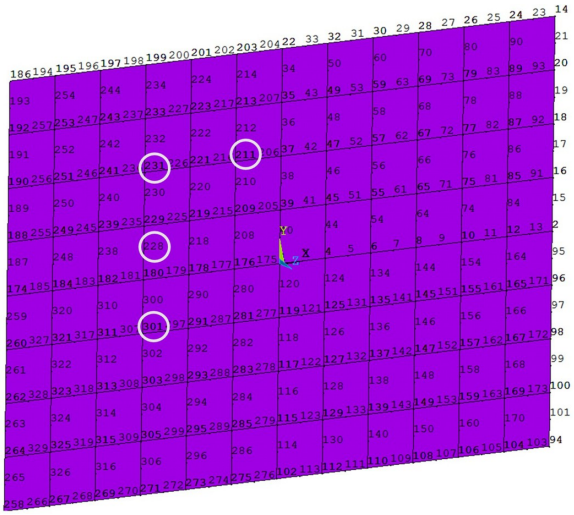

Fig. 8. Location of the sample points over the plate for harmonic displacements evaluation.

point in the design space).

5. Numerical results

5.1. Harmonic response for the reference configuration

Before running the optimisation procedure, the *reference response* must be calculated. To this purpose, firstly the numerical harmonic homogenisation process is performed on a RVE characterised by the material properties listed in Table 1 in order to obtain the *reference ply material properties*.

Secondly, the reference viscoelastic behaviour of the ply is implemented into the FE model of the multilayer plate for which both a non-linear modal analysis and a harmonic analysis are performed to calculate the *reference damped natural frequencies* and the *reference harmonic response*. The reference damped eigenfrequencies are listed in Table 5.

Table 7
Optimisation parameters for the GA ERASMUS.

Parameters	One-shot analysis
N. of individuals	50
N. of populations	2
N. of iterations	100
Crossover probability.	0.85
Mutation probability.	0.02
Isolation time	10

Table 8
Optimisation parameters for the gradient-based algorithm.

Parameters	Value
Solver algorithm	active-set
Max function evaluation	10000
Tolerance on the objective function	10^{-15}
Tolerance on the gradient norm	10^{-15}

For modal and harmonic analyses the frequency samples vary between $f_{LB} = 100$ Hz and $f_{UB} = 7500$ Hz: for the reference solution $n_f = 5$ damped natural frequencies fall into this interval.

The sampling of the considered spectrum is made according to the sequence reported in Table 6.

The value of δ_i is computed according to the following formula:

$$\delta_i(f_{in}) = -4.34 \times 10^{-12}(f_{in})^2 + 2.6 \times 10^{-7}(f_{in}) + 6.53 \times 10^{-4}, \quad (34)$$

which has been chosen in order to have a value of $\delta_i(f_{in})$ that increases with the frequency. Indeed, by looking at the viscoelastic effect on the amplitude of the FRF (evaluated at the fours sampled points highlighted in Fig. 8), as shown in Fig. 9, it is possible to observe that the damping effect is more pronounced at high frequencies.

The exciting nodal force (as illustrated in Fig. 7) has a value $|F_z| = 1\ N$ and it is not applied at the plate center, in order to be able to

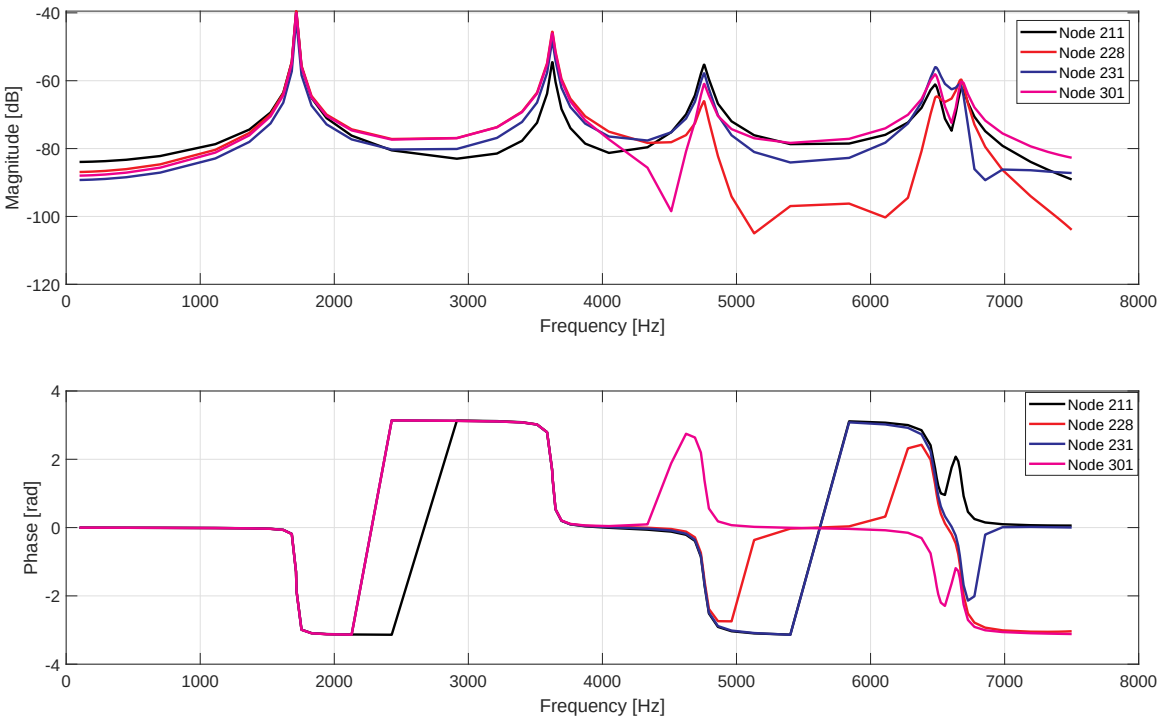

Fig. 9. Amplitude and phase of the FRF for the reference solution at the four sampling points highlighted in Fig. 8.

excite even and odd modes. Finally, the number of sampling frequencies is $N_s = 87$, for each plate point, whose number is $N_p = 329$.

5.2. Results of the inverse problem

The optimisation process has been performed by selecting the main optimisation parameters tuning the behaviour of the GA ERASMUS as a result of a statistic analysis to evaluate their effects on the optimum solutions, according to the best practices discussed in Montemurro et al. (2012). The parameters governing both the GA and the deterministic algorithm are listed in Tables 7 and 8, respectively.

The GA ERASMUS is run with two populations, each one composed of 50 individuals evolving along 100 generations. The exchange of information among populations is realised by using a ring-type operator every 10 generations: the probability of success of the ring-type operator is automatically computed by the GA. As far as the constraint-handling technique is concerned, the Automatic Dynamic Penalisation (ADP) method is used, see Montemurro et al. (2013).

The choice of using multiple populations, with a small number of individual, is due to the fact that the main goal is to find the global minimum without increasing too much the computational time. In this way, the GA has the possibility to explore the design domain by exchanging information between best individuals belonging to different populations. More details about the use of multiple populations can be found in Montemurro (2018).

The inverse problem is solved by considering a fibre volume fraction $V_F = 0.555$ (Soutis and Beaumont, 2005) and a fibre diameter equal to $d_f = 6.8$ μm (Cytec Industries Inc., 2012). The RVE dimensions are obtained as follows:

$$a_3 = \frac{d_f}{4}\sqrt{\frac{2\pi}{V_f}}, \quad a_2 = a_3, \quad a_1 = a_2/4. \tag{35}$$

For each point in the design space, the FE analyses, constituted of the union of a numerical homogenisation analysis, of the solution of the non-linear eigenvalue problem and of the computation of the harmonic responses, need about 104 s to be executed (on an Intel® Xeon® 2.70 GHz CPU with two processors and with a RAM of 128 GB). These analyses must be performed for each individual, at each iteration, which implies an overall time of about 26.3 days to get an optimum solution.

The optimum solutions obtained from the genetic calculation and the local gradient-based optimisation in terms of microscopic material properties, for both fibre and matrix, are listed in Table 9, while the relative eigenfrequencies values are summarised in Table 10.

As it can be easily inferred from the analysis of these results, the microscopic viscoelastic properties of the optimum solution are in good agreement with the reference data: the absolute percentage difference ranges from 0.10% for E_1^f to 11.94% for E_2^f. Only the material parameters E_1^m and G_{12}^f are characterised by significant percentage errors which are equal to 15.49% and 19.73%, respectively. This is a quite expected result because of the kinematic model at the basis of ANSYS shell elements. In fact, the effect of these material parameters on the dynamic response at the macroscopic scale is negligible and this is also due to the particular stacking sequence (orientation angles and thickness) used for the reference structure: the considered plate is not thick enough to observe a significant influence of G_{12}^f and E_1^m on its dynamic response.

Nevertheless, both the damped eigenfrequencies and the FRF, at each sample point, are in excellent agreement with the reference values and the numerical results found at the end of the optimisation perfectly match the reference data with an absolute percentage difference ranging from 3.58×10^{-2} % (for the first mode) to 2.19×10^{-1} % (for the fourth mode).

6. Conclusions and perspectives

In this paper, an extension of the Multi-Scale Identification Strategy (MSIS) (initially presented in Cappelli et al. (2018)) is proposed. The MSIS is here applied to characterise the viscoelastic behaviour of the matrix and the elastic behaviour of the fibres, by exploiting the information included into the dynamic response of the composite at the macroscopic scale. The proposed MSIS shows several features that make it a general methodology, that can be easily applied for different classes of materials and structures, e.g. multilayer, fabrics, etc, for identification of material properties without performing destructive tests.

In this study, the multi-scale inverse problem has been solved by means of a “one-shot” hybrid optimisation strategy. The multi-scale *inverse problem* is stated as an equivalent constrained non-linear programming problem (CNLPP) aiming at minimising the distance between the numerical and reference harmonic responses for the considered multilayer composite plate.

The scale transition is ensured by means of the strain energy homogenisation method for periodic media, which has been generalised to the viscoelastic case. In this way, the ply viscoelastic properties can be computed and used to build the FE model of the multilayer plate. At the microscopic scale the matrix viscoelastic behaviour is described through the Bagley-Torvik model that requires only four material parameters.

Moreover, the modal and harmonic analyses performed on the multilayer plate at the macroscopic scale are non-linear due to the viscoelastic behaviour of the ply. The main issue is related to the non-linear modal analysis: no dedicated solvers are available in commercial FE software. To this purpose, the Arnoldi’s method (Voss, 2004) for non-linear eigenvalue problems has been coded into the MATLAB® environment and interfaced with the ANSYS code.

The effectiveness of the proposed strategy is evaluated through a numerical benchmark in which a composite laminate made of unidirectional carbon/epoxy pre-preg plies T650/F584 is considered as a reference structure.

The results provided by the MSIS are quite satisfactory: all viscoelastic properties are identified with a good level of accuracy, except the in-plane shear modulus of the fibre G_{12}^f and the viscoelastic matrix parameter E_1^m which are affected by an absolute percentage error of 19% and 15%, respectively. These errors are mainly due to the very low sensitivity of the objective function to these parameters. On the one hand, this low sensitivity is due to the geometry of the considered laminate which is not thick enough to highlight the influence of these properties on its dynamical response. On the other hand, the laminate stacking sequence plays a fundamental role: the stack considered in this work is a standard symmetric balanced stack taken from the literature which has not been designed to maximise the influence of some material properties on the laminate dynamic behaviour.

Table 9
Optimum solution of the inverse problem: results provided by the GA and the active-set algorithm. The percentage difference is indicated in parentheses.

Micro-scale viscoelastic properties	Reference data	GA results	Gradient-based results
E_1^f [MPa]	276000	275,730 (−0.10)	275724.86 (−0.10)
E_2^f [MPa]	17300	19366.50 (11.95)	19365.77 (11.94)
ν_{12}^f	0.25	0.26 (5.34)	0.26 (5.34)
ν_{23}^f	0.428	0.428 (0)	0.428 (0)
G_{12}^f [MPa]	11240	13457.20 (19.73)	13457.22 (19.73)
E_0^m [MPa]	4140	3802.49 (−8.15)	3802.44 (−8.15)
E_1^m [MPa]	30	25.35 (−15.50)	25.35 (−15.49)
b^m	0.0053	0.0050 (−5.92)	0.0050 (−5.92)
α^m	0.5	0.4989 (−0.21)	0.50 (−0.22)
ν_m	0.35	0.38 (7.92)	0.38 (7.92)

Table 10
The damped eigenfrequencies for the optimum solution of the inverse problem: results provided by the GA and the active-set algorithm. The percentage difference (with respect to the reference values) is indicated in parentheses.

Nat. freq.	f_{in}^{ref} [Hz]	f_{in} [Hz]GA results	f_{in} [Hz]Gradient-based results
f_{1n}	1716.34	1716.94 (3.49×10^{-2})	1715.73 (3.58×10^{-2})
f_{2n}	3626.36	3630.07 (1.02×10^{-1})	3622.61 (1.03×10^{-1})
f_{3n}	4758.54	4766.03 (1.57×10^{-1})	4751 (1.58×10^{-1})
f_{4n}	6481.66	6495.78 (2.18×10^{-1})	6467.49 (2.19×10^{-1})
f_{5n}	6677.52	6690.54 (1.95×10^{-1})	6664.44 (1.96×10^{-1})

The proposed strategy constitutes just a “first attempt”: the MSIS needs to be generalised to catch the true behaviour of the material of the constitutive phases. In order to achieve this ambitious goal, research is ongoing in order to include into the MSIS the following aspects:

- validation of the effectiveness of the proposed MSIS to characterise the viscoelastic behaviour of composite materials by exploiting the data resulting from experimental harmonic tests;
- design of a suitable stack to maximise the sensitivity of the objective function $\Phi(\mathbf{x})$ to the full set of the material properties to be identified;
- extension of the MSIS to the characterisation of the variability related to some parameters like the fibre volume fraction, misalignments of fibres, variation of the plies orientation angles, etc. (as partially done in Cappelli et al. (2019));
- application of the proposed strategy to different macroscopic specimen geometries and microscopic RVE topologies (in terms of constituent phases configurations).

As far as the experimental validation of the MSIS is concerned, two major difficulties must be faced before programming a campaign of harmonic/modal tests.

Firstly, the variability of the material properties should be included into the inverse problem formulation. This requires the development of a suitable numerical model to properly describe the variability related to the viscoelastic behaviour of the composite, at each pertinent scale. Even if some models are available in the literature to properly describe the uncertainty of the elastic properties of both fibre and matrix, few research studies focuses on the modelling of the variability of their viscoelastic behaviour (to the best of the authors’ knowledge). Therefore, a preliminary numerical/theoretical study should be conducted in order to find/develop a pertinent model to describe the variability characterising the viscoelastic behaviour, at each pertinent scale of the composite.

Secondly, experimental results are unavoidably affected by noise. In the literature, one can find several methods/techniques to take into account the influence of noise on the characterisation of the elastic properties of the composite (very often at the mesoscopic scale). However, to the best of the authors’ knowledge, the influence of noise on the identification of the parameters governing the viscoelastic behaviour of the microscopic constituents of the composite has not fully investigated yet. This aspect is also of paramount importance and should be addressed before starting an experimental campaign which aims at validating the proposed MSIS.

Due to its versatility, the MSIS can be used to characterise the geometrical parameters of the RVE of the composite material. The variables defining the shape of the inclusion or its volume fraction can be easily integrated into the vector of optimisation variables, without altering the overall architecture of the MSIS. Furthermore, laminate parameters can be included among the unknowns to be identified, e.g. the orientation angle and the thickness of each ply. Research is ongoing on these aspects as well.

Acknowledgements

This research work has been carried out within the project FULLCOMP (FULLy analysis, design, manufacturing, and health monitoring of COMPosite structures), funded by the European Union Horizon 2020 Research and Innovation program under the Marie Skodowska-Curie grant agreement no. 642121.

Supplementary material

Supplementary material associated with this article can be found, in the online version, at 10.1016/j.mechmat.2019.103137

References

Abedi, M., 2016. Viscoelastic characterization of out-of-autoclave composite laminates: experimental and finite element studies.
Ansys, 2013. ANSYS Mechanical APDL Basic Analysis Guide. Release 15.0.
ASTM International, 1975. ASTM D3379-75(1989)e1, Standard Test Method for Tensile Strength and Young’s Modulus for High-Modulus Single-Filament Materials (Withdrawn 1998). West Conshohocken, PA
ASTM International, 2012. ASTM D5379 / D5379M-12, Standard Test Method for Shear Properties of Composite Materials by the V-Notched Beam Method. West Conshohocken, PA
ASTM International, 2014. ASTM D638-14, Standard Test Method for Tensile Properties of Plastics. West Conshohocken, PA
ASTM International, 2017. ASTM D3039 / D3039M-17, Standard Test Method for Tensile Properties of Polymer Matrix Composite Materials. West Conshohocken, PA
ASTM International, 2017. ASTM D790-17, Standard Test Methods for Flexural Properties of Unreinforced and Reinforced Plastics and Electrical Insulating Materials. West Conshohocken, PA
Bagley, R.L., Torvik, P.J., 1986. On the fractional calculus model of viscoelastic behavior. J. Rheol. 30 (1), 133–155. https://doi.org/10.1122/1.549887.
Barbero, E.J., 2007. Finite Element Analysis of Composite Materials. CRC Press, Taylor and Francis Group.
Barkanov, E., Skukis, E., Petitjean, B., 2009. Characterisation of viscoelastic layers in sandwich panels via an inverse technique. J. Sound Vib. 327 (3), 402–412. https://doi.org/10.1016/j.jsv.2009.07.011.
Bilasse, M., Charpentier, I., Daya, E.M., Koutsawa, Y., 2009. A generic approach for the solution of nonlinear residual equations. Part II: homotopy and complex nonlinear eigenvalue method. Comput. Methods Appl. Mech.Eng. 198 (49), 3999–4004. https://doi.org/10.1016/j.cma.2009.09.015.
Cappelli, L., Balokas, G., Montemurro, M., Dau, F., Guillaumat, L., 2019. Multi-scale identification of the elastic properties variability for composite materials through a hybrid optimisation strategy. Compos. Part B 176. https://doi.org/10.1016/j.compositesb.2019.107193.
Cappelli, L., Montemurro, M., Dau, F., Guillaumat, L., 2018. Characterisation of composite elastic properties by means of a multi-scale two-level inverse approach. Compos. Struct. 204, 767–777. https://doi.org/10.1016/j.compstruct.2018.08.007.
Catapano, A., Montemurro, M., 2014. A multi-scale approach for the optimum design of sandwich plates with honeycomb core. Part I: homogenisation of core properties. Compos. Struct. 118, 664–676.
Catapano, A., Montemurro, M., 2014. A multi-scale approach for the optimum design of sandwich plates with honeycomb core. Part II: the optimisation strategy. Compos. Struct. 118, 677–690.
Chandra, R., Singh, S., Gupta, K., 2003. Experimental evaluation of damping of fiber-reinforced composites. J. Compos. Technol. Res. 25 (2), 1–12. https://doi.org/10.1520/CTR10952J.
Cortés, F., Elejabarrieta, M.J., 2006. An approximate numerical method for the complex eigenproblem in systems characterised by a structural damping matrix. J. Sound Vib. 296 (1), 166–182. https://doi.org/10.1016/j.jsv.2006.02.016.
Costa, G., Montemurro, M., Pailhés, J., 2018. A general hybrid optimization strategy for curve fitting in the non-Uniform rational basis spline framework. J. Optim. Theory Appl. 176 (1), 225–251.
Cytec Industries Inc., 2012. THORNEL T-650/35 PAN-BASED FIBER.
Daya, E.M., Potier-Ferry, M., 2001. A numerical method for nonlinear eigenvalue problems application to vibrations of viscoelastic structures. Comput. Struct. 79 (5), 533–541. https://doi.org/10.1016/S0045-7949(00)00151-6.
Elkhaldi, I., Charpentier, I., Daya, E.M., 2012. A gradient method for viscoelastic behaviour identification of damped sandwich structures. Comptes Rendus Méc. 340 (8), 619–623. https://doi.org/10.1016/j.crme.2012.05.001.
Finegan, I.C., Tibbetts, G.G., Gibson, R.F., 2003. Modeling and characterization of damping in carbon nanofiber/polypropylene composites. Compos. Sci. Technol. 63 (11), 1629–1635. https://doi.org/10.1016/S0266-3538(03)00054-X.
Ghorbal, G.B., Tricoteaux, A., Thuault, A., Louis, G., Chicot, D., 2017. Mechanical characterization of brittle materials using instrumented indentation with knoop indenter. Mech. Mater. 108, 58–67. https://doi.org/10.1016/j.mechmat.2017.03.009.
Hamdaoui, M., Akoussan, K., Daya, E.M., 2016. Comparison of non-linear eigensolvers for modal analysis of frequency dependent laminated visco-elastic sandwich plates. Finite Elem. Anal. Des. 121, 75–85. https://doi.org/10.1016/j.finel.2016.08.001.
Hamdaoui, M., Druesne, F., Daya, E.M., 2015. Variability analysis of frequency dependent

visco-elastic three-layered beams. Compos. Struct. 131, 238–247. https://doi.org/10.1016/j.compstruct.2015.05.011.
Hexcell Corporation, 2016. Hexply F584.
Jayendiran, R., Arockiarajan, A., 2015. Micromechanical modeling and experimental characterization on viscoelastic behavior of 1–3 active composites. Compos. Part B 79, 105–113. https://doi.org/10.1016/j.compositesb.2015.04.033.
Jones, R.M., 1975. Mechanics of Composite Materials. McGraw-Hill.
Kostopoulos, V., Korontzis, D.T., 2003. A new method for the determination of viscoelastic properties of composite laminates: a mixed analytical-experimental approach. Compos. Sci. Technol. 63 (10), 1441–1452. https://doi.org/10.1016/S0266-3538(03)00086-1.
Krasnobrizha, A., 2015. Modelisation des mecanismes d'hysteresis des composites tisses a l'aide d'un modele collaboratif elasto-plastique endommageable a derivees fractionnaires. Université Nantes Angers Le Mans, France Ph.D. thesis.
Krasnobrizha, A., Rozycki, P., Gornet, L., Cosson, P., 2016. Hysteresis behaviour modelling of woven composite using a collaborative elastoplastic damage model with fractional derivatives. Compos. Struct. 158, 101–111. https://doi.org/10.1016/j.compstruct.2016.09.016.
Ledi, K.S., Hamdaoui, M., Robin, G., Daya, E.M., 2018. An identification method for frequency dependent material properties of viscoelastic sandwich structures. J. Sound Vib. 428, 13–25. https://doi.org/10.1016/j.jsv.2018.04.031.
Luciano, R., Barbero, E.J., 1995. Analytical expressions for the relaxation moduli of linear viscoelastic composites with periodic microstructure. ASME. J. Appl. Mech. 62 (3), 786–793. https://doi.org/10.1115/1.2897015.
Mahmoudi, S., Kervoelen, A., Robin, G., Duigou, L., Daya, E.M., Cadou, J.M., 2019. Experimental and numerical investigation of the damping of flax-epoxy composite plates. Compos. Struct. 208, 426–433. https://doi.org/10.1016/j.compstruct.2018.10.030.
Melo, J.D.D., Radford, D.W., 2005. Time and temperature dependence of the viscoelastic properties of CFRP by dynamic mechanical analysis. Compos. Struct. 70 (2), 240–253. https://doi.org/10.1016/j.compstruct.2004.08.025.
Meng, L., Raghavan, B., Bartier, O., Hernot, X., Mauvoisin, G., Breitkopf, P., 2017. An objective meta-modeling approach for indentation-based material characterization. Mech. Mater. 107, 31–44. https://doi.org/10.1016/j.mechmat.2017.01.011.
Moler, C., Stewart, G., 1973. An algorithm for generalized matrix eigenvalue problems. SIAM J. Numer. Anal. 10 (2), 241–256. https://doi.org/10.1137/0710024.
Montemurro, M., 2018. A Contribution to the Development of Design Strategies for the Optimisation of Lightweight Structures. Université de Bordeaux. HDR thesis, http://hdl.handle.net/10985/15155.
Montemurro, M., Catapano, A., 2016. Variational analysis and aerospace engineering: mathematical challenges for the aerospace of the future. A new paradigm for the optimum design of variable angle tow laminates, First ed. Springer Optimization and Its Applications Vol. 116. Springer International Publishing, pp. 375–400. https://doi.org/10.1007/978-3-319-45680-5.
Montemurro, M., Catapano, A., 2017. On the effective integration of manufacturability constraints within the multi-scale methodology for designing variable angle-tow laminates. Compos. Struct. 161, 145–159.
Montemurro, M., Catapano, A., Doroszewski, D., 2016. A multi-scale approach for the simultaneous shape and material optimisation of sandwich panels with cellular core. Compos. Part B 91, 458–472.
Montemurro, M., Izzi, M.I., El-Yagoubi, J., Fanteria, D., 2019. Least-weight composite plates with unconventional stacking sequences: design, analysis and experiments. J. Compos. Mater. 53 (16), 2209–2227.
Montemurro, M., Nasser, H., Koutsawa, Y., Belouettar, S., Vincenti, A., Vannucci, P., 2012. Identification of electromechanical properties of piezoelectric structures through evolutionary optimisation techniques. Int. J. Solids Struct. 49 (13), 1884–1892.
Montemurro, M., Pagani, A., Fiordilino, G.A., Pailhès, J., Carrera, E., 2018. A general multi-scale two-level optimisation strategy for designing composite stiffened panels. Compos. Struct. 201, 968–979. https://doi.org/10.1016/j.compstruct.2018.06.119.
Montemurro, M., Vincenti, A., Vannucci, P., 2013. The automatic dynamic penalisation method (ADP) for handling constraints with genetic algorithms. Comput. Methods Appl. Mech.Eng. 256, 70–87.
Panettieri, E., Montemurro, M., Catapano, A., 2019. Blending constraints for composite laminates in polar parameters space. Compos. Part B 168, 448–457. https://doi.org/10.1016/j.compositesb.2019.03.040.
Schiessel, H., Friedrich, C., Blumen, A., 2000. Applications to problems in polymer physics and rheology. In: Hilfer, R. (Ed.), Application of Fractional Calculus in Physics. World Scientific Publishing, pp. 331–376. https://doi.org/10.1142/9789812817747_0007.
Schreiber, K.,. Nonlinear Eigenvalue Problems: Newton-type Methods and Nonlinear Rayleigh Functionals. Ph.D. thesis. Technische Universität Berlin, Fakultät II - Mathematik und Naturwissenschaften. 10.14279/depositonce-1871.
Multi-scale modelling of composite material systems. The art of predictive damage modelling. In: Soutis, C., Beaumont, P.W.R. (Eds.), Woodhead Publishing Series in Composites Science and EngineeringElsevier, New York.
Suarez, S.A., Gibson, R.F., Sun, C.T., Chaturvedi, S.K., 1986. The influence of fiber length and fiber orientation on damping and stiffness of polymer composite materials. Exp. Mech. 26 (2), 175–184. https://doi.org/10.1007/BF02320012.
Sun, N.Z., 1999. Inverse Problems in Groundwater Modelling. Kluwer Academic Publishers, Boston. 6 of Theory and Applications of Transport in Porous Media
Swain, A., Roy, T., 2018. Viscoelastic modelling and dynamic characteristics of CNTs-CFRP-2DWF composite shell structures. Composites Part B: Engineering 141, 100–122. https://doi.org/10.1016/j.compositesb.2017.12.033.
Tarantola, A., 1988. Inverse Problem Theory: Methods for Data Fitting and Model Parameter Estimation. Elsevier, New York.
The Math Works Inc., 2017. Optimization Toolbox User's Guide. 3 Apple Ill Drive, Natick, MA. 01760-2098
Voss, H., 2004. An arnoldi method for nonlinear eigenvalue problems. BIT Numer. Math. 44 (2), 387–401. https://doi.org/10.1023/B:BITN.0000039424.56697.8b.
Voss, H., 2007. A Jacobi-Davidson method for nonlinear and nonsymmetric eigenproblems. Comput. Struct. 85 (17), 1284–1292. https://doi.org/10.1016/j.compstruc.2006.08.088.
Yap, Y.L., Toh, W., Koneru, R., Lin, K., Yeoh, K.M., Lim, C.M., Lee, J.S., Plemping, N.A., Lin, R., Ng, T.Y., Chan, K.I., Guang, H., Chan, W.Y.B., Teong, S.S., Zheng, G., 2019. A non-destructive experimental-cum-numerical methodology for the characterization of 3d-printed materials-polycarbonate-acrylonitrile butadiene styrene (PC-ABS). Mech. Mater. 132, 121–133. https://doi.org/10.1016/j.mechmat.2019.03.005.

Chapter 5

Multi-scale identification of the elastic properties variability for composite materials

5.1 Introduction and main motivations of the study

The article presented in the present Chapter has been published in *Composites Part B: Engineering*. It deals with the identification of the parameters describing the variability of the elastic properties of the constitutive phases of a composite (at the microscopic scale) starting from the analysis of the buckling strength of the structure at the macroscopic scale. To this purpose, the information contained into the probability distribution of the first buckling load of a multilayer plate (made of unidirectional fibre-reinforced pre-preg plies) are exploited to carry out the multi-scale identification process.

In this case the inverse problem is stated as the minimisation of the distance between the numerical and the reference buckling response of the plate in terms of probabilistic distribution response. Furthermore, thermodynamic constraints are considered to ensure the positive definiteness of the stiffness tensor of each constituent of the composite.

Due to the strong computational effort required to assess the probability distribution of the buckling load at the macroscopic scale for different combinations of the constitutive phases material properties (i.e. multi-scale numerical analysis under uncertainty), some modifications/improvements have been introduced into the original MSIS presented at Chapter 3.

On the one hand, an analytical homogenisation method is used to determine the effective elastic properties of the lamina (microscopic/mesoscopic scale transition).

On the other hand, the Monte Carlo technique combined with a suitable surrogate model of the composite (developed in the form of an Artificial Neural Network) has been used to determine the first-buckling load distribution of the multilayer plate, at the macroscopic scale, by taking into account for the elastic properties variability of the microscopic constituents. Of course, the learning phase of the surrogate model is performed by using a suitable FE model of the multilayer plate.

5.2 Multi-scale identification of the elastic properties variability for composite materials

Composites Part B 176 (2019) 107193

Contents lists available at ScienceDirect

Composites Part B

journal homepage: www.elsevier.com/locate/composites

Multi-scale identification of the elastic properties variability for composite materials through a hybrid optimisation strategy

Lorenzo Cappelli [a], Georgios Balokas [b], Marco Montemurro [a,*], Frédéric Dau [a], Laurent Guillaumat [c]

[a] Arts et Métiers ParisTech, Institut de Mécanique et d'Ingénierie (I2M) de Bordeaux CNRS UMR 5295, F-33400 Talence, France
[b] Structural Optimisation for Lightweight Design, Hamburg University of Technology, Hamburg, Germany
[c] Arts et Métiers ParisTech, Laboratoire Angevin de Mécanique, Procédés et innovAtion (LAMPA), F-49100 Angers, France

ARTICLE INFO

Keywords:
Composite materials
Homogenisation
Buckling
Uncertainty quantification
Surrogate model
Inverse problems
Optimisation

ABSTRACT

The problem of the identification of the variability characterising the elastic properties of the constitutive phases of a composite (at the microscopic scale) is addressed in this work. To this purpose, the information contained into the probability distribution of the first buckling load of a macroscopic composite specimen is considered, in order to develop a multi-scale identification strategy (MSIS).

The goal of the proposed MSIS is achieved by solving an inverse problem: the minimisation of the distance between the numerical and the reference buckling response of the plate, at the macroscopic scale, in terms of statistical moments. Furthermore, thermodynamic constraints are considered to ensure the positive definiteness of the stiffness tensor of each constituent of the composite.

The proposed strategy relies on: (a) a semi-analytical homogenisation method, to perform the microscopic / mesoscopic scale transition; (b) the Monte-Carlo technique and an Artificial Neural Network to determine the material properties variability; (c) a general hybrid optimisation algorithm able to deal with optimisation problems defined over a domain of variable dimension to perform the solution search. The effectiveness of the MSIS is proven through two meaningful benchmarks.

1. Introduction

Composite materials are nowadays widely used into mechanical components or engineering systems and structures belonging to different fields: from automotive to aerospace, from naval to biomedical. They are mainly employed due to their outstanding strength-to-weight and stiffness-to-weight ratios: these features are of paramount importance for lightweight applications, such as aircraft and space vehicles architectures [1]. Composites can be used to build integrated structures because both stiffness and strength can be tailored point-wise according to the requirements of the problem at hand. This feature allows for preserving structural continuity without introducing complex structural elements (and the related manufacturing aspects) by opportunely meeting geometrical and mechanical design requirements.

In the literature, research studies exploiting refined numerical and experimental techniques are increasingly used to characterise the mechanical behaviour of composite materials [2–4]. Nevertheless, especially in large-scale production, a large amount of uncertainty arises from unavoidable manufacturing imperfections for both geometrical and material properties. Intralaminar and/or matrix voids, excess of resin between adjacent laminae and incomplete cure of resin are only some examples: environmental factors and uncertain operational aggravate this issue.

As outlined in [5], the uncertainties are classified in three main categories: aleatory (variability of structural parameters), epistemic (lack of adequate information about the system) and prejudicial (absence of stochastic characterisation of the structural system). Composite structures are affected by all three forms of uncertainty and the characterisation of parameters tuning the variability law becomes of prime importance. However, experimental methods commonly used to characterise the material properties require a huge number of standard ASTM tests, if used for uncertainty characterisation, which are destructive and expensive [6]. Moreover, these tests are only suited to evaluate mesoscopic uncertainties, in terms of material and geometrical properties of the lamina, without providing any information about the variability characterising the properties of the constitutive phases at the microscopic scale.

Standard tests that can be carried out at the mesoscopic scale include the tension test for flat specimens (ASTM D3039 [7]), the

* Corresponding author.
E-mail addresses: marco.montemurro@ensam.eu, marco.montemurro@u-bordeaux.fr (M. Montemurro).

https://doi.org/10.1016/j.compositesb.2019.107193
Received 15 May 2019; Received in revised form 21 June 2019; Accepted 10 July 2019
Available online 12 July 2019
1359-8368/

three/four points bending test (ASTM D790 [8]), the compression tests (shear loading methods ASTM D3410 [9]) and the shear tests (in-plane shear tests ASTM D5379 [10]-D7078 [11]-D3518 [12], out-of-plane - interlaminar shear tests ASTM D2344 [13]-D5379). As far as the microscopic scale is concerned, only few standard experimental tests can be found in the literature: single fibre tensile test (ASTM D3379 [14]) and matrix tensile test (ASTM D638 [15]) to characterise the Young's moduli of the fibre in the longitudinal direction and that of the matrix, respectively. In order to characterise the rest of the constitutive phases elastic properties, only non-standard tests are available in the literature: pull-out [16], micro-indentation [17], fragmentation tests [18], etc. These tests are not able to evaluate the 3D set of the material properties of the constituents and they are very difficult to be carried out, due to the fibre diameter size.

In order to get statistically representative results, the aforementioned tests must be performed a huge number of times. Of course, this implies significant costs (and time) and the variability results (e.g. mean and standard deviation of material properties) are strongly affected by the errors introduced to carry out the experimental campaign, especially for those tests conducted at the microscopic scale. To this purpose, Sepahvand et al. developed the inverse stochastic method based on the general polynomial chaos (gPC) [19–25] to identify uncertain lamina elastic parameters from experimental modal data. Further examples of probabilistic methods are the parametric probabilistic approach [26] and the Bayesian inference techniques wherein all information are included into a prior distribution model [27–30]. However, in the case of composite structures, the uncertainty affecting the ply elastic behaviour is strictly related to the variability of the elastic properties of the constitutive phases. To the best of the authors' knowledge, only few works on the identification of the variability parameters characterising the material properties of the microscopic constituents of the composite are available in the literature [31]. The majority of researches in this field is devoted to the characterisation of the material properties uncertainty parameters at the ply-level [32–35].

The research activity here presented focuses on the development of a multi-scale identification strategy (MSIS) which smartly exploits the data resulting from macroscopic buckling tests to characterise the uncertainty of the constitutive phases elastic properties. The proposed MSIS has been initially proposed in [36] to identify the elastic properties of the composite (at each relevant scale), starting from the harmonic response of the multilayer composite plate at the macroscopic scale. Here, the MSIS is extended to the multi-scale characterisation of the variability related to the elastic properties at the microscopic scale of the composite.

The MSIS is characterised by some original features. Firstly, it relies on a particular hybrid optimisation tool used to perform the solution search, which is an in-house code made by the union of a special genetic algorithm (GA), i.e. ERASMUS (EvolutionaRy Algorithm for optimiSation of ModUlar Systems) developed by Montemurro [37] (which is able to deal with problems characterised by a number of design variables that can change during the optimisation process [38]) and of a gradient-based one, belonging to the MATLAB® *fmincon* family [39]. Secondly, the MSIS makes use of the Chamis' micromechanical model [40,41] to perform the microscopic/mesoscopic scale transition. Finally, the MSIS makes use of the Monte Carlo framework that allows describing the statistical nature of the elastic response. To improve the efficiency of the Monte Carlo technique (i.e. to minimise the computational effort related to such a method), an Artificial Neural Network (ANN) [41] is developed as a surrogate model: the probability distribution of the first buckling load is predicted starting from the probability density functions of the elastic properties of the constituent phases. The effectiveness of the MSIS is proven by means of two meaningful benchmarks.

Concerning the state-of-the-art of the approaches combining optimisation and uncertainty, three specific research areas can be identified in the literature, as outlined in [42]: reliability-based optimisation (RBO), robust design optimisation (RDO) and model updating. The RBO technique concerns the solution of an optimisation problem in which the main goal is to design for safety by considering extreme events: common objective functions are defined by the structural weight and the constraints are both deterministic and probabilistic (e.g. probability of failure of the structure) [43–46]. The RDO method is usually implemented in order to minimise the influence of stochastic variations on the mean design [47]. Finally, the typical goal of the model updating technique is to reduce the differences between model prediction and data from tests [48,49]. In this context, the MSIS can be considered as a model updating technique that allows identifying the elastic properties of the composite (and the related uncertainty) at each scale. This information can be later used in the framework of both RBO and RDO approaches.

The paper is organised as follows. The problem description and the MSIS are presented in Section 2. The analytical and the finite element (FE) models, developed at each pertinent scale, are shown in Section 3. The uncertainty microscopic quantification with the Monte-Carlo technique and the implemented ANN are described in Section 4. The sensitivity analyses concerning the meta-model of the considered benchmarks are presented in Section 5, while the mathematical formulation of the inverse problem is discussed in Section 6. The numerical results provided by the MSIS are given in Section 7. Finally, Section 8 ends the paper with conclusions and perspectives.

2. Multi-scale identification of the variability of composite elastic properties

2.1. The multi-scale identification strategy

The goal of the MSIS is the characterisation of the variability related to the elastic properties of the microscopic constituents of the composite, by using only the information contained into the statistical sample of the first buckling load of the multilayer plate at the macroscopic scale. In this way, only cheap, standard tests have to be realised, with the main advantage of reducing the characterisation time, the associated costs and the necessity of specialised skills.

The *reference* macroscopic response can be evaluated either by means of an extensive experimental campaign of buckling tests or through a wide numerical campaign of tests on a reference configuration of the multilayer plate. To prove the effectiveness of the MSIS, this latter case has been considered in this work.

To this purpose, the problem of characterising the variability related to the elastic properties of the fibre and the matrix is stated as a multi-scale constrained inverse problem. Of course, the numerical models involved in the MSIS are characterised by some fundamental hypotheses. As far as the microscopic scale is concerned, the main hypotheses are: (a) linear elastic isotropic behaviour for the matrix; (b) linear elastic transversely isotropic behaviour for the fibre; (c) the matrix/fibre interface is perfect; (d) the damping capability of both phases is neglected; (e) the uncertainty of the elastic properties is described by means of a Gaussian probability distribution.

At the laminate macroscopic scale the following hypotheses hold: (a) the constitutive lamina has a linear elastic transversely isotropic behaviour; (b) the interface between two adjacent plies is perfect; (c) the damping capability of the lamina is neglected; (d) the kinematics of the laminate is described by the first-order shear deformation theory (FSDT).

The general flow chart of the MSIS is illustrated in Fig. 1. The details of the optimisation algorithms employed within the MSIS are given in [36,37].

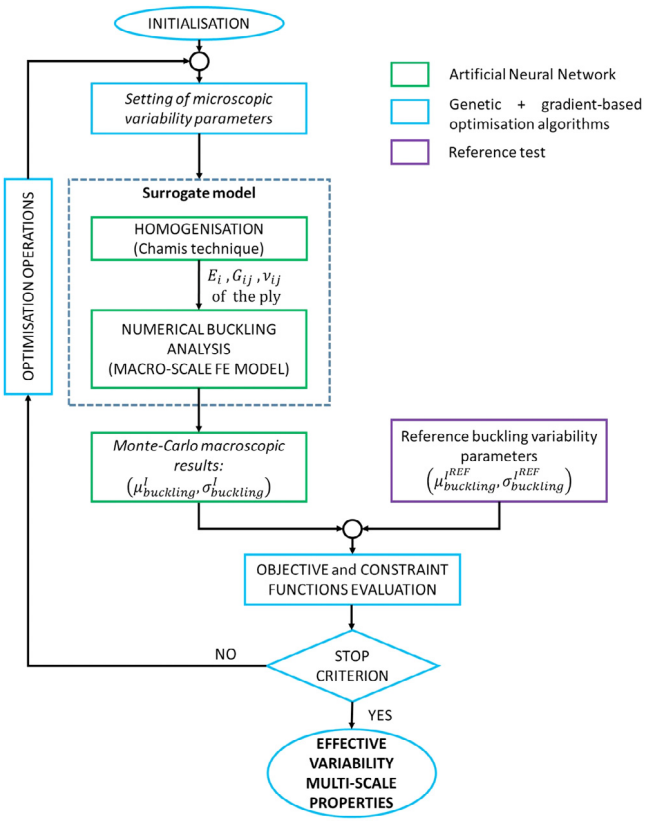

Fig. 1. Flow chart of the MSIS.

2.2. Problem description

The proposed multi-scale inverse approach for uncertainty characterisation is here applied to a reference multilayer composite plate made of unidirectional laminae: the relevant geometrical parameters are shown in Fig. 2. Two different benchmarks are investigated to evaluate the identification capability of the proposed MSIS. In particular the geometry of the reference laminate is the same for both cases, the only difference being the considered stacking sequence, i.e.

- benchmark 1 (BK1) $[0°/-45°/45°/90°]_S$;
- benchmark 2 (BK2) $[45]_8$.

For both laminates, the thickness of the elementary lamina is $t_{\text{ply}} = 0.282$ mm. The orientation angle of the generic ply is positive according to counter-clockwise rotation around the z-axis: the x-axis indicates the 0° orientation, as illustrated in Fig. 2.

The constitutive ply is made of carbon-epoxy fibre-reinforced Hexcel $T650/F584$ pre-impregnated tapes: its elastic properties are listed in Table 1. The mean values are taken from [50,51], while the standard deviation and the relative shapes of the probability density functions are not available experimentally for both the microscopic and the mesoscopic material properties. To this purpose, a Gaussian probability density function $\chi_i = \chi_i(x_i)$ is selected as a reference distribution for describing the uncertainty of the generic property x_i at the scale of the constituent phases. The analytical formula of such a distribution is

$$\chi_i(x_i) = \frac{1}{\sigma(x_i)\sqrt{2\pi}} e^{\frac{(x_i-\mu(x_i))^2}{2\sigma^2(x_i)}}, \quad \text{with } x_i \in \Re. \tag{1}$$

In particular, the Gaussian distribution involves two parameters, i.e. the mean value $\mu(x_i)$ and the variance $\sigma^2(x_i)$ of the *i-th* material

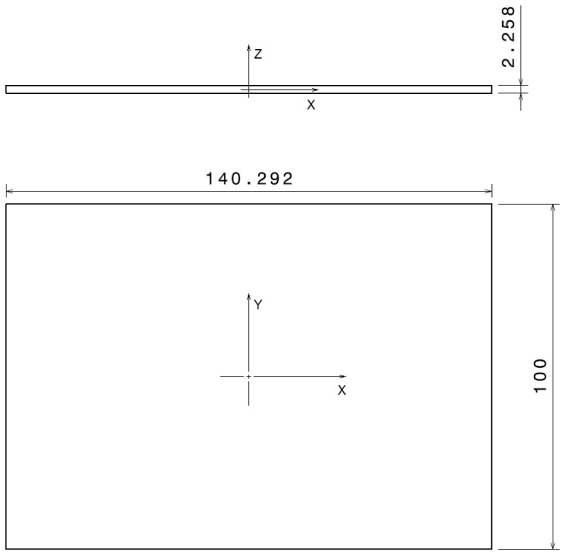

Fig. 2. Geometrical parameters of the reference multilayer composite plate (dimensions are in [mm]).

property x_i. If x_{i_j} is the *j-th* value of x_i occurring with a probability p_{i_j}, the relative mean value and the variance can be expressed as:

$$\begin{aligned} \mu(x_i) &= \sum_{j=1}^{N_i} x_{i_j} p_{i_j}, \\ \sigma^2(x_i) &= \mu(\beta_i(x_i)), \\ \beta_i(x_i) &= (x_i - \mu(x_i))^2. \end{aligned} \tag{2}$$

Usually, the coefficient of variation $\text{COV}(x_i)$ is introduced as a standard measure of the dispersion of the probability distribution function:

$$\text{COV}(x_i) = \frac{\sigma(x_i)}{\mu(x_i)}. \tag{3}$$

In this work, the *reference* distribution of the first buckling load of the structure is determined by means of a multi-scale numerical analysis on the *reference* configuration of the plate for both benchmarks. In particular, the *reference* material properties of the constitutive phases, listed in Table 1, are implemented, firstly, to compute the *reference* distribution of the ply elastic properties. Secondly, the resulting distribution of the lamina elastic properties is used to compute the *reference* distribution of the first buckling load of the composite plate, for each considered benchmark (as described in Section 7.1).

3. Analytical and numerical models at different scales

3.1. Microscopic/mesoscopic scale transition: the Chamis' model

Multi-scale modelling strategies are widely used to assess the behaviour of the composite at each relevant scale [52,53]. The transition from the scale of the constitutive phases (microscopic scale) to that of the elementary ply (mesoscopic scale) is performed by means of a homogenisation calculation. This phase can be performed either numerically, e.g. by implementing the well-known strain energy homogenisation technique of periodic media (SEHTPM) [54], or analytically by using a suitable homogenisation scheme for composites, as the Chamis' model [40]. As discussed in [36], the SEHTPM has already been integrated into the MSIS to determine the equivalent elastic behaviour of general periodic materials with complex microstructures. Despite its general nature, the SEHTPM can be quite time consuming (depending on the problem at hand) since the equivalent elastic properties at the

Table 1
Mean value and standard deviation of the elastic properties for the fibre $T650/35-3K$ and the matrix $F584$ (the mean values are taken from [50,51]).

	Fibre					Matrix		
	E_1^f [GPa]	E_2^f [GPa]	ν_{12}^f	ν_{23}^f	G_{12}^f [GPa]	E^m [GPa]	ν^m	V_F
$\mu(x_i)$	276	17.3	0.25	0.428	11.24	4.14	0.35	0.555
$\sigma(x_i)$	27.6	1.73	0.025	0.0428	1.124	0.414	0.035	0.0555

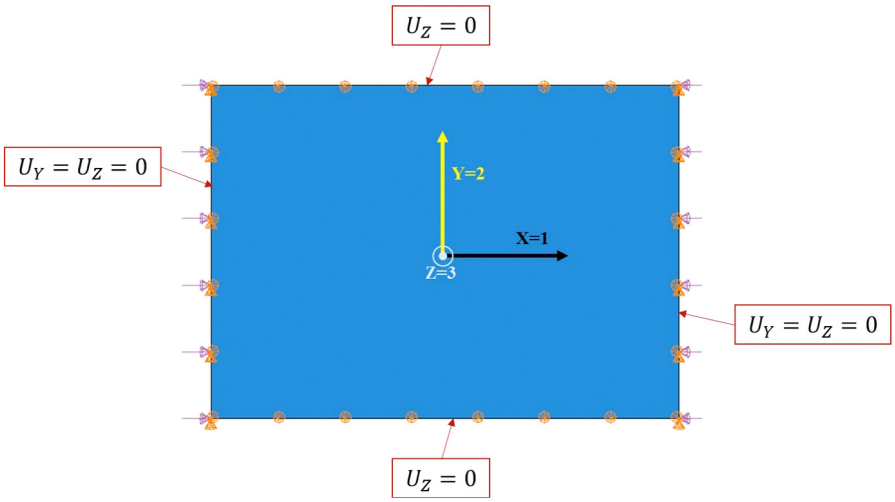

Fig. 3. Loads and boundary conditions (BCs) of the macroscopic FE model.

upper scale are the result of six static FE analyses (i.e. the equivalent stiffness tensor of the homogenised material is evaluated column-wise). When dealing with uncertainty quantification, the SEHTPM requires a strong computational effort to evaluate the propagation of the uncertainty from the microscopic scale to the mesoscopic one. Therefore, to reduce the computational cost, an efficient analytical homogenisation scheme has been considered in this work, i.e. the aforementioned Chamis' model. Moreover, this choice allows avoiding the integration of further FE model-related parameters like the mesh size. In particular, according to the Chamis' model, the ply engineering constants can be determined as follows:

$$
\begin{aligned}
E_1 &= V_F E_1^f + \left(1 - V_F\right) E^m, \\
E_2 = E_3 &= \frac{E^m}{1 - \sqrt{V_F}\left(1 - \frac{E^m}{E_2^f}\right)}, \\
G_{12} = G_{13} &= \frac{\frac{E^m}{2\left(1+\nu^m\right)}}{1 - \sqrt{V_F}\left(1 - \frac{\frac{E^m}{2\left(1+\nu^m\right)}}{G_{12}^f}\right)}, \\
G_{23} &= \frac{\frac{E^m}{2\left(1+\nu^m\right)}}{1 - \sqrt{V_F}\left(1 - \frac{E^m\left(1+\nu_{23}^f\right)}{E_2^f\left(1+\nu^m\right)}\right)}, \\
\nu_{12} = \nu_{13} &= \nu^m + V_F\left(\nu_{12}^f - \nu^m\right), \\
\nu_{23} &= \frac{E_2}{2G_{23}} - 1.
\end{aligned}
\tag{4}
$$

In Eq. (4), E_1^f, E_2^f, G_{12}^f, ν_{12}^f, ν_{23}^f are the elastic constants of the transversely isotropic fibre, while E^m and ν^m are the Young's modulus and the Poisson's ratio of the isotropic matrix. The volume fraction of the fibre is indicated as V_F. Moreover, the homogenised elastic properties of the ply are denoted as E_1, E_2, E_3, G_{12}, G_{13}, G_{23}, ν_{12}, ν_{13}, ν_{23}.

3.2. Mesoscopic/macroscopic scale transition: the finite element model

The distribution of the first buckling load of the multilayer plate is the result of an eigenvalue buckling analysis which is carried out by considering the distribution of the ply elastic properties evaluated by means of the Chamis' model. The FE model is developed into the Abaqus® environment [55]: the Abaqus® shell layered element S4R having *four* nodes and six degrees of freedom (DOFs) per node has been used to build the FE model of the multilayer plate. The kinematics of the element is described in the framework of the first-order shear deformation theory (FSDT) [1]. Of course, this type of element is well suited to describe the buckling strength of the laminate when its aspect ratio is in the range [20, 100]. For the problem at hand the multilayer plate is characterised by an aspect ratio $AR = 44.29$. Fig. 3 illustrates the loads and boundary conditions (BCs) for the proposed benchmarks.

As far as the mesh size is concerned, a sensitivity study of the first buckling load of the laminate to the number of elements (not reported here for the sake of brevity) has been performed: a model with 3654 DOFs is sufficient, to evaluate the first buckling load of the composite plate. The mesh of the FE model is illustrated in Fig. 4.

4. Probabilistic modelling and uncertainty quantification

4.1. Monte Carlo Analysis

The Monte Carlo (MC) method [41] is the most straightforward and robust one, among the popular methods used for calculating the response variability in stochastic structural mechanics. Based on the law of large numbers, MC approximates the statistical moments (e.g. mean, variance, etc.) of the quantity of interest (QoI), by performing a sufficient number of model evaluations, while sampling random, independent variables from the input space. The generated finite sample of the QoI is then post-processed, to obtain the unbiased statistics of the response estimates. In mathematical terms, the first and second moment

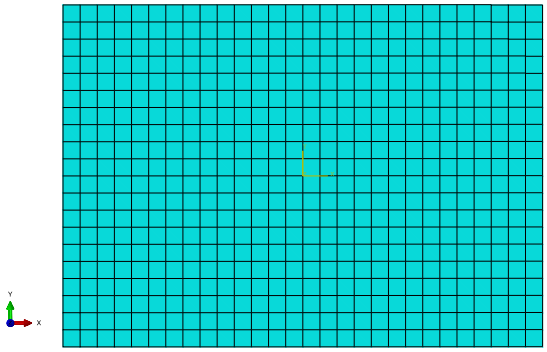

Fig. 4. Mesh of the macroscopic FE model.

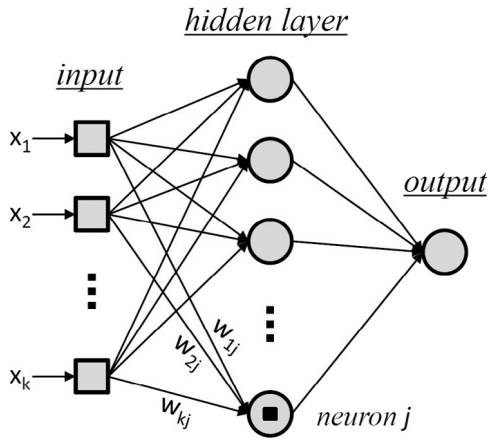

Fig. 5. Architecture of a single layer feed-forward neural network.

described in Eq. (2) for the discrete case, can be approximated after N realisations as:

$$\mu(\mathbf{r}) = \frac{1}{N}\sum_{j=1}^{N} r_j,$$
$$\sigma^2(\mathbf{r}) = \frac{1}{N-1}\sum_{j=1}^{N}\left[r_j - \mu(\mathbf{r})\right]^2. \tag{5}$$

where $\mathbf{r} = \{r_i,\ i = 1,\dots,N\}$ is the sample of the response QoI (e.g. displacement, force, bucking load etc.). Although MC can practically handle every problem, regardless of the complexity of the response surface topology, the large number of required model evaluations sets the method prohibitive for high-fidelity models (e.g. FE models), especially for applications of reliability or uncertainty quantification.

4.2. Variance-based global sensitivity analysis

In order to understand the cause-and-effect relationship between the input variables and the response, a classification of the random parameters in terms of output variability can be achieved through a global sensitivity analysis (GSA). The total variance of the QoI is decomposed into parts induced from single input parameters, but also potential interactions of the latter. Thus, the uncertain parameters can be qualitatively quantified, and the dominating ones can be later used into the models involved into the optimisation process introduced in Section 6.

Let $f(x_1, x_2, \dots\ x_k)$ be a square integrable scalar function over the k-dimensional unit hypercube Ω^k model. According to Sobol [56], f can be decomposed into sums of increasing dimensions as follows:

$$f = f_0 + \sum_i f_i + \sum_{j>i} f_{ij} + \cdots + f_{12\dots k}, \tag{6}$$

where $f_i = f_i(x_i)$, $f_{ij} = f_{ij}(x_i, x_j)$ etc. After several algebraic manipulations (the reader is referred to [56] or [41] for details), the final expression for the variance decomposition is reached:

$$\mathrm{Var}(y) = \sum_{i=1}^{k} V_i + \sum_{j>i}^{k} V_{ij} + \cdots + V_{12\dots k}, \tag{7}$$

$$\text{where} \quad V_i = \mathrm{Var}_{x_i}(E_{x_{\sim i}}(y|x_i)), \tag{8}$$

$$V_{ij} = \mathrm{Var}_{x_{ij}}(E_{x_{\sim ij}}(y|x_i, x_j)) - V_i - V_j \quad , \text{ etc.} \tag{9}$$

The $x_{\sim i}$ notation indicates the set of all variables except x_i. By dividing the term of interest by the unconditional variance $\mathrm{Var}(y)$, the first-order Sobol index is obtained as a fractional contribution:

$$S_i = \frac{V_i}{\mathrm{Var}(y)}. \tag{10}$$

In the case of non-analytical models, expressions such as Eq. (8) or (9) must be approximated via a sampling (e.g. Monte Carlo) procedure. Firstly, two (N, k) matrices with random samples from the input space are generated, namely A and B, with N being the number of realisations and k the stochastic dimension of the problem. After that, a third matrix A_B^i is formed, identical to A, except its ith column which is replaced by the ith column of B ($i = 1,\dots,k$). Finally, the model is evaluated with respect to the aforementioned input matrices, according to the following estimator for the first-order Sobol index, for every input parameter i:

$$V_i = \mathrm{Var}_{x_i}(E_{x_{\sim i}}(y|x_i)) \approx \frac{1}{N}\sum_{j=1}^{N} f(B)_j(f(A_B^i)_j - f(A)_j). \tag{11}$$

It is noteworthy that there are several other options available, regarding estimators of this sort [56]. A drawback of GSA, is that formulae like Eq. (11) require excessive realisations in order to converge (order of 10^4 or 10^5). In the context of computationally expensive simulations, such as FE analyses, a possible remedy is the emulation of the input–output relationship via a surrogate model, as it is described in the next section.

4.3. Surrogate modelling with Artificial Neural Networks

Surrogate models (or metamodels) are mathematical functions able to mimic the response of a model, when trained with a relatively small training set of model evaluations. Afterwards, the demanding model can be substituted from these inexpensive proxy models, for applications requiring an excessive amount of simulations (e.g. optimisation, reliability, GSA etc.) Popular choices, among relevant research studies, are ANNs, Gaussian processes (or Kriging), polynomial chaos expansions (PCE) and support vector machines (SVM), as outlined in [57].

In this work, a surrogate is appropriately trained to emulate the multi-scale modelling strategy described in Section 3. The material properties of the different phases at the micro-scale, listed in Eq. (15), are used as input, while the output response is the plate first buckling load. The aim of the surrogate is twofold. Firstly, it is used for the GSA and the evaluations required by the estimator of Eq. (11). Secondly, as explained in Section 1, it is used into the multi-scale identification strategy to boost the optimisation process. Concerning the surrogate type, ANNs are selected in this study, mostly because, despite their versatility and their good generalisation, they only have few parameters to be tuned within their training procedure, which is beneficial for the optimisation algorithm.

In particular, an ANN is a parallel information-processing system, consisting of at least three layers: the input, the output and one (or more) hidden layer. The nodes inside every layer are called *neurons* and they are linked by the so-called *synapses*. When information is circulated only in a single direction, the network is called feed-forward.

An illustration of a typical single-layer, feed-forward ANN configuration is shown in Fig. 5. It is noteworthy that the input neurons (squares) connect the network to the external environment, without further processing information, while the hidden layer neurons (circles) process information from a previous layer and feed it to the next one.

The learning procedure of an ANN is based on a general unconstrained optimisation problem, where the weight parameters w_{ij} assigned to every synapse are the design variables, and the objective function is the sum squared error between the predicted output $t(w_{ij})$ and the target output y_0:

$$E(w_{ij}) = \frac{1}{2}\sum[t(w_{ij}) - y_0]^2. \tag{12}$$

During the process, the weights are updated through an iterative procedure, until the desired error level is achieved or the maximum number of cycles is reached:

$$w_{ij}^{(t+1)} = w_{ij}^{(t)} + \Delta w_{ij}, \tag{13}$$

where Δw_{ij} is the correction of the weight at the tth learning step. In order to avoid overfitting, a fraction of the sample data is used as a validation dataset and the error is monitored over the iterations to stop the training early enough. Regarding the internal process in every neuron, each input from the previous neuron is placed into a weighted sum as the following:

$$z_j = \sum_{i=1}^{k} x_i w_{ij} + b, \tag{14}$$

which then goes through an activation function where the nonlinearity of the decision boundary is introduced (usually of sigmoid type). The term b in the previous equation is a bias term allowing the neuron to cover a broader range. For more details on ANNs, the interested reader is addressed to [41].

5. Sensitivity analysis of the meta-model

5.1. Global sensitivity analyses for the two benchmarks

The implementation of the Artificial Neural Network, described in Section 4.3, allows to apply the variance-based GSA described in Section 4.2, since the computational effort needed to perform the convergence of the Sobol index is negligible. All the material and geometrical variables of the constitutive phases with the related uncertainty are considered here: through the total output variance decomposition, it is possible to identify the dominant microscopic input parameters, from a statistical point of view.

According to the hypotheses given in Section 1, a total of eight variables can be identified for the microscopic constituents of the composite, i.e.

$$\mathbf{x} = \left\{ E_1^f, E_2^f, G_{12}^f, \nu_{12}^f, \nu_{23}^f, E^m, \nu^m, V_F \right\}. \tag{15}$$

The related mean and standard deviation values are summarised in Table 1, in which, a COV equal to 10% is set, for all the parameters concerning the microscopic scale. The causes at the basis of this uncertainty are various and often very difficult to be identified. For example, the uncertainty of the fibre volume fraction is often related to the manufacturing process parameters.

The results of the variance-based GSA for every benchmark are shown in Figs. 6(a) and 7(a), in terms of the evolution of the Sobol index, defined in Eq. (11), over the number of simulations. It is possible to observe that the Sobol index converges after around 15000 simulations, for both benchmarks.

The pie diagrams shown in Figs. 6(b) and 7(b) highlight a result of paramount importance: the sensitivity of the first buckling load to the material and geometrical properties of the constitutive phases (and the related uncertainty as well) is strongly influenced by the nature of the stacking sequence. In particular, for benchmark BK1, which is characterised by a quasi-isotropic symmetric stack, the sensitivity of the first buckling load to the elastic properties E_2^f, G_{12}^f, ν_{12}^f, ν_{23}^f, E^m, ν^m is negligible. Accordingly, only E_1^f and V_F affects the laminate behaviour in terms of first buckling load.

Conversely, since the multilayer plate of benchmark BK2 is characterised by an angle-ply orthotropic symmetric stacking sequence, the first buckling load is influenced by the following properties: E_1^f, E_2^f, E^m and V_F. The sensitivity of the laminate buckling strength to the other elastic properties remains negligible also for this configuration of the plate.

According to the aforementioned remarks, the number of parameters (characterising the material and geometrical properties uncertainty) to be identified varies with the considered benchmark. These aspects are discussed in detail in the following Section.

Table 2
Benchmark BK1: bounds of the design variables.

Microscopic parameters	Lower bound	Upper bound
$\mu\left(E_1^f\right)$ [GPa]	220.8	331.2
$\sigma\left(E_1^f\right)$ [GPa]	22.08	33.12
$\mu\left(V_F\right)$	0.444	0.666
$\sigma\left(V_F\right)$	0.0444	0.0666

6. Mathematical formulation of the inverse problem

6.1. Optimisation variables, objective function and constraints

The multi-scale identification problem is stated as a classical constrained inverse problem: the identification of the elastic properties variability of the composite constitutive phases can be achieved by minimising the Euclidean distance between the reference distribution of the buckling load and that resulting from the numerical simulation.

As discussed in Section 5, the sensitivity of the buckling load distribution to the material and geometrical parameters of the microscopic constituents is strongly affected by the stacking sequence of the laminate. Therefore, the number of optimisation variables (i.e. the parameters of the distribution law, for each property at the microscopic scale, to be identified) depends upon the considered benchmark. As a result of the GSA discussed in Section 5, the parameters tuning the distribution of the most relevant elastic and geometrical properties of the constitutive phases can be arranged in the vector of design variables $\boldsymbol{\xi}^{\alpha}$, $(\alpha = \mathrm{BK1}, \mathrm{BK2})$ as follows:

$$\boldsymbol{\xi}^{\mathrm{BK1}} = \left\{ \mu\left(E_1^f\right), \sigma\left(E_1^f\right), \mu\left(V_F\right), \sigma\left(V_F\right) \right\}, \tag{16}$$

$$\boldsymbol{\xi}^{\mathrm{BK2}} = \left\{ \mu\left(E_1^f\right), \sigma\left(E_1^f\right), \mu\left(E_2^f\right), \sigma\left(E_2^f\right), \mu\left(E^m\right), \sigma\left(E^m\right), \mu\left(V_F\right), \sigma\left(V_F\right) \right\}. \tag{17}$$

Accordingly, benchmark BK1 is characterised by four design variables, whilst benchmark BK2 has eight design variables. In both cases, the elastic properties excluded from the vector of design variables (due to the negligible sensitivity of the first buckling load to these quantities) have been set to the reference mean values listed in Table 1.

Each design variable can vary into a suitable definition domain which depends upon the considered benchmark. Lower and upper bounds of design variables for benchmarks BK1 and BK2 are given in Tables 2 and 3, respectively.

Moreover, in order to ensure the positive definiteness of the stiffness tensors of both the lamina (mesoscopic scale) and the constitutive phases (microscopic scale) [36], every combination of elastic properties generated through the Monte-Carlo technique, must satisfy a set of non-linear constraints $\mathbf{g}(\boldsymbol{\xi}^{\alpha})$ [36]. Of course, these constraints must be

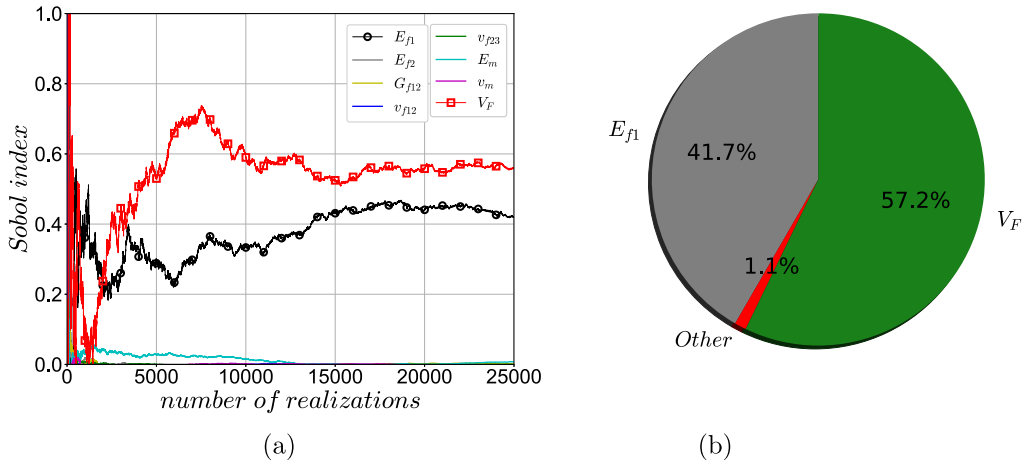

Fig. 6. (a) Convergence of the Sobol index and (b) sensitivity analysis results, for the first benchmark (BK1).

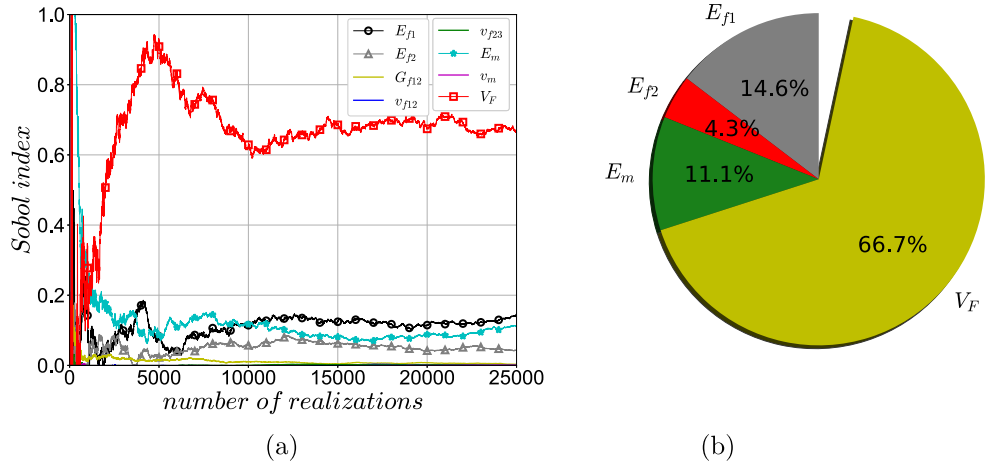

Fig. 7. (a) Convergence of the Sobol index and (b) sensitivity analysis results, for the second benchmark (BK2).

Table 3
Benchmark BK2: bounds of the design variables.

Microscopic parameters	Lower bound	Upper bound
$\mu\left(E_1^f\right)$ [GPa]	220.8	331.2
$\sigma\left(E_1^f\right)$ [GPa]	22.08	33.12
$\mu\left(E_2^f\right)$ [GPa]	13.84	20.76
$\sigma\left(E_2^f\right)$ [GPa]	1.384	2.076
$\mu(E^m)$ [GPa]	3.312	4.968
$\sigma(E^m)$ [GPa]	0.3312	0.4968
$\mu(V_F)$	0.444	0.666
$\sigma(V_F)$	0.0444	0.0666

imposed at the lamina-level and at the constitutive phases-level. For the elementary lamina, these constraints read:

$$
\begin{aligned}
&g_1(\xi^\alpha) = |\nu_{12}(\xi^\alpha)| - \sqrt{\frac{E_1(\xi^\alpha)}{E_2(\xi^\alpha)}} < 0,\\
&g_2(\xi^\alpha) = |\nu_{23}(\xi^\alpha)| - \sqrt{\frac{E_2(\xi^\alpha)}{E_3(\xi^\alpha)}} < 0,\\
&g_3(\xi^\alpha) = 2\nu_{12}(\xi^\alpha)\nu_{13}(\xi^\alpha)\nu_{23}(\xi^\alpha)\frac{E_3(\xi^\alpha)}{E_1(\xi^\alpha)} + \cdots\\
&+\nu_{12}(\xi^\alpha)^2\frac{E_2(\xi^\alpha)}{E_1(\xi^\alpha)} + \nu_{23}(\xi^\alpha)^2\frac{E_3(\xi^\alpha)}{E_2(\xi^\alpha)} + \nu_{13}(\xi^\alpha)^2\frac{E_3(\xi^\alpha)}{E_1(\xi^\alpha)} - 1 < 0,
\end{aligned}
\tag{18}
$$

whilst for the constitutive phases they can be written as

$$
\begin{aligned}
&g_4(\xi^\alpha) = |\nu_{12}^f| - \sqrt{\frac{E_1^f(\xi^\alpha)}{E_2^f(\xi^\alpha)^f}} < 0,\\
&g_5(\xi^\alpha) = |\nu_{23}^f| - 1 < 0,\\
&g_6(\xi^\alpha) = \frac{E_1^f(\xi^\alpha)}{E_2^f(\xi^\alpha)}\left[2\nu_{23}^f\left(\nu_{12}^f\right)^2 + 2\left(\nu_{12}^f\right)^2\right] - 1 < 0.
\end{aligned}
\tag{19}
$$

The objective function $\Phi(\xi^\alpha)$ is defined as the Euclidean distance between the *reference* and the numerical mechanical response, in terms of the probabilistic parameters $\mu_{buckling}$ and $\sigma_{buckling}$ of the first buckling load. In particular, this objective function is a least-square error estimator defined as:

$$
\Phi(\xi^\alpha) = \left(\frac{\mu_{buckling}(\xi^\alpha) - \mu_{buckling}^{\text{ref}}}{\mu_{buckling}^{\text{ref}}}\right)^2 + \left(\frac{\sigma_{buckling}(\xi^\alpha) - \sigma_{buckling}^{\text{ref}}}{\sigma_{buckling}^{\text{ref}}}\right)^2. \tag{20}
$$

Finally, the multi-scale inverse problem is stated as a classical CNLPP as:

$$
\begin{aligned}
&\min_{\xi^\alpha} \Phi(\xi^\alpha),\\
&\text{subject to:}\\
&g_j(\xi^\alpha) \le 0, \quad j = 1, \ldots, 6.
\end{aligned}
\tag{21}
$$

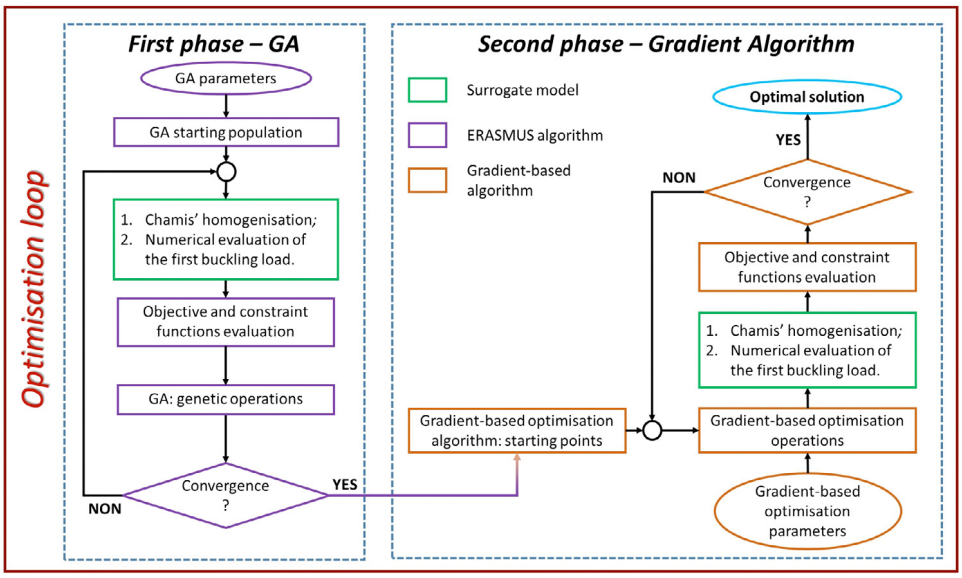

Fig. 8. Optimisation strategy for the resolution of problem (21).

6.2. The numerical strategy

Problem (21) is a non-convex CNLPP, in terms of constraints and objective function. The number of parameters, describing the variability of material and geometrical properties of the constitutive phases, depends on the considered benchmark: the first benchmark (BK1) allows to characterise four parameters, while the second benchmark (BK2) allows to characterise up to eight parameters. Of course, the non-convexity of problem (21) implies the lack of uniqueness of its solution [36].

Taking into account all these aspects, the CNLPP of Eq. (21) is solved by means of a hybrid optimisation tool based on the GA ERASMUS (EvolutionaRy Algorithm for optimiSation of ModUlar Systems), which is interfaced with the MATLAB® *fmincon* algorithm [39], as shown in Fig. 8. The GA ERASMUS has already been used successfully to solve different classes of real-world engineering problems [58–66].

The procedure illustrated in Fig. 8 is articulated in two phases. The first one represents the global solution search and it is carried out through the GA ERASMUS: the goal is to find potential suboptimal solutions which will constitute the starting points for the gradient-based optimisation algorithm. The genotype of the individual is characterised by one chromosome and four genes for the first benchmark (BK1) and eight genes for the second benchmark (BK2).

The second step is the local optimisation phase and it is performed by means of the MATLAB® *fmincon* tool. The selected optimisation solver is the *active-set* algorithm, i.e. a Quasi-Newton method, in which an approximation of the Hessian matrix is used to compute the descent direction [39].

Each optimisation algorithm has been interfaced to the ANN, presented in Section 4, which emulate both the homogenisation phase and the eigenvalue buckling analysis. The ANN has been employed in order to reduce significantly the computational effort.

In particular, the output of the ANN is the current value of both the objective and the constraint functions which are passed to the optimisation tool in order to execute the optimisation operations: these operations are repeated until the user-defined convergence criteria are met.

Table 4
Variability parameters of the *reference* first buckling load.

Benchmark	$\mu\left(\sigma^{I}_{buckling}\right)$ [MPa]	COV $\left(\sigma^{I}_{buckling}\right)$
BK1	83.41	0.12
BK2	59.3	0.098

7. Numerical results

7.1. Buckling response for the reference configuration

The multi-scale inverse problem defined in Eq. (21) requires the computation of the objective function $\Phi(\xi^{\alpha})$ of Eq. (20): this function depends upon the buckling *reference* response which must be evaluated before starting the optimisation process. Due to the difficulty to get experimental data in terms of variability of the microscopic material properties and the related buckling probability distribution at the macroscopic scale, a numerical test is performed in order to obtain the *reference* data.

To deal with this task, the *reference* variability parameters of material and geometrical properties of the microscopic constituents, listed in Table 1, are considered for each benchmark.

Firstly, a Monte-Carlo simulation is performed to generate randomly a statistically representative number of samples. Secondly, for each sample, the homogenisation step is performed by using the Chamis' model, described in Section 3, to get the lamina elastic properties that are used into the macroscopic FE model, to compute the first buckling load of the plate. After carrying out these operations for the whole set of samples, it is possible to determine the mean value and the relative COV of the first buckling load, according to Eqs. (2) and (3), respectively. The variability parameters of the *reference* first buckling load distribution are then summarised in Table 4: these quantities have been obtained by performing 1000 realisations.

Furthermore, a small sub-set of 20 realisations has been used to train the ANN, for each benchmark. In order to check the accuracy of the ANN, 50 samples generated with the Monte-Carlo technique have been selected as a *validation set* and a comparison between them and the results provided by the ANN is carried out, as shown in Fig. 9 (only the results related to the first benchmark have been reported for the sake of brevity). As a matter of fact, the results provided by the ANN

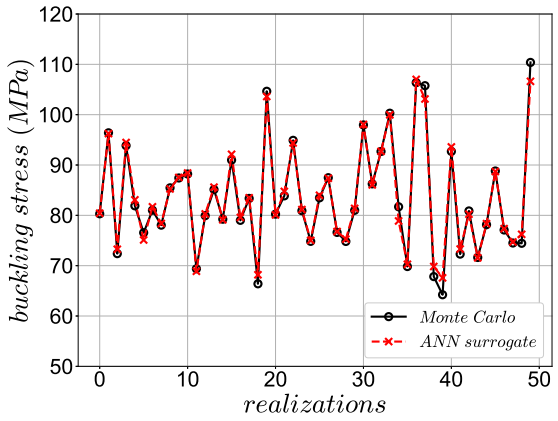

Fig. 9. Comparison between the validation set of samples and the results provided by the ANN.

Table 5
Optimisation parameters for the genetic algorithm, for benchmarks BK1 and BK2.

Parameters	BK1	BK2
N. of individuals	40	80
N. of populations	2	2
N. of iterations	100	100
Crossover probability.	0.85	0.85
Mutation probability.	0.025	0.0125
Isolation time	20	20

Table 6
Optimisation parameters for the gradient-based algorithm, for benchmarks BK1 and BK2.

Parameters	BK1	BK2
Solver	Active-set	Active-set
Max n. of function evaluation	10000	10000
Tol. on the objective function	10^{-15}	10^{-15}
Tol. on the gradient norm	10^{-15}	10^{-15}

are in very good agreement with the samples constituting the validation set.

7.2. Numerical results of the MSIS for benchmarks BK1 and BK2

As discussed in Section 2, two benchmarks are investigated in order to show the effectiveness of the proposed MSIS, by varying the stacking sequence of the multilayer plate.

The parameters tuning the GA and the deterministic algorithms are summarised in Tables 5 and 6, respectively, according to the main guidelines described in [67].

The GA calculation is performed with two populations, in which, the number of individuals, evolving along the selected maximum number of generations, depends on the considered benchmark. Indeed, the best practice is to set the number of individuals greater than or equal to ten times the number of optimisation variables. Accordingly, benchmarks BK1 and BK2 are characterised by two populations composed of 40 and 80 individuals, respectively. The two populations exchange the best individual every ten iterations, by using a ring-type operator, whose probability is automatically computed by the considered GA. Moreover, as far as the constraint-handling technique is concerned, the Automatic Dynamic Penalisation (ADP) method is used [68].

It is noteworthy that, the choice of multiple populations, with a small number of individuals, allows finding the global minimum without increasing too much the computational effort. In this way, the GA has the possibility to explore the design domain in the most effective way, by exchanging information between the best individuals belonging to each population: the reader is addressed to [37] for more details about these aspects.

Inasmuch as the proposed strategy makes use of a metaheuristic algorithm, the GA is run three times for each benchmark. The best individual obtained at the end of the genetic calculation is used as a starting guess for the gradient-based algorithm, in order to execute the subsequent local optimisation.

In terms of computational effort, the training phase of the ANN needs several seconds to be performed. Then, the hybrid optimisation strategy needs 37.8 and 68.2 h for the benchmarks BK1 and BK2, respectively, on an Intel® Xeon® 2.70 GHz CPU with two processors and with a RAM of 128 GB.

Table 7
Optimum solution of the multi-scale inverse problem provided by the GA, for benchmark BK1.

Analysis name	$\mu\left(E_1^f\right)$ [GPa]	$\sigma\left(E_1^f\right)$ [GPa]	$\mu\left(V_F\right)$	$\sigma\left(V_F\right)$
REF	276	27.6	0.555	0.0555
GE1A	238	27.1	0.628	0.0562
GE1B	237	27.1	0.630	0.0562
GE1C	237	27.1	0.630	0.0564
GE2A	257	25.5	0.589	0.0595
GE2B	257	25.5	0.589	0.0595
GE2C	257	25.4	0.589	0.0597
GE3A	221	25.3	0.665	0.0597
GE3B	223	25.5	0.662	0.0593
GE3C	223	25.5	0.661	0.0593

The results provided by the ERASMUS GA for benchmarks BK1 and BK2 are summarised in Tables 7 and 9, respectively, whilst those provided by the gradient-based algorithm are reported in Tables 8 and 10, respectively. In order to compare the obtained results with the *reference* ones, the average of the solutions provided by the gradient-based algorithm is performed for each identified parameter, as it can be seen in Tables 8 and 10, for each benchmark.

As it can be easily inferred from the analysis of these results, the mean value and the standard deviation of the microscopic material properties are in good agreement with the *reference* data: the absolute percentage error ranges from 2.8% to 13.4% for the first benchmark and from 0.2% to 3.2% for the second benchmark.
The discrepancy between the values of $\mu\left(E_1^f\right)$ and $\mu\left(V_F\right)$ provided by the MSIS and the reference ones, for benchmark BK1, is related to the nature of the laminate stack. Indeed, for this benchmark, the considered sequence has an isotropic membrane stiffness matrix but a completely anisotropic bending stiffness matrix. This aspect has a strong influence on the solution search for the multi-scale inverse problem because the first buckling load is dominated by the bending stiffness of the laminate. In particular, if the bending stiffness matrix is not orthotropic, problem (21) becomes strongly non-convex and several equivalent optimal solutions exist. Therefore, finding the global minimum is anything but trivial in such a case.
These results prove that a particular care should be put in the choice of the stacking sequence, which strongly affects both the number of parameters that is possible to identify and the quality of the final result.

8. Conclusions

In this work the multi-scale identification strategy (MSIS), initially presented in [36], has been extended to the characterisation of the uncertainty of the geometrical and the elastic properties of the fibre and the matrix at the microscopic scale, by using information restrained in the macroscopic response of the laminate, i.e. the first buckling load of the multilayer plate.

In this context, the multi-scale characterisation problem, is stated as a constrained inverse problem. The goal is the minimisation of the distance between the numerical and the reference variability parameters that describe the probability distribution of the first buckling load.

Table 8
Optimum solution of the multi-scale inverse problem provided by the gradient-based algorithm, for benchmark BK1; the percentage difference between the solution and the microscopic *reference* data are given in parentheses.

Analysis name	$\mu\left(E_1^f\right)$ [GPa]	$\sigma\left(E_1^f\right)$ [GPa]	$\mu\left(V_F\right)$	$\sigma\left(V_F\right)$	$\Phi(\mathbf{x})$
REF	276	27.6	0.555	0.0555	0
GR1A	238	27.1	0.625	0.0564	3.01E−05
GR1B	244	27.6	0.616	0.0567	5.58E−07
GR1C	235	27.1	0.632	0.0526	1.62E−05
GR2A	257	25.6	0.588	0.0594	7.33E−06
GR2B	257	25.5	0.589	0.0596	3.00E−07
GR2C	255	25.2	0.594	0.0586	2.88E−07
GR3A	221	25.3	0.665	0.0597	2.48E−07
GR3B	223	27.1	0.663	0.0512	2.11E−06
GR3C	223	25.5	0.661	0.0593	7.37E−08
AVERAGE	239 (−13.4)	26.2(−5)	0.626 (12.8)	0.0571 (2.8)	

Table 9
Optimum solution of the multi-scale inverse problem provided by the GA, for benchmark BK2.

Analysis name	$\mu\left(E_1^f\right)$ [GPa]	$\sigma\left(E_1^f\right)$ [GPa]	$\mu\left(E_2^f\right)$ [GPa]	$\sigma\left(E_2^f\right)$ [GPa]	$\mu(E^m)$ [GPa]	$\sigma(E^m)$ [GPa]	$\mu\left(V_F\right)$	$\sigma\left(V_F\right)$
REF	276	27.6	17.3	1.73	4.14	0.414	0.555	0.0555
GE1A	255	31.2	15.7	1.50	3.64	0.412	0.620	0.0540
GE1B	311	30.3	20.1	2.02	4.49	0.366	0.482	0.0547
GE1C	313	30.2	20.0	1.59	4.47	0.363	0.482	0.0554
GE2A	304	22.4	18.3	1.51	3.43	0.484	0.568	0.0523
GE2B	304	22.4	18.3	1.51	3.43	0.484	0.568	0.0523
GE2C	258	24.5	16.0	1.93	4.23	0.467	0.581	0.0593
GE3A	233	24.8	16.0	1.59	4.16	0.404	0.615	0.0633
GE3B	233	24.8	16.0	1.59	4.16	0.409	0.615	0.0632
GE3C	233	24.8	16.0	1.60	4.16	0.404	0.615	0.0633

Table 10
Optimum solution of the multi-scale inverse problem provided by the gradient-based algorithm, for benchmark BK2; the percentage difference between the solution and the microscopic *reference* data are given in parentheses.

Analysis name	$\mu\left(E_1^f\right)$ [GPa]	$\sigma\left(E_1^f\right)$ [GPa]	$\mu\left(E_2^f\right)$ [GPa]	$\sigma\left(E_2^f\right)$ [GPa]	$\mu(E^m)$ [GPa]	$\sigma(E^m)$ [GPa]	$\mu\left(V_F\right)$	$\sigma\left(V_F\right)$	$\Phi(\mathbf{x})$
REF	276	27.6	17.3	1.73	4.14	0.414	0.555	0.0555	0
GR1A	288	31.3	17.7	1.74	4.24	0.433	0.520	0.0514	4.50E−04
GR1B	280	28.8	18.8	1.75	4.33	0.401	0.529	0.0539	1.77E−06
GR1C	306	29.4	19.5	1.58	4.38	0.377	0.497	0.0548	4.27E−07
GR2A	288	31.3	17.7	1.74	4.24	0.433	0.520	0.0514	1.71E−09
GR2B	304	22.4	18.3	1.51	3.43	0.484	0.568	0.0523	3.59E−08
GR2C	258	26.1	16.4	1.96	4.14	0.450	0.569	0.0579	2.76E−04
GR3A	236	24.7	16.0	1.61	4.14	0.402	0.610	0.0634	2.05E−05
GR3B	233	24.8	16.0	1.59	4.16	0.409	0.615	0.0632	1.45E−07
GR3C	233	24.7	16.2	1.59	4.14	0.407	0.617	0.0634	1.98E−07
AVERAGE	270 (−2.3)	27 (−2)	17.4 (0.5)	1.67 (−3.2)	4.13 (−0.2)	0.422 (1.9)	0.561 (1)	0.0569 (2.5)	

In this case, the solution search is performed by a hybrid optimisation tool, in which, a metaheuristic algorithm and a gradient-based one have been interfaced to solve the related non-convex CNLPP.

The MSIS makes use of an analytical homogenisation scheme, i.e. the Chamis' model, to perform the microscopic/mesoscopic scale transition. The elastic properties of the elementary lamina evaluated by means of the Chamis' model are then used into the FE model of the multilayer plate to evaluate its first buckling load.

Moreover, a Monte-Carlo simulation campaign has been performed to compute the probability distribution of the first buckling load, starting from a Gaussian probability distribution of the material properties of the constituent phases. The obtained samples have been used to train an ANN which emulates the multi-scale mechanical response of the plate: the inputs are the geometrical and elastic properties of the microscopic constituents of the composite and the output is the first-buckling load of the laminate. Then, the obtained surrogate model has been used into the optimisation process to reduce the computational effort.

Before executing the hybrid optimisation process, a sensitivity study has been performed to determine the most relevant microscopic parameters influencing the first buckling load at the macroscopic scale. In particular, numerical results show that this sensitivity is strongly affected by the nature of the stacking sequence. Therefore to prove the effectiveness of the proposed MSIS two different stacking sequences have been considered: the first benchmark is characterised by a symmetric quasi-isotropic stack, while the second one is characterised by a symmetric orthotropic one.

As a consequence, also the obtained results, in terms of the identification of the parameters tuning the variability of the elastic and geometrical properties of the constitutive phases of the composite, are strongly influenced by the nature of the laminate lay-up. In particular, for the first benchmark the absolute percentage error ranges from 2.8% to 13.4% for the standard deviation of the fibre volume fraction $\sigma\left(V_F\right)$ and the mean value of the fibre longitudinal elastic modulus $\mu\left(E_1^f\right)$, respectively. Conversely, for the second benchmark the absolute percentage error ranges from 0.2% to 3.2% for the mean value of the matrix elastic modulus $\mu(E^m)$ and the standard deviation of the fibre transverse elastic modulus $\sigma\left(E_2^f\right)$.

Nevertheless, thanks to the proposed MSIS, it is possible to retrieve the variability of both longitudinal and transversal effective properties of the constitutive phases and this task cannot be easily performed by means of standard ASTM tests.

As far as perspectives of this work are concerned, research is ongoing in order to include into the MSIS the following aspects:

- the validation of the MSIS by means of experimental data. In this case, the influence of noise on the results provided by the MSIS should be properly taken into account. To this purpose, suitable regularisation techniques, as the Tikhonov–Morozov one, which is widely used in different engineering fields [69,70], must be efficiently integrated into the multi-scale identification process to handle noise;
- the formulation of a dedicated optimisation problem to find a suitable stack which maximise the sensitivity of the first buckling load to each parameter defined at the microscopic scale of the composite;
- the extension of the MSIS to the characterisation of the variability of the viscoelastic properties of the microscopic constituent and the evaluation of the variability effects related to further geometrical parameters, e.g. fibre misalignment, macroscopic geometrical defects, etc.

Finally, thanks to the versatility of the proposed MSIS, it is possible to increase the accuracy in terms of variability parameters by introducing more general probability density functions for both the buckling load and the microscopic parameters. In this way, it will be possible to go beyond the limits of the Gaussian model, in which the shape of the distribution is imposed a priori.

Acknowledgements

This research work has been carried out within the project FULLCOMP (FULLy analysis, design, manufacturing, and health monitoring of COMPosite structures), funded by the European Union Horizon 2020 Research and Innovation program under the Marie Skłodowska-Curie grant agreement No. 642121.

References

[1] Jones RM. Mechanics of composite materials. McGraw-Hill; 1975.
[2] Funari MF, Greco F, Lonetti P, Luciano R, Penna R. An interface approach based on moving mesh and cohesive modeling in Z-pinned composite laminates. Composites B 2018;135:207–17. http://dx.doi.org/10.1016/j.compositesb.2017.10.018.
[3] Funari MF, Greco F, Lonetti P. A moving interface finite element formulation for layered structures. Composites B 2016;96:325–37. http://dx.doi.org/10.1016/j.compositesb.2016.04.047.
[4] Funari MF, Greco F, Lonetti P. A numerical model based on ALE formulation to predict crack propagation in sandwich structures. Fract. Struct. Integr. 2019;47:277–93, Ten years of 'Frattura ed Integrità Strutturale'. http://dx.doi.org/10.3221/IGF-ESIS.47.21.
[5] Naskar S, Mukhopadhyay T, Sriramula S. Probabilistic micromechanical spatial variability quantification in laminated composites. Composites B 2018;151:291–325. http://dx.doi.org/10.1016/j.compositesb.2018.06.002.
[6] Sepahvand K, Marburg S. Identification of composite uncertain material parameters from experimental modal data. Probab Eng Mech 2014;37:148–53. http://dx.doi.org/10.1016/j.probengmech.2014.06.008.
[7] ASTM D3039 / D3039M-17, Standard test method for tensile properties of polymer matrix composite materials. West Conshohocken, PA: ASTM International; 2017.
[8] ASTM D790-17, Standard test methods for flexural properties of unreinforced and reinforced plastics and electrical insulating materials. West Conshohocken, PA: ASTM International; 2017.
[9] ASTM D3410 / D3410M-16, Standard test method for compressive properties of polymer matrix composite materials with unsupported gage section by shear loading. West Conshohocken, PA: ASTM International; 2016.
[10] ASTM D5379 / D5379M-12, Standard test method for shear properties of composite materials by the v-notched beam method. West Conshohocken, PA: ASTM International; 2012.
[11] ASTM D7078 / D7078M-12, Standard test method for shear properties of composite materials by v-notched rail shear method. West Conshohocken, PA: ASTM International; 2012.
[12] ASTM D3518 / D3518M-13, Standard test method for in-plane shear response of polymer matrix composite materials by tensile test of a 45 Laminate. West Conshohocken, PA: ASTM International; 2013.
[13] ASTM D2344 / D2344M-16, Standard test method for short-beam strength of polymer matrix composite materials and their laminates. West Conshohocken, PA: ASTM International; 2016.
[14] ASTM D3379-75(1989)e1, Standard test method for tensile strength and young's modulus for high-modulus single-filament materials (withdrawn 1998). West Conshohocken, PA: ASTM International; 1975.
[15] ASTM D638-14, Standard test method for tensile properties of plastics. West Conshohocken, PA: ASTM International; 2014.
[16] Nairn JA. Analytical fracture mechanics analysis of the pull-out test including the effects of friction and thermal stresses. Adv Compos Lett 2000;9(6):373–83.
[17] Maurin R, Davies P, Baral N, Baley C. Transverse properties of carbon fibres by nano-indentation and micro-mechanics. Appl Compos Mater 2018;15:61–73.
[18] Feih S, Wonsyld K, Minzari D, Westermann P, Lilholt H. Testing procedure for the single fiber fragmentation test, vol. 1483(EN). Denmark: Forskningscenter Risoe. Risoe-R; 2004.
[19] Sepahvand K, Marburg S. On construction of uncertain material parameter using generalized polynomial chaos expansion from experimental data. Procedia IUTAM 2013;6:4–17, IUTAM Symposium on Multiscale Problems in Stochastic Mechanics. http://dx.doi.org/10.1016/j.piutam.2013.01.001.
[20] Pajonk O, Rosić BV, Litvinenko A, Matthies HG. A deterministic filter for non-Gaussian Bayesian estimation— Applications to dynamical system estimation with noisy measurements. Physica D 2012;241(7):775–88. http://dx.doi.org/10.1016/j.physd.2012.01.001.
[21] Desceliers C, Ghanem R, Soize C. Maximum likelihood estimation of stochastic chaos representations from experimental data. Internat J Numer Methods Engrg 2006;66(6):978–1001. http://dx.doi.org/10.1002/nme.1576.
[22] Marzouk YM, Najm HN, Rahn LA. Stochastic spectral methods for efficient Bayesian solution of inverse problems. J Comput Phys 2007;224(2):560–86. http://dx.doi.org/10.1016/j.jcp.2006.10.010.
[23] Soize C. A computational inverse method for identification of non-Gaussian random fields using the Bayesian approach in very high dimension. Comput Methods Appl Mech Engrg 2011;200(45):3083–99. http://dx.doi.org/10.1016/j.cma.2011.07.005.
[24] Narayanan VAB, Zabaras N. Stochastic inverse heat conduction using a spectral approach. Internat J Numer Methods Engrg 2004;60(9):1569–93. http://dx.doi.org/10.1002/nme.1015.
[25] Proppe C. Reliability computation with local polynomial chaos approximations. ZAMM Z Angew Math Mech 2009;89(1):28–37. http://dx.doi.org/10.1002/zamm.200800072.
[26] Batou A, Soize C. Stochastic modeling and identification of an uncertain computational dynamical model with random fields properties and model uncertainties. Arch Appl Mech 2012;1–18.
[27] Wang J, Zabaras N. Hierarchical Bayesian models for inverse problems in heat conduction. Inverse Problems 2004;21(1):183–206. http://dx.doi.org/10.1088/0266-5611/21/1/012.
[28] Ghanem RG, Doostan A. On the construction and analysis of stochastic models: Characterization and propagation of the errors associated with limited data. J Comput Phys 2006;217(1):63–81, Uncertainty Quantification in Simulation Science. http://dx.doi.org/10.1016/j.jcp.2006.01.037.
[29] Chen C, Duhamel D, Soize C. Probabilistic approach for model and data uncertainties and its experimental identification in structural dynamics: Case of composite sandwich panels. J Sound Vib 2006;294(1):64–81. http://dx.doi.org/10.1016/j.jsv.2005.10.013.
[30] Rosić BV, Litvinenko A, Pajonk O, Matthies HG. Sampling-free linear Bayesian update of polynomial chaos representations. J Comput Phys 2012;231(17):5761–87. http://dx.doi.org/10.1016/j.jcp.2012.04.044.
[31] Vu-Bac N, Rafiee R, Zhuang X, Lahmer T, Rabczuk T. Uncertainty quantification for multiscale modeling of polymer nanocomposites with correlated parameters. Composites B 2015;68:446–64. http://dx.doi.org/10.1016/j.compositesb.2014.09.008.
[32] Riley EJ, Koudela KL, Narayanan RM. Characterization of the electromagnetic parameter uncertainty in single-ply unidirectional carbon-fiber-reinforced-polymer laminas. Composites B 2019;162:361–8. http://dx.doi.org/10.1016/j.compositesb.2018.10.089.
[33] Dey S, Mukhopadhyay T, Sahu S, Li G, Rabitz H, Adhikari S. Thermal uncertainty quantification in frequency responses of laminated composite plates. Composites B 2015;80:186–97. http://dx.doi.org/10.1016/j.compositesb.2015.06.006.
[34] Dong C. Uncertainties in flexural strength of carbon/glass fibre reinforced hybrid epoxy composites. Composites B 2016;98:176–81. http://dx.doi.org/10.1016/j.compositesb.2016.05.035.
[35] Alazwari MA, Rao SS. Modeling and analysis of composite laminates in the presence of uncertainties. Composites B 2019;161:107–20. http://dx.doi.org/10.1016/j.compositesb.2018.10.052.
[36] Cappelli L, Montemurro M, Dau F, Guillaumat L. Characterisation of composite elastic properties by means of a multi-scale two-level inverse approach. Compos Struct 2018;204:767–77. http://dx.doi.org/10.1016/j.compstruct.2018.08.007.
[37] Montemurro M. A contribution to the development of design strategies for the optimisation of lightweight structures [Hdr thesis], Université de Bordeaux; 2018, URL http://hdl.handle.net/10985/15155.
[38] Montemurro M. Optimal design of advanced engineering modular systems through a new genetic approach [Ph.D. thesis], France: UPMC, Paris VI; 2012, URL http://tel.archives-ouvertes.fr/tel-00955533.

[39] Optimization Toolbox User's Guide. 3 Apple Ill Drive, Natick, MA 01760-2098: The MathWorks, Inc.; 2017.
[40] Chamis CC. Mechanics of composite materials: Past, present, and future. J Compos Technol Res 1989;11(1):3–14.
[41] Balokas G, Czichon S, Rolfes R. Neural network assisted multiscale analysis for the elastic properties prediction of 3D braided composites under uncertainty. Compos Struct 2018;183:550–62. http://dx.doi.org/10.1016/j.compstruct.2017.06.037.
[42] Schuller G, Jensen H. Computational methods in optimization considering uncertainties – An overview. Comput Methods Appl Mech Engrg 2008;198(1):2–13. http://dx.doi.org/10.1016/j.cma.2008.05.004.
[43] Enevoldsen I, Sørensen J. Reliability-based optimization in structural engineering. Struct Saf 1994;15(3):169–96. http://dx.doi.org/10.1016/0167-4730(94)90039-6.
[44] Gasser M, Schuëller G. Reliability-based optimization of structural systems. Math Methods Oper Res 1997;46(3):287–307. http://dx.doi.org/10.1007/BF01194858.
[45] Jensen HA. Design and sensitivity analysis of dynamical systems subjected to stochastic loading. Comput Struct 2005;83(14):1062–75. http://dx.doi.org/10.1016/j.compstruc.2004.11.016.
[46] Papadrakakis M, Lagaros N, Plevris V. Design optimization of steel structures considering uncertainties. Eng Struct 2005;27(9):1408–18. http://dx.doi.org/10.1016/j.engstruct.2005.04.002.
[47] Doltsinis I, Kang Z. Robust design of structures using optimization methods. Comput Methods Appl Mech Engrg 2004;193(23):2221–37. http://dx.doi.org/10.1016/j.cma.2003.12.055.
[48] Farhat C, Hemez F. Updating finite element dynamic models using an element-by-element sensitivity methodology. AIAA J 1993;31(9):1702–11. http://dx.doi.org/10.2514/3.11833.
[49] Hemez FM, Doebling SW. Review and assessment of model updating for non-linear, transient dynamics. Mech Syst Signal Process 2001;15(1):45–74. http://dx.doi.org/10.1006/mssp.2000.1351.
[50] Soutis C, Beaumont PWR, editors. Multi-scale modelling of composite material systems. the art of predictive damage modelling. In: Woodhead Publishing Series in Composites Science and Engineering, New York: Elsevier; 2005.
[51] Hexply F584. Hexcell Corporation; 2016.
[52] Feo L, Greco F, Leonetti L, Luciano R. Mixed-mode fracture in lightweight aggregate concrete by using a moving mesh approach within a multiscale framework. Compos Struct 2015;123:88–97. http://dx.doi.org/10.1016/j.compstruct.2014.12.037.
[53] Bruno D, Greco F, Luciano R, Blasi PN. Nonlinear homogenized properties of defected composite materials. Comput Struct 2014;134:102–11. http://dx.doi.org/10.1016/j.compstruc.2013.11.018.
[54] Barbero E. Finite element analysis of composite materials. CRC Press, Taylor and Francis Group; 2007.
[55] Système D. Abaqus Analysis user's guide. Providence, RI, USA: Dassault Systèmes Simulia Corp.; 2013.
[56] Sobol IM. Global sensitivity indices for nonlinear mathematical models and their Monte Carlo estimates. Math Comput Simulation 2001;55(1–3):271–80. http://dx.doi.org/10.1016/S0378-4754(00)00270-6.
[57] Dey S, Mukhopadhyay T, Adhikari S. Metamodel based high-fidelity stochastic analysis of composite laminates: A concise review with critical comparative assessment. Compos Struct 2017;171:227–50. http://dx.doi.org/10.1016/j.compstruct.2017.01.061.
[58] Montemurro M, Catapano A, Doroszewski D. A multi-scale approach for the simultaneous shape and material optimisation of sandwich panels with cellular core. Composites B 2016;91:458–72. http://dx.doi.org/10.1016/j.compstruct.2014.07.058.
[59] Montemurro M, Catapano A. On the effective integration of manufacturability constraints within the multi-scale methodology for designing variable angle-tow laminates. Compos Struct 2017;161:145–59. http://dx.doi.org/10.1016/j.compstruct.2016.11.018.
[60] Montemurro M, Catapano A. A general b-spline surfaces theoretical framework for optimisation of variable angle-tow laminates. Compos Struct 2019;209:561–78. http://dx.doi.org/10.1016/j.compstruct.2018.10.094.
[61] Costa G, Montemurro M, Pailhès J. A general hybrid optimization strategy for curve fitting in the non-uniform rational basis spline framework. J Optim Theory Appl 2018;176(1):225–51. http://dx.doi.org/10.1007/s10957-017-1192-2.
[62] Montemurro M, Izzi MI, El-Yagoubi J, Fanteria D. Least-weight composite plates with unconventional stacking sequences: Design, analysis and experiments. J Compos Mater 2019;51(16):2209–27. http://dx.doi.org/10.1177/0021998318824783.
[63] Panettieri E, Montemurro M, Catapano A. Blending constraints for composite laminates in polar parameters space. Composites B 2019;168:448–57. http://dx.doi.org/10.1016/j.compositesb.2019.03.040.
[64] Bertolino G, Montemurro M, Pasquale GD. Multi-scale shape optimisation of lattice structures : an evolutionary-based approach. Int J Interact Des Manuf 2019 [in press]. http://dx.doi.org/10.1007/s12008-019-00580-9.
[65] Audoux Y, Montemurro M, Pailhes J. A surrogate model based on non-uniform rational b-splines hypersurfaces. Procedia CIRP 2018;70:463–8, 28th CIRP Design Conference 2018, 23-25 May 2018, Nantes, France. http://dx.doi.org/10.1016/j.procir.2018.03.234.
[66] Garulli T, Catapano A, Montemurro M, Jumel J, Fanteria D. Quasi-trivial stacking sequences for the design of thick laminates. Compos Struct 2018;200:614–23. http://dx.doi.org/10.1016/j.compstruct.2018.05.120.
[67] Montemurro M, Nasser H, Koutsawa Y, Belouettar S, Vincenti A, Vannucci P. Identification of electromechanical properties of piezoelectric structures through evolutionary optimisation techniques. Int J Solids Struct 2012;49(13):1884–92.
[68] Montemurro M, Vincenti A, Vannucci P. The automatic dynamic penalisation method (ADP) for handling constraints with genetic algorithms. Comput Methods Appl Mech Engrg 2013;256:70–87.
[69] Faghidian S. Inverse determination of the regularized residual stress and eigenstrain fields due to surface peening. J Strain Anal Eng Des 2015;50(2):84–91. http://dx.doi.org/10.1177/0309324714558326.
[70] Faghidian SA. A regularized approach to linear regression of fatigue life measurements. Int J Struct Integr 2016;7(1):95–105. http://dx.doi.org/10.1108/IJSI-12-2014-0071.

Conclusions and perspectives

General conclusions

This Ph.D. thesis has been developed in the context of the research project FULLCOMP, which is an H2020 Marie Sklodowska-Curie project. It is framed into one of the three main research axes characterising the project, i.e. the *Virtual characterisation and manufacturing effects*.

The main subject of this work is the development of a suitable methodology able to characterise the composite material properties at each characteristic scale. The basic idea consisted in developing a suitable multi-scale identification strategy (MSIS) by formulating the multi-scale characterisation problem as an unconventional inverse problem. In particular, the use of non-destructive tests and the related advantages like the recycling of the specimens and the reduction of experimental activities costs with respect to the standard characterisation procedures have been highlighted. If on the one hand the MSIS relies on the exploitation of the information coming from non-destructive tests, on the other hand it makes use of the following numerical methods

- a general numerical homogenisation procedure based on the strain energy of periodic media to perform the scale transition;
- classical deterministic algorithms and original meta-heuristics developed at the I2M laboratory to solve the inverse problem at each pertinent scale;
- stochastic methods (like Monte Carlo algorithm) and surrogate models (like artificial neural networks) when the parameters tuning the variability of the material properties are integrated among the identification parameters;
- a dedicated solver for non-linear eigenvalue problems when the non-linear viscoelastic behaviour of the composite is the object of the inverse problem.

In Chapter 3, the MSIS is applied to the problem of characterising the elastic properties of the composite at each characteristic scale. The MSIS, relies on a single non-destructive harmonic test performed at the macroscopic scale of the composite specimen. In this background, the problem of characterising the elastic properties of the composite at different scales has been split into two related inverse problems. The first-level inverse problem concerns the macroscopic / mesoscopic scale transition. At this level, the goal is to determine the ply elastic properties by minimising the distance between the numerical harmonic response and the reference one.

As far as the second-level inverse problem is concerned, it focuses on the mesoscopic / microscopic scale transition: in this case, the main goal is to find the optimum value of elastic properties of both fibre and matrix matching the set of the lamina elastic properties provided by the first-level problem.

The effectiveness of the MSIS is proven through a numerical benchmark: a multilayer plate made of unidirectional carbon/epoxy pre-preg plies $T650/F584$ is considered as the reference structure.

At the mesoscopic scale, the results of the identification process are very good: the maximum absolute percentage error is 5.78% on the ply transverse Poisson's ratio ν_{23}. At the scale of the constitutive phases, all elastic properties are identified with a good level of accuracy, except for parameters ν_{12}^f, ν_{23}^f and ν^m, which are affected by an absolute percentage error of about 10%, 14% and 10%, respectively. The relatively small error on the transverse Poisson's ratio of the lamina is due to the very low sensitivity of the objective function to this material property (the laminate is not thick enough). On the other hand, this error propagates at the lower scale and affect the Poisson's ratii of both fibre and matrix for which the percentage error is amplified, due to the non-linear nature of the considered problem.

Nevertheless, the first fundamental result is that the MSIS allows determining the full set of elastic properties of the microscopic constituents of the composite: this task cannot be easily performed by means of standard ASTM tests. Moreover, such a result has been obtained by using a unique macroscopic non-destructive harmonic test that allows to recycle the specimen and , thus, to strongly reduce the experiments cost.

In Chapter 4 the MSIS has been extended to the characterisation of the viscoelastic behaviour of the matrix and the elastic behaviour of the fibre, by exploiting the information restrained into the non-linear dynamic response of the composite at the specimen scale. In this case, the multi-scale inverse problem has been solved by using a "one-shot" hybrid optimisation strategy. The inverse problem is stated as an equivalent CNLPP aiming at minimising the distance between the numerical non-linear harmonic response and the reference one for the considered composite plate.

To deal with this problem, the energy homogenisation method of periodic media has been generalised to the case of viscoelastic heterogeneous materials. At the microscopic scale, the matrix viscoelastic behaviour is modelled through the Bagley-Torvik law, that requires only four material parameters and which constitutes the design variables affecting the matrix behaviour.

The main consequence deriving from the viscoelastic behaviour of the matrix is that the elastic properties of the constitutive lamina (at the mesoscopic scale) are frequency-dependent. This means that the modal and harmonic analyses at the macroscopic scale of the sample becomes non-linear. Unfortunately, no dedicated solvers are available in commercial FE software to solve non-linear eigenvalue problems. To overcome this issue, the Arnoldi's method has been coded in MATLAB® environment to solve the non-linear eigenvalue problem and interfaced with the ANSYS® code.

In this case, the effectiveness of the MSIS is evaluated through a numerical benchmark: a composite plate made of unidirectional carbon/epoxy pre-preg plies T650/F584 is considered as a reference structure. The results are quite satisfactory: all viscoelastic properties are identified with a good level of accuracy, except the in-plane shear modulus of the fibre, G_{12}^f and the viscoelastic matrix parameter E_1^m, which are affected by an absolute percentage error of 19% and 15%, respectively. These errors are mainly due to the very low sensitivity of the objective function to these parameters. This low sensitivity is due, on the one hand, to the geometry of the considered laminate which is not thick enough to highlight the influence of these properties on its dynamical response. On the other hand, the laminate stacking sequence plays a fundamental role: the stack considered in this work is a standard symmetric balanced stack taken from the literature

which has not been designed to maximise the influence of some material properties on the laminate dynamic behaviour. Nevertheless, the MSIS allows identifying the viscoelastic behaviour of both the lamina and the constitutive phases, by using a unique macroscopic non-destructive harmonic test, without introducing any simplifying assumption.

Finally, in Chapter 5, the MSIS has been extended to the characterisation of the uncertainty characterising geometrical and elastic properties of both fibre and matrix, by exploiting the information restrained in the first buckling load of the laminate.

Also in this case, the multi-scale identification problem is stated as a CNLPP. However, in this context, the goal is the minimisation of the distance between the numerical and the reference variability parameters affecting the probability distribution of the first buckling load of the laminate. In this case, in order to reduce the computational effort of the whole procedure, the microscopic / mesoscopic scale transition is performed through an analytical homogenisation scheme, i.e. the Chamis' model, and the ply material properties are then used into the FE model of the composite laminate to evaluate its first buckling load.

A Monte-Carlo simulation campaign is carried out in order to compute the probability distribution of the first buckling load, starting from a Gaussian probability distribution of the material properties of the constituent phases. The obtained samples are used to train an Artificial Neural Network (ANN), which is able to emulate the multi-scale mechanical response of the specimen: the geometrical and elastic properties of the constitutive phases are the inputs and the first-buckling load of the laminate is the output. Then, the ANN has been interfaced with the optimisation algorithm, to reduce the computational time.

The numerical results show that the identification process is strongly affected by the nature of the stacking sequence. Accordingly, two benchmarks with different stacking sequences are considered: the first benchmark is characterised by a symmetric quasi-isotropic stack, while the second one is characterised by a symmetric balanced one.

In particular, for the first benchmark the absolute percentage error ranges from 2.8% to 13.4% for the standard deviation of the fibre volume fraction $\sigma\left(V_F\right)$ and the mean value of the fibre longitudinal elastic modulus $\mu\left(E_1^f\right)$, respectively. Conversely, for the second benchmark the absolute percentage error ranges from 0.2% to 3.2% for the mean value of the matrix elastic modulus $\mu\left(E^m\right)$ and the standard deviation of the fibre transverse elastic modulus $\sigma\left(E_2^f\right)$.

In any case, the MSIS proved to be an efficient and versatile tool to identify the material properties variability of the constitutive phases. To the best of the author's knowledge, this task cannot be achieved with conventional ASTM tests.

Perspectives

This work constitutes just a "first attempt" and the MSIS needs to be further generalised in order to catch the true behaviour of the composite at each characteristic scale.

Firstly, the effectiveness of the method must be proven by using experimental data. This can be easily done by exploiting the results of non-destructive experimental modal tests to characterise the viscoelastic behaviour of the composite.

A second point of paramount importance is the design of a suitable stack maximising the sensitivity of the objective function to the full set of the material properties to be identified (in this way, a dedicated sample is generated, giving the possibility to standardise the proposed procedure).

Moreover, the MSIS is a really versatile procedure that can be used for the evaluation of the variability affecting the microscopic geometrical parameters, e.g. fibre misalignment, porosity, etc.

Furthermore, the MSIS could be easily generalised to characterise the geometrical features of the RVE of the composite material: the parameters defining the shape of the inclusion or its volume fraction can be easily integrated among the optimisation variables, without altering the overall architecture of the identification methodology. On the other hand, also geometric parameters of the laminate (mesoscopic scale) can be included among the unknowns to be identified, e.g. the orientation angles and the thickness of each lamina.

Finally, one can imagine also to use the MSIS for identifying the topology of the damaged zone and the parameters governing the beaviour of the damage models typically used in the analysis of composite structures subject to impacts. In this case the MSIS could constitute a sound alternative to classical non-destructive testing methods.

Appendix

Journal papers

1. Cappelli L., Montemurro M., Dau F., Guillaumat L. *Characterisation of composite elastic properties by means of a multi-scale two-level inverse approach.* Composite Structures 2018;204:767-777.
https://doi.org/10.1016/j.compstruct.2018.08.007

2. Cappelli L., Balokas G., Montemurro M., Dau F., Guillaumat L. *Multi-scale identification of the elastic properties variability for composite materials through a hybrid optimisation strategy.* Composites Part B: Engineering 2019;176:107193.
https://doi.org/10.1016/j.compositesb.2019.107193

3. Cappelli L., Montemurro M., Dau F., Guillaumat L. *Multi-scale identification of the viscoelastic behaviour of composite materials through a non-destructive test.* Mechanics of Materials 2019;137:103137.
https://doi.org/10.1016/j.mechmat.2019.103137

Books, Book chapters

1. Cappelli L., Montemurro M., Dau F., Guillaumat L. (2019) *Multiscale Identification of Material Properties for Anisotropic Media: A General Inverse Approach.* In: Petrolo M. (eds) *Advances in Predictive Models and Methodologies for Numerically Efficient Linear and Nonlinear Analysis of Composites.* PoliTO Springer Series. Springer, Cham.
https://doi.org/10.1007/978-3-030-11969-0_10

Conference proceedings

1. Cappelli L., Montemurro M., Dau F., Guillaumat L., *Multi-scale characterisation of material properties of composite fabrics through modal tests*, 20ème Journées Nationales Composites, 28-30 Juin 2017, Ecole des ponts et chausses, Champs/Marne.
https://hal.archives-ouvertes.fr/hal-01621617

Conferences

1. 19th International Conference on Composite Structures (ICCS19) - September 05-09 2016, Porto (Portugal).

2. Journées Nationales sur les Composites (JNC20) - 2017, June 28-30 - Champs-sur-Marne (France).

3. 20th International Conference on Composite Structures (ICCS20) - 2017, September 04-07 September 2017, Paris (France).

4. 6th European Conference on Computational Mechanics (Solids, Structures and Coupled Problems) (ECCM 6) and the 7th European Conference on Computational Fluid Dynamics (ECFD 7) conference - 2018, June 11-15, Glasgow (United Kingdom).

5. First International Conference of Mechanics of Advanced Materials and Structures (ICMAMS) conference - 2018, June 17-20, Turin (Italy).

Bibliography

[1] M. Montemurro. *Optimal design of advanced engineering modular systems through a new genetic approach.* PhD thesis, UPMC, Paris VI, France, 2012. http://tel.archives-ouvertes.fr/tel-00955533.

[2] R. M. Jones. *Mechanics of composite materials.* McGraw-Hill, 1975.

[3] M. Petrolo. *Advances in Predictive Models and Methodologies for Numerically Efficient Linear and Nonlinear Analysis of Composites.* Springer International Publishing, 2019.

[4] E. Carrera. *Theories and finite elements for multilayered, anisotropic, composite plates and shells.* Springer Netherlands, 2002.

[5] E. Carrera, M. Cinefra, M. Petrolo, and E. Zappino. *Finite element analysis of structures through unified formulation.* Chichester, West Sussex : John Wiley & Sons, 2014.

[6] Subramani Sockalingam, Sanjib C Chowdhury, Jr John W Gillespie, and Michael Keefe. Recent advances in modeling and experiments of kevlar ballistic fibrils, fibers, yarns and flexible woven textile fabrics a review. *Textile Research Journal*, 87(8):984–1010, 2017.

[7] A. Gasser, P. Boisse, and S. Hanklar. Mechanical behaviour of dry fabric reinforcements. 3d simulations versus biaxial tests. *Computational Materials Science*, 17(1):7 – 20, 2000.

[8] Giurgiutiu V. *Structural health monitoring with piezoelectric wafer active sensors.* 2nd edn. Academic, Oxford, 2014.

[9] Ling Liu, Bo-Ming Zhang, Dian-Fu Wang, and Zhan-Jun Wu. Effects of cure cycles on void content and mechanical properties of composite laminates. *Composite Structures*, 73(3):303 – 309, 2006.

[10] S.W. Yurgartis. Measurement of small angle fiber misalignments in continuous fiber composites. *Composites Science and Technology*, 30(4):279 – 293, 1987.

[11] A.R. Melro, P.P. Camanho, and S.T. Pinho. Generation of random distribution of fibres in long-fibre reinforced composites. *Composites Science and Technology*, 68(9):2092 – 2102, 2008.

[12] F.D. Adams, A.L. Carlsson, and R.B. Pipes. *Experimental characterization of advanced composite materials.* CRC Press LLC, New York, 2003.

[13] J. A. Nairn. Analytical fracture mechanics analysis of the pull-out test including the effects of friction and thermal stresses. *Advanced Composite Letters*, 9(6):373–383, 2000.

[14] R. Maurin, P. Davies, N. Baral, and C. Baley. Transverse Properties of Carbon Fibres by Nano-Indentation and Micro-mechanics. *Applied Composite Materials*, 15:61–73, 2018.

[15] S. Feih, K. Wonsyld, D. Minzari, P. Westermann, and H. Lilholt. *Testing Procedure for the Single Fiber Fragmentation Test*, volume No. 1483(EN). Denmark. Forskningscenter Risoe. Risoe-R, 2004.

[16] ASTM International, West Conshohocken, PA. *ASTM D3039 / D3039M-17, Standard Test Method for Tensile Properties of Polymer Matrix Composite Materials*, 2017.

[17] ASTM International, West Conshohocken, PA. *ASTM D790-17, Standard Test Methods for Flexural Properties of Unreinforced and Reinforced Plastics and Electrical Insulating Materials*, 2017.

[18] ASTM International, West Conshohocken, PA. *ASTM D3410 / D3410M-16, Standard Test Method for Compressive Properties of Polymer Matrix Composite Materials with Unsupported Gage Section by Shear Loading*, 2016.

[19] ASTM International, West Conshohocken, PA. *ASTM D695-15, Standard Test Method for Compressive Properties of Rigid Plastics*, 2015.

[20] ASTM International, West Conshohocken, PA. *ASTM D6641 / D6641M-16e1, Standard Test Method for Compressive Properties of Polymer Matrix Composite Materials Using a Combined Loading Compression (CLC) Test Fixture*, 2016.

[21] ASTM International, West Conshohocken, PA. *ASTM D5379 / D5379M-12, Standard Test Method for Shear Properties of Composite Materials by the V-Notched Beam Method*, 2012.

[22] ASTM International, West Conshohocken, PA. *ASTM D7078 / D7078M-12, Standard Test Method for Shear Properties of Composite Materials by V-Notched Rail Shear Method*, 2012.

[23] ASTM International, West Conshohocken, PA. *ASTM D3518 / D3518M-13, Standard Test Method for In-Plane Shear Response of Polymer Matrix Composite Materials by Tensile Test of a 45 Laminate*, 2013.

[24] ASTM International, West Conshohocken, PA. *ASTM D2344 / D2344M-16, Standard Test Method for Short-Beam Strength of Polymer Matrix Composite Materials and Their Laminates*, 2016.

[25] ASTM International, West Conshohocken, PA. *ASTM D3379-75(1989)e1, Standard Test Method for Tensile Strength and Young's Modulus for High-Modulus Single-Filament Materials (Withdrawn 1998)*, 1975.

[26] ASTM International, West Conshohocken, PA. *ASTM D638-14, Standard Test Method for Tensile Properties of Plastics*, 2014.

[27] T. J. Young. *Characterisation of Interfaces in Micro- and Nano-composites*. PhD thesis, University of Surrey, 2012.

[28] S. A. Suarez, R. F. Gibson, C. T. Sun, and S. K. Chaturvedi. The influence of fiber length and fiber orientation on damping and stiffness of polymer composite materials. *Experimental Mechanics*, 26(2):175 – 184, Jun 1986.

[29] Alina Krasnobrizha, Patrick Rozycki, Laurent Gornet, and Pascal Cosson. Hysteresis behaviour modelling of woven composite using a collaborative elastoplastic damage model with fractional derivatives. *Composite Structures*, 158:101 – 111, 2016.

[30] V. Kostopoulos and D.Th. Korontzis. A new method for the determination of viscoelastic properties of composite laminates: a mixed analyticalexperimental approach. *Composites Science and Technology*, 63(10):1441 – 1452, 2003.

[31] S. Naskar, T. Mukhopadhyay, and S. Sriramula. Probabilistic micromechanical spatial variability quantification in laminated composites. *Composites Part B: Engineering*, 151:291 – 325, 2018.

[32] K. Sepahvand and S. Marburg. Identification of composite uncertain material parameters from experimental modal data. *Probabilistic Engineering Mechanics*, 37:148 – 153, 2014.

[33] A. Batou and C. Soize. Stochastic modeling and identification of an uncertain computational dynamical model with random fields properties and model uncertainties. *Arch Appl Mech*, pages 1–18, 2012.

[34] Jingbo Wang and Nicholas Zabaras. Hierarchical bayesian models for inverse problems in heat conduction. *Inverse Problems*, 21(1):183–206, dec 2004.

[35] Roger G. Ghanem and Alireza Doostan. On the construction and analysis of stochastic models: Characterization and propagation of the errors associated with limited data. *Journal of Computational Physics*, 217(1):63 – 81, 2006. Uncertainty Quantification in Simulation Science.

[36] C. Chen, D. Duhamel, and C. Soize. Probabilistic approach for model and data uncertainties and its experimental identification in structural dynamics: Case of composite sandwich panels. *Journal of Sound and Vibration*, 294(1):64 – 81, 2006.

[37] Bojana V. Rosi, Alexander Litvinenko, Oliver Pajonk, and Hermann G. Matthies. Sampling-free linear bayesian update of polynomial chaos representations. *Journal of Computational Physics*, 231(17):5761 – 5787, 2012.

[38] Klaus Mosegaard and Albert Tarantola. Probabilistic approach to inverse problems. *International Handbook of Earthquake and Engineering Seismology*, pages 237–265, 2002.

[39] Carl Friedrich Gauss. *Theoria motus corporum coelestium in sectionibus conicis solem ambientium*. Hamburgi : sumtibus Frid. Perthes et I. H. Besser, 1809.

[40] Jacques Hadamard. *Le problème de Cauchy et les quations aux drives partielles linaires hyperboliques leons professes l'Universit Yale*. dition revue et notablement augmente edition, 1932.

[41] V. I. Keilis-Borok and T. B. Yanovskaja. Inverse Problems of Seismology (Structural Review). *Geophysical Journal International*, 13(1-3):223–234, 07 1967.

[42] Frank Press. Earth models obtained by monte carlo inversion. *Journal of Geophysical Research (1896-1977)*, 73(16):5223–5234, 1968.

[43] George Backus. Inference from inadequate and inaccurate data, i. *Proceedings of the National Academy of Sciences*, 65(1):1–7, 1970.

[44] George Backus. Inference from inadequate and inaccurate data, ii. *Proceedings of the National Academy of Sciences*, 65(2):281–287, 1970.

[45] George Backus. Inference from inadequate and inaccurate data, iii. *Proceedings of the National Academy of Sciences*, 67(1):282–289, 1970.

[46] G. E. Backus and J. F. Gilbert. Numerical Applications of a Formalism for Geophysical Inverse Problems. *Geophysical Journal International*, 13(1-3):247–276, 07 1967.

[47] George Backus and Freeman Gilbert. The Resolving Power of Gross Earth Data. *Geophysical Journal International*, 16(2):169–205, 10 1968.

[48] G. Backus, F. Gilbert, and Edward Crisp Bullard. Uniqueness in the inversion of inaccurate gross earth data. *Philosophical Transactions of the Royal Society of London. Series A, Mathematical and Physical Sciences*, 266(1173):123–192, 1970.

[49] Brian Kennett and Guust Nolet. Resolution Analysis for Discrete Systems. *Geophysical Journal International*, 53(2):413–425, 05 1978.

[50] Ralph A. Wiggins. Monte carlo inversion of body-wave observations. *Journal of Geophysical Research (1896-1977)*, 74(12):3171–3181, 1969.

[51] Joel N Franklin. Well-posed stochastic extensions of ill-posed linear problems. *Journal of Mathematical Analysis and Applications*, 31(3):682 – 716, 1970.

[52] Parzen Emanuel, Kunio Tanabe, and Genshiro Kitagawa. *Selected Papers of Hirotugu Akaike*. Springer, New York, NYr, 1998.

[53] Klaus Mosegaard and Albert Tarantola. Monte carlo sampling of solutions to inverse problems. *Journal of Geophysical Research: Solid Earth*, 100(B7):12431–12447, 1995.

[54] A. Tarantola. *Inverse Problem Theory: Methods for Data Fitting and Model Parameter Estimation*. Elsevier, New York, 1987.

[55] David E. Goldberg. *Genetic Algorithms in Search, Optimization and Machine Learning*. Addison-Wesley Longman Publishing Co., Inc., Boston, MA, USA, 1st edition, 1989.

[56] Nicholas Metropolis and S. Ulam. The monte carlo method. *Journal of the American Statistical Association*, 44(247):335–341, 1949.

[57] Nicholas Metropolis, Arianna W. Rosenbluth, Marshall N. Rosenbluth, Augusta H. Teller, and Edward Teller. Equation of state calculations by fast computing machines. *The Journal of Chemical Physics*, 21(6):1087–1092, 1953.

[58] W. K. Hastings. Monte Carlo sampling methods using Markov chains and their applications. *Biometrika*, 57(1):97–109, 1970.

[59] Roger Fletcher. *Practical Methods of Optimization*. John Wiley & Sons, New York, NY, USA, second edition, 1987.

[60] M. J. D. Powell. *Approximation Theory and Methods*. Cambridge University Press, 1981.

[61] L. E. Scales. *Introduction to Non-Linear Optimization*. Macmillan, 1985.

[62] John A Scales, Martin L Smith, and Terri L Fischer. Global optimization methods for multimodal inverse problems. *Journal of Computational Physics*, 103(2):258 – 268, 1992.

[63] Pierre-Simon de Laplace. *Trait de mcanique cleste, Tome III, No. 39*. J.-B.-M. Duprat (Paris), 1799.

[64] A. Benjeddou and M. Hamdi. Robust inverse identification of the effective three-dimensional elastic behaviour of a piezoceramic patch bonded to a multilayer unidirectional fibre composite. *Composite Structures*, 151:58 – 69, 2016.

[65] Hexcell Corporation. *Hexply 200*, 2016.

[66] Hexcell Corporation. *Hexply F584*, 2016.

[67] SAATI S.p.A. *EF452 epoxy matrix*, 2011.

[68] JG Michopoulos, JC Hermanson, A Iliopoulos, SG Lambrakos, and T. Furukawa. Data-driven design optimization for composite material characterization. *ASME. J. Comput. Inf. Sci. Eng.*, 11(2), 2011.

[69] John Steuben, John Michopoulos, Athanasios Iliopoulos, and Cameron Turner. Inverse characterization of composite materials via surrogate modeling. *Composite Structures*, 132:694 – 708, 2015.

[70] G. Rus, R. Palma, and J. Suarez. *Piezoelectric ceramics*, chapter Characterization of properties and damage in piezoelectrics. IntechOpen, 2010.

[71] A. L. Araújo, C.M. Mota Soares, and C.A. Mota Soares. Inverse techniques for the characterisation of mechanical and piezoelectric properties on composite and adaptive structures: A survey. *Computational Technology Reviews*, 2:103 – 123, 2010.

[72] A.L. Araújo, C.M. Mota Soares, J. Herskovits, and P. Pedersen. Development of a finite element model for the identification of mechanical and piezoelectric properties through gradient optimisation and experimental vibration data. *Composite Structures*, 58(3):307 – 318, 2002.

[73] A.L. Araújo, C.M. Mota Soares, J. Herskovits, and P. Pedersen. Estimation of piezoelastic and viscoelastic properties in laminated structures. *Composite Structures*, 87(2):168 – 174, 2009.

[74] A.L. Araújo, H.M.R. Lopes, M.A.P. Vaz, C.M. Mota Soares, J. Herskovits, and P. Pedersen. Parameter estimation in active plate structures. *Computers & Structures*, 84(22):1471 – 1479, 2006.

[75] M. Montemurro, H. Nasser, Y. Koutsawa, S. Belouettar, A. Vincenti, and P. Vannucci. Identification of electromechanical properties of piezoelectric structures through evolutionary optimisation techniques. *International Journal of Solids and Structures*, 49(13):1884–1892, 2012.

[76] P. Pedersen. *Mechanics of composite materials and structures*, chapter Identification techniques in composite laminates. Kluwer Academic Publisher, 1999.

[77] P. Pedersen and P. S. Frederiksen. Identification of orthotropic material moduli by a combined experimental/numerical method. *Measurement*, 10(3):113–118, 1992.

[78] H Sol. *Identication of anisotropic plate rigidities using free vibration data*. PhD thesis, Vrije Universiteit Brussel, Belgium, 1986.

[79] Hugo Sol and C.W.J. Oomens. *Material identification using mixed numerical experimental methods : proceedings of the EUROMECH colloquium held in Kerkrade, The Netherlands, 7-9 April 1997*. EUROMECH-Colloquium : proceedings. Kluwer Academic Publishers, Netherlands, 1997.

[80] Jakob Kuttenkeuler. *Aircraft composites and aeroelastic tailoring*. PhD thesis, KTH, Aeronautical Engineering, 1998.

[81] C. M. Mota Soares, M. Moreira de Freitas, A. L. Arjo, and P. Pedersen. Identification of material properties of composite plate specimens. *Composite Structures*, 25:277–285, 1993.

[82] Luigi Bruno. Mechanical characterization of composite materials by optical techniques: A review. *Optics and Lasers in Engineering*, 104:192 – 203, 2018.

[83] S. W. Tsai and T. Hahn. *Introduction to composite materials*. Technomic, 1980.

[84] Pierron Fabrice and Grdiac Michel. *The Virtual Fields Method: extracting constitutive mechanical parameters from Full-field deformation measurements*. Springer, New York, NY, 2012.

[85] M. Grdiac, F. Pierron, S. Avril, and E. Toussaint. The virtual fields method for extracting constitutive parameters from full-field measurements: a review. *Strain*, 42(4):233–253, 2006.

[86] X. Gu and F. Pierron. Towards the design of a new standard for composite stiffness identification. *Composites Part A: Applied Science and Manufacturing*, 91:448 – 460, 2016.

[87] Marco Rossi and Fabrice Pierron. On the use of simulated experiments in designing tests for material characterization from full-field measurements. *International Journal of Solids and Structures*, 49(3):420 – 435, 2012.

[88] N. Nigamaa and S.J. Subramanian. Identification of orthotropic elastic constants using the eigenfunction virtual fields method. *International Journal of Solids and Structures*, 51(2):295 – 304, 2014.

[89] M. Rossi, P. Lava, F. Pierron, D. Debruyne, and M. Sasso. Effect of dic spatial resolution, noise and interpolation error on identification results with the vfm. *Strain*, 51(3):206–222, 2015.

[90] B. Rahmani, I. Villemure, and M. Levesque. Regularized virtual fields method for mechanical properties identification of composite materials. *Computer Methods in Applied Mechanics and Engineering*, 278:543 – 566, 2014.

[91] Patrick Ienny, Anne-Sophie Caro-Bretelle, and Emmanuel Pagnacco. Identification from measurements of mechanical fields by finite element model updating strategies. *European Journal of Computational Mechanics*, 18(3-4):353–376, 2009.

[92] Marwala Tshilidzi. *Finite-element-model Updating Using Computional Intelligence Techniques. Applications to Structural Dynamics*. Springer, London, 2010.

[93] B. Rahmani, F. Mortazavi, I. Villemure, and M. Levesque. A new approach to inverse identification of mechanical properties of composite materials: Regularized model updating. *Composite Structures*, 105:116 – 125, 2013.

[94] Asim Kumar Mishra and Sushanta Chakraborty. Inverse detection of constituent level elastic parameters of frp composite panels with elastic boundaries using finite element model updating. *Ocean Engineering*, 111:358 – 368, 2016.

[95] M.R. Hematiyan, A. Khosravifard, and Y.C. Shiah. A new stable inverse method for identification of the elastic constants of a three-dimensional generally anisotropic solid. *International Journal of Solids and Structures*, 106-107:240 – 250, 2017.

[96] E. Florentin and G. Lubineau. Identification of the parameters of an elastic material model using the constitutive equation gap method. *Comput Mech*, (46:521), 2010.

[97] Fabien Amiot, Jean-Noël Pri, and Stphane Roux. *Equilibrium Gap Method*, chapter 12, pages 331–362. John Wiley & Sons, Ltd, 2012.

[98] Stphane Andrieux, Huy Duong Bui, and Andrei Constantinescu. *Reciprocity Gap Method*, chapter 13, pages 363–378. John Wiley & Sons, Ltd, 2012.

[99] Ali Moussawi, Gilles Lubineau, Eric Florentin, and Benoit Blaysat. The constitutive compatibility method for identification of material parameters based on full-field measurements. *Computer Methods in Applied Mechanics and Engineering*, 265:1 – 14, 2013.

[100] Marc Bonnet and Andrei Constantinescu. Inverse problems in elasticity. *Inverse Problems*, 21(2):R1–R50, 2005.

[101] S. Avril, M. Bonnet, and AS. et al. Bretelle. Overview of identification methods of mechanical parameters based on full-field measurements. *Exp Mech*, (48:381), 2008.

[102] S. Mahmoudi, A. Kervoelen, G. Robin, L. Duigou, E.M. Daya, and J.M. Cadou. Experimental and numerical investigation of the damping of flaxepoxy composite plates. *Composite Structures*, 208:426 – 433, 2019.

[103] R. Jayendiran and A. Arockiarajan. Micromechanical modeling and experimental characterization on viscoelastic behavior of 13 active composites. *Composites Part B: Engineering*, 79:105 – 113, 2015.

[104] Ashirbad Swain and Tarapada Roy. Viscoelastic modelling and dynamic characteristics of cnts-cfrp-2dwf composite shell structures. *Composites Part B: Engineering*, 141:100 – 122, 2018.

[105] Jos Daniel D. Melo and Donald W. Radford. Time and temperature dependence of the viscoelastic properties of cfrp by dynamic mechanical analysis. *Composite Structures*, 70(2):240 – 253, 2005.

[106] Ioana C. Finegan, Gary.G. Tibbetts, and Ronald F. Gibson. Modeling and characterization of damping in carbon nanofiber/polypropylene composites. *Composites Science and Technology*, 63(11):1629 – 1635, 2003.

[107] R. Chandra, S. Singh, and K. Gupta. Experimental evaluation of damping of fiber-reinforced composites. *Journal of Composites Technology and Research*, 25(2):1 – 12, 2003.

[108] M. Abedi. Viscoelastic characterization of out-of-autoclave composite laminates: Experimental and finite element studies. 2016.

[109] Liang Meng, Balaji Raghavan, Olivier Bartier, Xavier Hernot, Gerard Mauvoisin, and Piotr Breitkopf. An objective meta-modeling approach for indentation-based material characterization. *Mechanics of Materials*, 107:31 – 44, 2017.

[110] Yee Ling Yap, William Toh, Rahul Koneru, Kehua Lin, Kirk Ming Yeoh, Chin Mian Lim, Jia Shing Lee, Nur Adilah Plemping, Rongming Lin, Teng Yong Ng, Keen Ian Chan, Huanyu Guang, Wai Yew Brian Chan, Soo Soon Teong, and Guoying Zheng. A non-destructive experimental-cum-numerical methodology for the characterization of 3d-printed materialspolycarbonate-acrylonitrile butadiene styrene (pc-abs). *Mechanics of Materials*, 132:121 – 133, 2019.

[111] Ghailen BEN Ghorbal, Arnaud Tricoteaux, Anthony Thuault, Ghislain Louis, and Didier Chicot. Mechanical characterization of brittle materials using instrumented indentation with knoop indenter. *Mechanics of Materials*, 108:58 – 67, 2017.

[112] E. Barkanov, E. Skukis, and B. Petitjean. Characterisation of viscoelastic layers in sandwich panels via an inverse technique. *Journal of Sound and Vibration*, 327(3):402 – 412, 2009.

[113] Imen Elkhaldi, Isabelle Charpentier, and El Mostafa Daya. A gradient method for viscoelastic behaviour identification of damped sandwich structures. *Comptes Rendus Mcanique*, 340(8):619 – 623, 2012.

[114] F. Cortés and M.J. Elejabarrieta. An approximate numerical method for the complex eigenproblem in systems characterised by a structural damping matrix. *Journal of Sound and Vibration*, 296(1):166 – 182, 2006.

[115] K.S. Ledi, M. Hamdaoui, G. Robin, and E.M. Daya. An identification method for frequency dependent material properties of viscoelastic sandwich structures. *Journal of Sound and Vibration*, 428:13 – 25, 2018.

[116] E. J. Barbero. *Finite element analysis of composite materials*. Taylor and Francis Group, 2008.

[117] A. Krasnobrizha. *Modelisation des mecanismes d'hysteresis des composites tisses a l'aide d'un modele collaboratif elasto-plastique endommageable a derivees fractionnaires*. PhD thesis, LUniversit Nantes Angers Le Mans, France, 2015.

[118] RE Rouse. The theory of the linear viscoelastic properties of dilute solutions of coiling polymers. *Chemical Physics*, 21:1272–1280, 1953.

[119] R. Gorenflo and F. Mainardi. *Fractional Calculus*, pages 223–276. Springer Vienna, Vienna, 1997.

[120] C. Friedrich. Relaxation and retardation functions of the maxwell model with fractional derivatives. *Rheologica Acta*, 30(2):151–158, 1991.

[121] RC. Koeller. Applications of fractional calculus to the theory of viscoelasticity. *ASME. J. Appl. Mech.*, 51(2):299–307, 1984.

[122] H Schiessel and A Blumen. Hierarchical analogues to fractional relaxation equations. *Journal of Physics A: Mathematical and General*, 26(19):5057–5069, oct 1993.

[123] N. Heymans and J.-C. Bauwens. Fractal rheological models and fractional differential equations for viscoelastic behavior. *Rheologica Acta*, 33(3):210–219, 1994.

[124] M. Caputo and F. Mainardi. A new dissipation model based on memory mechanism. *Pure and Applied Geophysics PAGEOPH*, 91(1):134–147, 1971.

[125] YN Rabotnov. Ravnovesie uprugoj sredi s posledstvie. *Prikladnaya Matematika i Mechanika*, 12:53–62, 1948.

[126] R.L. Bagley. On the fractional calculus model of viscoelastic behavior. *Journal of Rheology*, 30(1):133–155, 1986.

[127] F.C. Meral, T.J. Royston, and R. Magin. Fractional calculus in viscoelasticity: An experimental study. *Communications in Nonlinear Science and Numerical Simulation*, 15(4):939 – 945, 2010.

[128] M. Fukunaga and N. Shimizu. Fractional derivative models of viscoelastic materials for large extension. In *ICFDA'14 International Conference on Fractional Differentiation and Its Applications 2014*, pages 1–5, June 2014.

[129] Grdiac Michel, Hild Franois, and Pineau André. *FullField Measurements and Identification in Solid Mechanics*. John Wiley & Sons, Inc., 2012.

[130] Kenneth T. Kavanagh and Ray W. Clough. Finite element applications in the characterization of elastic solids. *International Journal of Solids and Structures*, 7(1):11 – 23, 1971.

[131] Emmanuel Pagnacco, Anne-Sophie Caro-Bretelle, and Patrick Ienny. *Parameter Identification from Mechanical Field Measurements using Finite Element Model Updating Strategies*, chapter 9, pages 247–274. John Wiley & Sons, Ltd, 2012.

[132] C. Farhat and F.M. Hemez. Updating finite element dynamic models using an element-by-element sensitivity methodology. *American Institute of Aeronautics and Astronautics*, 31(9):1702–1711, 1993.

[133] Marc Bonnet. *Introduction to Identification Methods*, chapter 8, pages 223–246. John Wiley & Sons, Ltd, 2012.

[134] P. Ladeveze and D. Leguillon. Error estimate procedure in the finite element method and applications. *SIAM Journal on Numerical Analysis*, 20(3):485–509, 1983.

[135] P. Ladeveze, D. Nedjar, and M. Reynier. Updating of finite element models using vibration tests. *AIAA Journal*, 32(7):1485–1491, 1994.

[136] Giuseppe Geymonat, Franois Hild, and Stphane Pagano. Identification of elastic parameters by displacement field measurement. *Comptes Rendus Mcanique*, 330(6):403 – 408, 2002.

[137] P. Feissel and O. Allix. Modified constitutive relation error identification strategy for transient dynamics with corrupted data: The elastic case. *Computer Methods in Applied Mechanics and Engineering*, 196(13):1968 – 1983, 2007.

[138] S. Andrieux and A. Ben Abda. The reciprocity gap: a general concept for flaws identification problems. *Mechanics Research Communications*, 20(5):415 – 420, 1993.

[139] S. Andrieux, A.B. Abda, and H.D. Bui. Reciprocity principle and crack identification. *Inverse Problems*, 15(1):59–65, 1999.

[140] Michel Grdiac. The use of full-field measurement methods in composite material characterization: interest and limitations. *Composites Part A: Applied Science and Manufacturing*, 35(7):751 – 761, 2004.

[141] Damien Claire, Franois Hild, and Stéphane Roux. Identification of damage fields using kinematic measurements. *Comptes Rendus Mcanique*, 330(11):729 – 734, 2002.

[142] D. Claire, F. Hild, and S. Roux. A finite element formulation to identify damage fields: The equilibrium gap method. *International Journal for Numerical Methods in Engineering*, 61(2):189–208, 2004.

[143] S. Roux and F. Hild. Digital image mechanical identification (dimi). *Experimental Mechanics*, 48(4):495–508, 2008.

[144] Laurent Crouzeix, Jean Nol Pri, Francis Collombet, and Bernard Douchin. An orthotropic variant of the equilibrium gap method applied to the analysis of a biaxial test on a composite material. *Composites Part A: Applied Science and Manufacturing*, 40(11):1732 – 1740, 2009.

[145] Jean Noël Pri, Hugo Leclerc, Stéphane Roux, and François Hild. Digital image correlation and biaxial test on composite material for anisotropic damage law identification. *International Journal of Solids and Structures*, 46(11):2388 – 2396, 2009.

[146] S. Avril, M. Grdiac, and F. Pierron. Sensitivity of the virtual fields method to noisy data. *Computational Mechanics*, 34(6):439–452, 2004.

[147] Julien Rthor, Stéphane Roux, and François Hild. Optimal and noise-robust extraction of fracture mechanics parameters from kinematic measurements. *Engineering Fracture Mechanics*, 78(9):1827 – 1845, 2011.

[148] F. Amiot, F. Hild, and J.P. Roger. Identification of elastic property and loading fields from full-field displacement measurements. *International Journal of Solids and Structures*, 44(9):2863 – 2887, 2007.

[149] R. Gras, H. Leclerc, F. Hild, S. Roux, and J. Schneider. Identification of a set of macroscopic elastic parameters in a 3d woven composite: Uncertainty analysis and regularization. *International Journal of Solids and Structures*, 55:2 – 16, 2015.

[150] Stéphane Roux and François Hild. Optimal procedure for the identification of constitutive parameters from experimentally measured displacement fields. *International Journal of Solids and Structures*, 2018.

[151] Adrien Leygue, Michel Coret, Julien Rthor, Laurent Stainier, and Erwan Verron. Data-based derivation of material response. *Computer Methods in Applied Mechanics and Engineering*, 331:184 – 196, 2018.

[152] Srinivas Sriramula and Marios K. Chryssanthopoulos. Quantification of uncertainty modelling in stochastic analysis of frp composites. *Composites Part A: Applied Science and Manufacturing*, 40(11):1673 – 1684, 2009.

[153] D.J. Lekou and T.P. Philippidis. Mechanical property variability in frp laminates and its effect on failure prediction. *Composites Part B: Engineering*, 39(7):1247 – 1256, 2008.

[154] H.K. Jeong and R.A. Shenoi. Probabilistic strength analysis of rectangular frp plates using monte carlo simulation. *Computers and Structures*, 76(1):219–235, 2000.

[155] A.K. Onkar, C.S. Upadhyay, and D. Yadav. Probabilistic failure of laminated composite plates using the stochastic finite element method. *Composite Structures*, 77(1):79–91, 2007.

[156] K.D. Potter, M. Campbell, C. Langer, and M.R. Wisnom. The generation of geometrical deformations due to tool/part interaction in the manufacture of composite components. *Composites Part A: Applied Science and Manufacturing*, 36(2 SPEC. ISS.):301–308, 2005.

[157] K. Potter, C. Langer, B. Hodgkiss, and S. Lamb. Sources of variability in uncured aerospace grade unidirectional carbon fibre epoxy preimpregnate. *Composites Part A: Applied Science and Manufacturing*, 38(3):905–916, 2007.

[158] K. Potter, B. Khan, M. Wisnom, T. Bell, and J. Stevens. Variability, fibre waviness and misalignment in the determination of the properties of composite materials and structures. *Composites Part A: Applied Science and Manufacturing*, 39(9):1343–1354, 2008.

[159] M.C. Shiao and C.C. Chamis. Probabilistic evaluation of fuselage-type composite structures. *Probabilistic Engineering Mechanics*, 14(1-2):179–187, 1999.

[160] G. Fernlund, N. Rahman, R. Courdji, M. Bresslauer, A. Poursartip, K. Willden, and K. Nelson. Experimental and numerical study of the effect of cure cycle, tool surface, geometry, and lay-up on the dimensional fidelity of autoclave-processed composite parts. *Composites - Part A: Applied Science and Manufacturing*, 33(3):341–351, 2002.

[161] S.P. Yushanov and A.E. Bogdanovich. Stochastic theory of composite materials with random waviness of the reinforcements. *International Journal of Solids and Structures*, 35(22):2901–2930, 1998.

[162] K. Sepahvand and S. Marburg. On construction of uncertain material parameter using generalized polynomial chaos expansion from experimental data. *Procedia IUTAM*, 6:4 – 17, 2013. IUTAM Symposium on Multiscale Problems in Stochastic Mechanics.

[163] Oliver Pajonk, Bojana V. Rosi, Alexander Litvinenko, and Hermann G. Matthies. A deterministic filter for non-gaussian bayesian estimation applications to dynamical system estimation with noisy measurements. *Physica D: Nonlinear Phenomena*, 241(7):775 – 788, 2012.

[164] Christophe Desceliers, Roger Ghanem, and Christian Soize. Maximum likelihood estimation of stochastic chaos representations from experimental data. *International Journal for Numerical Methods in Engineering*, 66(6):978–1001, 2006.

[165] Youssef M. Marzouk, Habib N. Najm, and Larry A. Rahn. Stochastic spectral methods for efficient bayesian solution of inverse problems. *Journal of Computational Physics*, 224(2):560 – 586, 2007.

[166] C. Soize. A computational inverse method for identification of non-gaussian random fields using the bayesian approach in very high dimension. *Computer Methods in Applied Mechanics and Engineering*, 200(45):3083 – 3099, 2011.

[167] Velamur Asokan Badri Narayanan and Nicholas Zabaras. Stochastic inverse heat conduction using a spectral approach. *International Journal for Numerical Methods in Engineering*, 60(9):1569–1593, 2004.

[168] C. Proppe. Reliability computation with local polynomial chaos approximations. *ZAMM - Journal of Applied Mathematics and Mechanics / Zeitschrift fr Angewandte Mathematik und Mechanik*, 89(1):28–37, 2009.

[169] G.I. Schuller and H.A. Jensen. Computational methods in optimization considering uncertainties an overview. *Computer Methods in Applied Mechanics and Engineering*, 198(1):2 – 13, 2008.

[170] I. Enevoldsen and J.D. Srensen. Reliability-based optimization in structural engineering. *Structural Safety*, 15(3):169 – 196, 1994.

[171] M. Gasser and G.I. Schuller. Reliability-based optimization of structural systems. *Mathematical Methods of Operations Research*, 46(3):287 – 307, 1997.

[172] Hector A. Jensen. Design and sensitivity analysis of dynamical systems subjected to stochastic loading. *Computers & Structures*, 83(14):1062 – 1075, 2005.

[173] M. Papadrakakis, N.D. Lagaros, and V. Plevris. Design optimization of steel structures considering uncertainties. *Engineering Structures*, 27(9):1408 – 1418, 2005.

[174] Ioannis Doltsinis and Zhan Kang. Robust design of structures using optimization methods. *Computer Methods in Applied Mechanics and Engineering*, 193(23):2221 – 2237, 2004.

[175] Franois M. Hemez and Scott W. Doebling. Review and assessment of model updating for non-linear, transient dynamics. *Mechanical Systems and Signal Processing*, 15(1):45 – 74, 2001.

[176] M. Montemurro. *A contribution to the development of design strategies for the optimisation of lightweight structures*. Habilitation à diriger des recherches, Université de Bordeaux, 2018.

[177] The Nature of Mathematical Programming, Mathematical Programming Glossary, 2014, https://glossary.informs.org.

[178] J. Nocedal and S. Wright. *Numerical Optimization*. Springer-Verlag New York, 2006.

[179] F. W. Glover and G. A. Kochenberger. *Handbook of Metaheuristics*. Springer US, 2003.

[180] O. Mangasarian. *Nonlinear Programming*. Society for Industrial and Applied Mathematics, 1994.

[181] The MathWorks, Inc., 3 Apple Ill Drive, Natick, MA 01760-2098. *Optimization Toolbox User's Guide*, September 2011.

[182] A. Forsgren, P. E. Gill, and M. H. Wright. Interior methods for nonlinear optimization. *SIAM review*, 44(4):525–597, 2002.

[183] N. Gould, D. Orban, and P. Toint. Numerical methods for large-scale nonlinear optimization. *Acta Numerica*, 14:299361, 2005.

[184] I. Rechenberg. *Evolutionsstrategie: Optimierung technischer Systeme nach Prinzipien der biologischen Evolution*. Stuttgart: Frommann-Holzboog Verlag (in German), 1973.

[185] H. P. Schwefel. *Numerical optimization for computer models*. Chichester: John Wiley, 1981.

[186] Z. Michalewicz. *Genetic algorithms + data structures = evolution programs*. Berlin: Springer, 1994.

[187] L. J. Fogel, A. J. Owens, and M. J. Walsh. *Artificial intelligence through simulated evolution*. Chichester: John Wiley, 1966.

[188] F. Glover. Heuristics for integer programming using surrogate constraints. *Decision Sciences*, 8(1):156–166, 1977.

[189] J. H. Holland. *Adaptation in natural and artificial systems*. Ann Arbor: University of Michigan Press, 1975.

[190] D. E. Goldberg. *Genetic algorithms*. New York: Addison and Wesley, 1994.

[191] B. Baudry, F. Fleurey, J. M. Jezequel, and Y. Le Traon. Automatic test case optimization: a bacteriologic algorithm. *Software IEEE*, 22(2):76–82, 2005.

[192] G. Kjellström. On the efficiency of gaussian adaptation. *Journal of Optimization Theory and Applications*, 71(3):589–597, 1991.

[193] M. Dorigo, V. Maniezzo, and A. Colorni. Ant system: Optimization by a colony of cooperating agents. *IEEE Transactions on Systems, Man, and Cybernetics-Part B*, 26(1):29–41, 1996.

[194] J. Kennedy and R. Eberhart. Particle swarm optimization. pages 1942–1945, Perth, Australia, 1995. Proceedings of the IEEE International Conference on Neural Networks.

[195] H. Shah-Hosseini. The intelligent water drops algorithm: a nature-inspired swarm-based optimization algorithm. *International Journal of Bio-Inspired Computation*, 1:71–79, 2009.

[196] S. Kirkpatrick, C. D. Gelatt Jr., and M. P. Vecchi. Optimization by simulated annealing. *Science*, 220:671–680, 1983.

[197] F. Glover and M. Laguna. *Tabu Search*. Kluwer Academic Publishers, 1998.

[198] J. M. Renders. *Algorithmes génétiques et réseaux de neurones*. Paris: Hermes (in French), 1995.

[199] J. Rechenberg. *Cybernetic solution path of an experimental problem*. Royal Aircraft Establishment, Liberty translation 1122. Farnborough, UK., 1965.

[200] F. Greene. A method for utilizing diploid/dominance in genetic search. volume 1, pages 439–444, Orlando, 27-29 June 1994. Proceedings of the First IEEE International Conference on Evolutionary Computation, IEEE Service Center, Piscataway, NJ.

[201] M. Montemurro, A. Vincenti, and P. Vannucci. The automatic dynamic penalisation method (ADP) for handling constraints with genetic algorithms. *Computer Methods in Applied Mechanics and Engineering*, 256:70–87, 2013.

[202] A. Catapano and M. Montemurro. A multi-scale approach for the optimum design of sandwich plates with honeycomb core. Part I: homogenisation of core properties. *Composite Structures*, 118:664–676, 2014.

[203] R. L. Bagley and P. J. Torvik. On the fractional calculus model of viscoelastic behavior. *Journal of Rheology*, 30(1):133 – 155, 1986.

Lorenzo CAPPELLI

A general multi-scale identification strategy for the characterisation of the material behaviour of heterogeneous media

Résumé

Les matériaux composites sont largement utilisés en raison de leurs propriétés exceptionnelles. S'agissant de la caractérisation de leur comportement matériel, les principaux problèmes sont liés à la difficulté de caractériser les propriétés matérielles à chaque échelle. Les tests destructifs expérimentaux utilisés conduisent à des campagnes qui ne permettent pas d'identifier l'ensemble des propriétés élastiques 3D du pli.

En ce qui concerne l'identification microscopique des propriétés matériaux, seuls quelques tests standard et non standard sont effectués, lesquels montrent des dispersions de résultats significatives. Pour surmonter ces limitations, une stratégie d'identification multi-échelle (MSIS) est développée dans cette thèse.

De plus, la caractérisation du comportement non linéaire des matériaux composites permet de décrire la capacité d'amortissement sous des charges dynamiques. La réponse dynamique est affectée par le comportement viscoélastique des phase microscopiques et la caractérisation viscoélastique est tout sauf triviale. Expérimentalement, les techniques courantes peuvent fournir des informations uniquement à l'échelle du pli. Pour cette raison, le MSIS est étendu à la caractérisation viscoélastique des propriétés des matériaux composites à chaque échelle, en utilisant des tests non destructifs.

Concernant l'identification des propriétés des matériaux composites, il est important de caractériser la variabilité liée aux imperfections de fabrication. Les méthodes expérimentales d'identification de la variabilité ne peuvent pas évaluer l'incertitude des phases constitutives. Le grand nombre de tests requis implique des coûts importants pour obtenir des résultats qui sont toutefois affectés par les erreurs expérimentales. Différentes méthodes probabilistes sont décrites dans la littérature, qui ne permettent pas la caractérisation de la variabilité à l'échelle microscopique. Cet aspect représente le principal défi concernant l'identification de l'incertitude des structures composites, ainsi que la nécessité d'utiliser des techniques macroscopiques non destructives. Pour faire face à ce problème, le MSIS proposé est étendu pour intégrer la caractérisation de l'incertitude des propriétés des matériaux composites, à chaque échelle pertinente.

Mots-clés : Optimisation, Caractérisation, Problèmes inverses, Essais non-destructifs, Variabilité, Viscoélasticité.

Abstract:

Composite materials are widely employed due to their outstanding properties. When dealing with the characterisation of their material behaviour, the main issues are related to the difficulty of characterising the material properties at each scale. The commonly used experimental destructive tests lead to expensive campaigns, which are not able to identify the full set of 3D elastic properties of the ply.

Concerning the identification of the microscopic material properties, only few standard and non-standard tests can be performed, which show significant result dispersions. To overcome these limitations, a multi-scale identification strategy (MSIS) is developed in the presented thesis.

Moreover, the characterisation of the non-linear behaviour of composite materials allows to describe the damping capability under dynamic loads. Their dynamic response is affected by the viscoelastic behaviour of the microconstituents and the viscoelastic characterisation is anything but trivial. From an experimental viewpoint, common techniques can provide information only at the mesoscopic scale, whilst they cannot be used to characterise the microscopic viscoelastic properties. For these reasons, the MSIS is extended to the viscoelastic characterisation of composite materials properties at each pertinent scale, by using non-destructive tests.

Concerning the composite material properties, it is important to enhance the identification process by integrating the large amount of variability from manufacturing imperfections. Experimental methods for variability identification are only suited to evaluate mesoscopic uncertainty, without providing information about the constitutive phases. The huge number of required tests implies important costs to get results that are however affected by the experimental errors. Different probabilistic methods are found in literature, but they are not extended to the variability affecting the microscopic constituents. This aspect represents the main challenge concerning the uncertainty identification of composite structures, together with the need to use macroscopic non-destructive techniques. In order to face this problem, the proposed MSIS is extended to integrate the characterisation of the uncertainty of composite material properties, at each pertinent scale.

Keywords : Optimisation, Characterisation, Inverse problems, Non-destructive tests, Variability, Viscoelasticity.